Comptes Rendus
Géoscience — Sciences de la Planète
2021, 353, nº S1, p. 105-151
https://doi.org/10.5802/crgeos.69

Seismicity in France / *Sismicité en France*

Seismotectonics of southeast France: from the Jura mountains to Corsica

Christophe Larroque [*, a], Stéphane Baize [b], Julie Albaric [c], Hervé Jomard [b], Jenny Trévisan [a], Maxime Godano [a], Marc Cushing [b], Anne Deschamps [a], Christian Sue [c, d], Bertrand Delouis [a], Bertrand Potin [e], Françoise Courboulex [a], Marc Régnier [a], Diane Rivet [a], Didier Brunel [a], Jérôme Chèze [a], Xavier Martin [a], Christophe Maron [a] and Fabrice Peix [a]

[a] Géoazur, Université Côte d'Azur, CNRS, IRD, Observatoire de la Côte d'Azur, 06 560 Valbonne, France

[b] IRSN, PSE-ENV/SCAN/BERSSIN, BP 17, 92 262 Fontenay-aux-roses, France

[c] CNRS-UMR 6249, Bourgogne-Franche-Comté University, 25 000 Besançon, France

[d] CNRS, IRD, IFSTTAR, ISTerre, University Grenoble Alpes, University Savoie Mont Blanc, 38 000 Grenoble, France

[e] Departamento de Geofisica, Universidad de Chile, Blanco Encalada 2002, Santiago, 8320000, Chile

E-mails: larroque@geoazur.unice.fr (C. Larroque), Stephane.BAIZE@irsn.fr (S. Baize), julie.albaric@univ-fcomte.fr (J. Albaric), herve.jomard@irsn.fr (H. Jomard), trevisan@geoazur.unice.fr (J. Trévisan), godano@geoazur.unice.fr (M. Godano), Edward.CUSHING@irsn.fr (M. Cushing), deschamps@geoazur.unice.fr (A. Deschamps), christian.sue@univ-fcomte.fr (C. Sue), delouis@geoazur.unice.fr (B. Delouis), bertrand.potin@uchile.cl (B. Potin), courboulex@geoazur.unice.fr (F. Courboulex), regnier@geoazur.unice.fr (M. Régnier), diane.rivet@geoazur.unice.fr (D. Rivet), brunel@geoazur.unice.fr (D. Brunel), cheze@geoazur.unice.fr (J. Chèze), maron@geoazur.unice.fr (X. Martin), xavier.martin@geoazur.unice.fr (C. Maron), fabrice.peix@geoazur.unice.fr (F. Peix)

Abstract. The analysis of the seismicity catalog (1996 to 2019) covering the region from the Jura mountains to Corsica provides a first-order image of the distribution of earthquakes, highlighting large structures such as the Briançonnais and Piedmontais seismic arcs, the eastward deepening of the focal depths through the Western Alps, several large active faults (e.g. Belledonne, Middle Durance, Ligure). Over this period the magnitudes are moderate and the focal mechanisms of the main events display a diversity of seismic behaviors that can be explained by the complexity of the different geological domains with a more or less strong structural inheritage, by variable rheological characteristics at the scale of the crust and by the joint action of different mechanisms of deformation. The distribution of the historical events is in fairly good agreement with the instrumental seismicity, but several earthquakes of $M > 6$ are highlighted since the 14th century until the beginning of the 20th.

Keywords. Earthquakes, Faults, Jura–Bresse, Southeast basin, Western Alps, Ligurian Sea, Corsica.

Available online 5th August 2021

* Corresponding author.

1. Introduction

The southeast part of metropolitan France is one of the most seismic areas within the westernmost European continent (Figure 1). The first seismicity catalog for this zone was published by Rothé [1942] and since then the densification of monitoring networks, the technological improvement of seismometers and digital processing have led to spectacular progress in the detection and distribution of earthquakes and their focal mechanisms.

The seismic activity consists mainly of: (i) moderate magnitude events (i.e. no earthquakes $M_w > 6.0$ were recorded during the instrumental period), (ii) abundant and uneven microseismicity (i.e. $M_w < 3$) distributed throughout the SE region and (iii) numerous swarms. However, several strong historical earthquakes were reported (e.g. 1356, 1564, 1887, 1909). The rate of motions measured by spatial geodesy for more than 20 years are very low over the whole region: horizontal motions are less than 0.5 mm/yr through the Alpine and foreland domains and vertical motions are 3 mm/yr maximum, located in the northwestern Alps [e.g. Nocquet, 2012, Serpelloni et al., 2013, Nocquet et al., 2016, Walpersdorf et al., 2018]. So far, only the High Durance fault displays a present-day measurable slip-rate by spatial geodesy [Mathey et al., 2020]. The horizontal strain rate is in the range of 1–2 × 10^{-9}/yr [Masson et al., 2019], typical of intraplate domains.

An analysis of seismicity in France is proposed in the context of the 100th anniversary of the Bureau Central Sismologique Français (C.R. Geoscience, this issue). The present paper focusses on the southeastern quarter of the metropolitan territory. Southeast France is part of an intraplate region made of contrasting topographical and geological domains such as the Bresse graben, the Jura fold-and-thrust belt, the Southeast basin, the western Alpine belt, the Ligurian Sea and Corsica island. The Meso-Cenozoic geological evolution involved Paleozoic crystalline basement and Meso-Cenozoic sedimentary cover of variable thickness, together strongly structured by numerous faults resulting from the Hercynian, Pyrenean and Alpine orgeneses as well as Tethyan and western Mediterranean rifting phases [Chantraine et al., 2003]. The thickness of the crust also varies significantly: from 55 km at the maximum in the Alpine thickened area to less than 10 km in the Ligurian basin.

The objective of this paper is a synthesis of the knowledge on the seismicity of SE France. First, we present the evolution of the regional seismological networks that have provided data since the beginning of the 1960s. We then discuss the distribution of instrumental and historical seismicity over the whole SE region. This SE region being of particularly widespread seismicity, in a third part we discuss more precisely the relationship between seismicity and geology in the Jura–Bresse, the Southeast basin, the Western Alps and the Ligurian Sea and Corsica. In the last part we discuss some particular points of interest about (i) the precise relationships between earthquakes and faults, (ii) the seismogenic potential of faults according to their extension in depth, (iii) the very shallow earthquakes (iv) the forces allowing the stress loading of faults in the SE region. The seismic swarms detected in the region are not analyzed in detail (the reader can refer to the papers of Baques et al. [2021] and Guéguen et al. [2021]) and we do not adress the evaluation of the seismic hazard. Names and acronyms in italics correspond to web sites whose links are given in the references. Figures and tables numbered with the index "-S", as well as the high resolution seismicity maps can be found in the electronic supplement and also a kml file which helps to locate the places, cities and geological locations mentioned in the text.

2. The seismological networks and catalogs in southeast France

CEA-LDG (Laboratoire de Détection et de Géophysique du Commissariat à l'énergie atomique et aux énergies alternatives) deployed, in 1962, the first seismological high sensitivity network covering the whole metropolitan territory. In the 1970s, ten stations were deployed in SE France. In the same decade isolated seismic stations, run by universities or other institutions were dedicated to record large events and arrival times collected by *BCSF* (Bureau Central Sismologique Français) to locate main events [BCSF, 1983] (Figure A-Sa).

It is only from 1978 that the scientific community dedicated permanent seismic networks to follow regional and local microseismicity. Thus the first local network was installed by IPG Strasbourg (Insti-

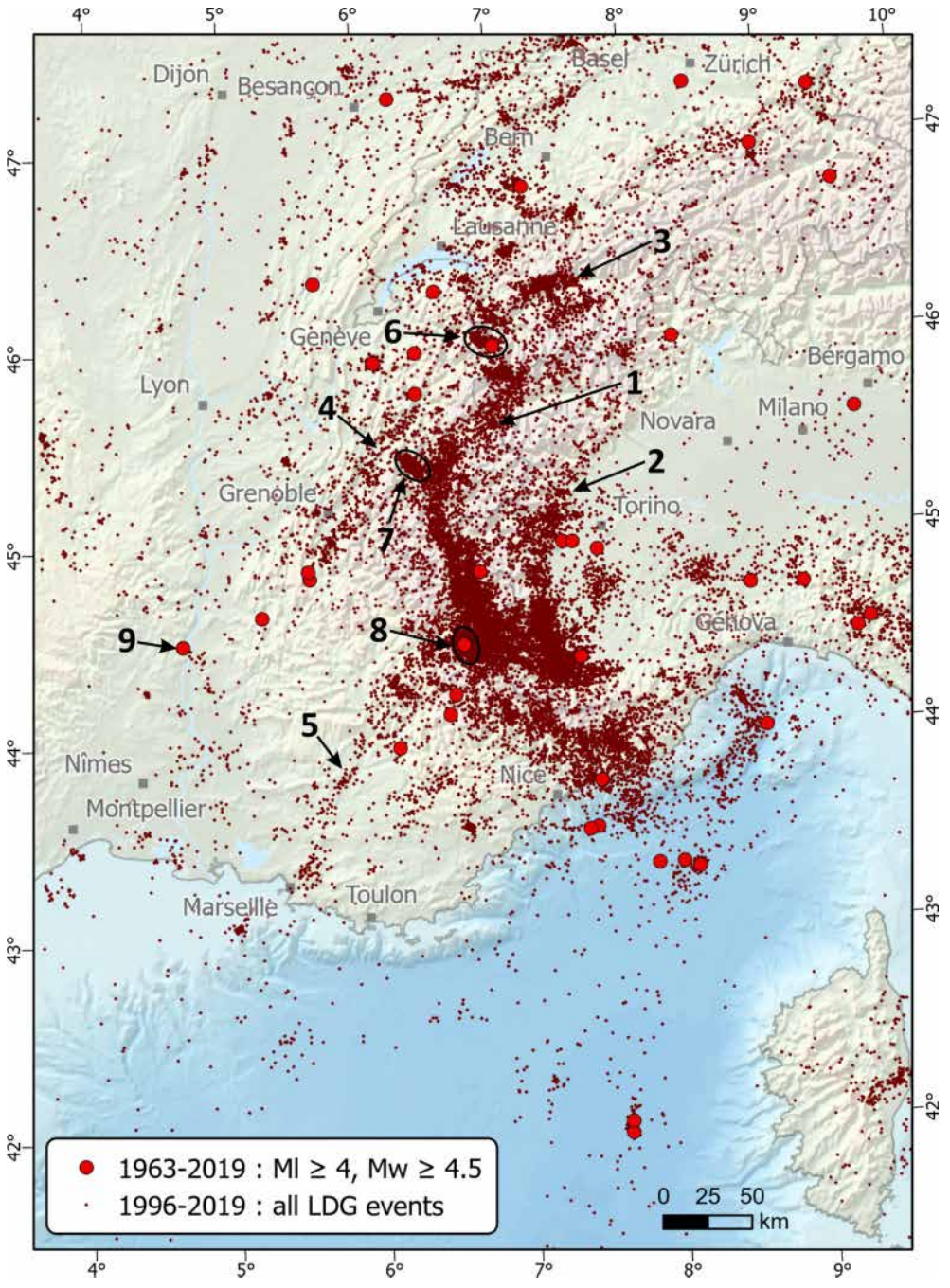

Figure 1. Seismicity map from the *CEA*_1996–2019 catalog supplemented by earthquakes of $M_L \geq 4.5$ or $M_w \geq 4.0$ from the *CEA* and the Si-Hex catalogs for the period 1963–1996. 1, 2: Briançonnais and Piemontais seismicity arcs respectively; 3–5: Rhône, Belledonne and Durance seismic alignments respectively; 6: Vallorcine cluster; 7: Maurienne cluster; 8: Ubaye cluster; 9: Epicenter of the Le Teil earthquake (M_w 4.9, 2019/11/11). The geographic extend of the map is NW: 47.615° N–3.663° E, NE: 47.615° N–9.974° E, SW: 41.235° N–3.694E, SE: 41.092° N–9.610° E.

tut de Physique du Globe) (under the responsibility of P. Hoang-Trong) covering the Nice area with seven vertical short-period stations being radio transmitted (Figure A-Sb). During the same period, radio-link stations were installed around Grenoble. These stations, equipped with sensitive short-period sensors (mostly providing the vertical component of shaking), suffered from limited data transfer capabilities, hence limiting the sampling rate. The digital content has evolved only slowly from 12 bits to 16 bits, and data of the largest events were mostly clipped allowing only arrival time picking. Timing control was performed using an encoded radio time (DCF77) provided by a German Institution *PTB* (Physikalisch-Technische Bundesanstalt), with a precision of 1/50 s. Some years later, a similar network was installed covering the Middle Durance fault, run by the *RéNaSS* (Réseau National de Surveillance Sismique). The Durance network was replaced after 1992 by a denser network operated by *IRSN* (Institut de Radioprotection et de Sureté Nucléaire) for 10 years [Dervin et al., 2007].

The main modern network covering southeast France was the *SISmalp* network installed from the end of the 1980s (Figure A-Sb). It was originally composed by 35 sites equipped with L4C 1 Hz vertical velocimeters and 16 bits digitizers. The data, locally triggered time windows of the continuous record, were collected on *public switched telephone network* lines for a centralized analysis. Only a part of the Sismalp stations were contributing to BCSF seismological events location [BCSF, 2002]. It provided the first robust imaging of microseismicity with the possibility of determining a lot of focal mechanisms. During its 25 years of operation, the network was regularly upgraded by installing some three component sensors, 24-bit digitizers and GPS time control integration, partly integrating broad-band network. It stopped running after 2015 and a large part of the stations have been integrated into the *RESIF–EPOS* (Réseau Sismologique et Géodésique Français-European Plate Observing System) network.

The last evolution of the network over SE France began with the installation of the first broad-band sensors connected to 24-bit digitizers and GPS time control. The migration to continuous 100 Hz real-time transmission of the data (2005) using seedlink protocol allows a more efficient sharing of the data and therefore a simplified use for microseismicity analysis. The last stage is the implementation of *RESIF–EPOS* infrastructure in which CNRS, University observatories and *CEA-LDG* gather most of the data from their stations in France (Figure A-Sc): these initiatives push forward the aim of uniform coverage of the national territory and open diffusion of all the data and tends to enhance the completeness of the catalogs.

Several catalogs have been published by different institutions operating seismic networks. In recent years a special effort has been made to harmonize the catalogs in order to provide moment magnitudes [*SI-Hex* catalog, Cara et al., 2015] or to improve earthquake location through 3D tomographic modeling of the crust and top of the mantle [Potin, 2016]. For the analysis carried out in this paper, given the size of the study area, bordering Switzerland and Italy and including the Ligurian Sea and Corsica, we have used the *CEA* catalog (Table A-S) which covers the largest area beyond the borders, unless otherwise stated in the text.

In SE France, the *CEA* catalog gathers the earthquake locations obtained using station records from the various French networks: the *CEA* network since the early 1960s, *SISmalp*, *RéNaSS* and *OCA* networks since 1977, 1986 and 1992 respectively; and also in order to complete outside the borders, the stations from *GEOFON* (Germany), *SED* (Switzerland) and *RSNI* (Italy) seismic networks are also used [Duverger et al., 2021]. The magnitude versus time distribution (Figure 2) clearly highlights the gain in detection capability over the years. For instance, the improvement during the 1977–2000 period is mainly related to the *SISmalp* network deployment.

3. Seismicity in the southeast of France

3.1. *Instrumental seismicity*

From 1963 to 2019, the *CEA* catalog displays the location and local magnitude (M_L) of 37,935 natural earthquakes (quarry blasts and marine explosions excluded). We have chosen to analyze only the last 23 years (1996–2019) during which the balance between magnitude completeness and event detection is optimal for a set of 30,493 events (Figure 1). The locations were determined based on manual P- and S-wave picks, using a 1D velocity model [Duverger et al., 2021]. In order to complete this map of instrumental

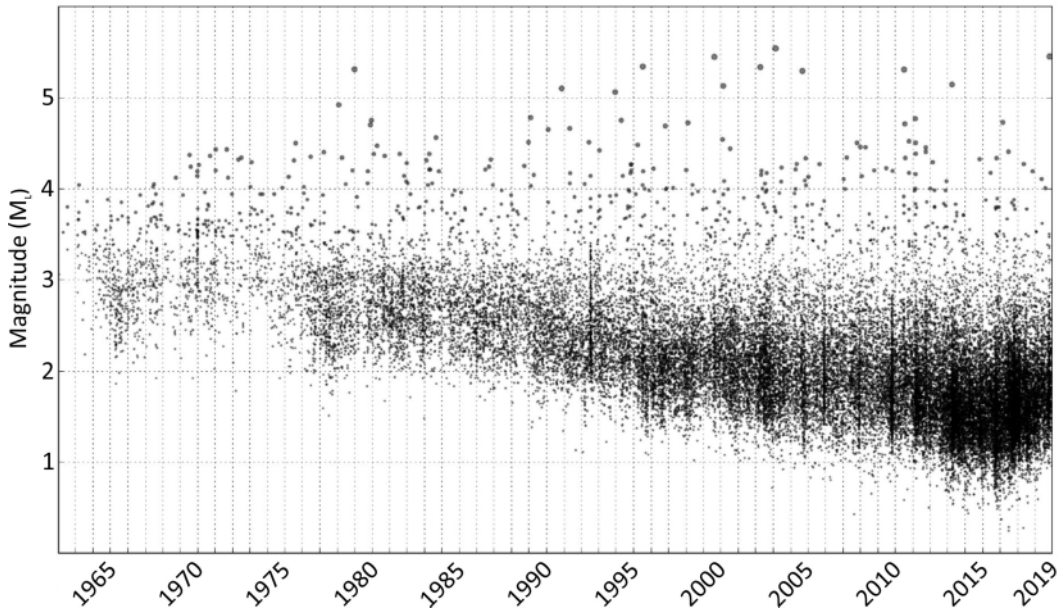

Figure 2. Magnitude versus time of earthquakes in SE France from the *CEA*_1963–2019 catalog.

seismicity for the period 1963–1995, we have added 25 earthquakes of $M_L \geq 4.5$ or $M_w \geq 4$ from the *CEA* and *Si-Hex* catalogs respectively which can be assumed to have been located with a sufficient number of stations and therefore of a reasonable accuracy (Figure 1 and Table B-S).

From 1996 to 2019, the maximum magnitude, M_L 5.4 (M_w 4.9), corresponds to the Le Teil earthquake (2019/11/11), but over the period up to 1963, the strongest earthquake had occurred in the Ligurian Sea (1963/07/19, M_w 6.0) and a total of 43 earthquakes exceeded M_L 4.5 or M_w 4.0 (Table B-S). These moderate earthquakes are distributed throughout the SE domain of France.

The magnitude–frequency distribution of the entire catalog of SE France shows a magnitude of completeness around 1.5 and a *b*-value of 1.12 (Figure 3). This high *b*-value deviates from the first-order *b*-value ~1 [Gutenberg and Richter, 1944] and indicates a relative excess of low magnitude earthquakes versus large magnitude ones. Such excess could be explained by large swarms (Figure 1) in Ubaye [2003–2004, 2012–2016; Jenatton et al., 2007; Thouvenot et al., 2016; Baques et al., 2021], near Sampeyre [2010, Godano et al., 2013] and in Maurienne [2017–2018, Guéguen et al., 2021] as can be seen on the monthly distribution since 1996 (Figure 4). One can notice that the 2003–2004 Ubaye swarm [16,000 earthquakes in two years, Jenatton et al., 2007] does not appear in this data set, certainly in relation to the low detection capacity of the permanent network for $M_L < 1.7$ at that time. The 30,493 earthquakes of the 1996–2019 *CEA* catalog are mainly located in the upper crust between 2 and 12 km depth with about 500 events lying between 30 and 50 km and about 15 beyond 50 km depth (Figure B-S).

As mentioned in previous works [e.g. Nicolas et al., 1998, Eva et al., 2020], at the scale of SE France and NW Italy the distribution of epicenters is very heterogeneous. A large part of the seismicity is diffuse and has no particular distribution or relationship with identified geological structures. Nevertheless, according to their geometry, several types of epicenter concentrations are highlighted, mainly in the Alpine domain and its foreland (Figure 1): (i) the major ones are the so-called "Briançonnais and Piemont arcs", previously identified by Rothé [1942]: they extend over more than 150 km from Aosta in the north to Cuneo in the south; (ii) obvious alignments of epicenters underline large geological structures such as the Rhône fault (Valais, Switzerland), the Belledonne Border fault (near Grenoble) and the Middle Durance fault (Provence, France); and (iii) several clusters of epicenters are found throughout the entire Alpine

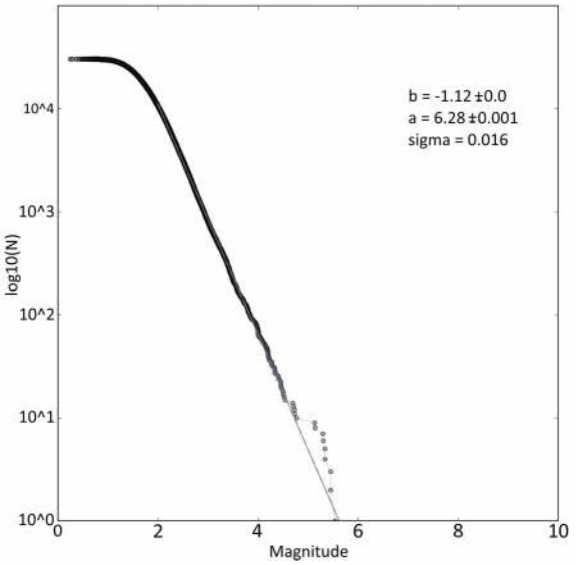

Figure 3. Magnitude–frequency distribution of earthquakes in SE France from the *CEA*_DG 1996–2019 catalog.

chain, the major ones are the Vallorcine, Maurienne and Ubaye clusters.

Other areas are characterized by an almost total absence of seismicity over this period: the Bresse depression, the Diois–Barronies–Ventoux chain and the Vaucluse plateau, the Maures massif and the external crystalline massifs of the Alpes. The lower Rhône valley, between Montélimar and Avignon is also rather poorly seismic; but it should be mentioned that the strongest earthquake recorded in metropolitan France since 50 years occurred 10 km to Montélimar [M_w 4.9, 2019/11/11; Ritz et al., 2020; Cornou et al. and Delouis et al., 2021].

3.2. *Historical seismicity*

Prior to 1963 and the onset of sufficiently dense seismological networks, the most complete data set concerning the regional seismicity comes from macroseismic catalogs. In this review, we present data from the *SISFRANCE* database. *SISFRANCE* database compiles intensity information from written historical archives, as well as from macroseismic inquiries, in particular those collected by the *BCSF* since 1921 [Fréchet, 2008] and by the Bureau de Recheches Géologiques et Minières (*BRGM*) between 1978 and 1987. Intensities are established in the MSK-64 macroseismic scale [Medvedev et al., 1967, Scotti et al., 2004].

Up to 1963, a total of 2055 events are reported along with an epicentral location (Figure 5). This only represents the best part of the available knowledge, considering that historical archives are often not precise enough to attribute either a location or an epicentral intensity to a single or a group of events. The 2055 events are distributed as follows (Figure 6 and Jomard et al., 2021 for the precise definition of each intensity class): (i) 1085 events without attributed epicentral intensity (mainly poorly known events and aftershocks), (ii) 176 locally felt events (II ≤ Io ≤ III–IV: weak events for which the felt area is small), (iii) 558 widely felt events (IV ≤ Io ≤ V–VI: wider macroseismic fields and more significant impact on the population in the epicentral area), (iv) 200 damaging events (VI ≤ Io ≤ VII: structural damages on buildings, without causing their collapse or in rare cases, of high building vulnerability), (v) 36 strongly damaging events (Io ≥ VII–VIII: collapse of a significant number of buildings).

Besides the very first located earthquake in Vienne in 463 A.D. (Figure 5), the seismicity catalog of the region really starts with the 12th century events. In particular, an exceptional archive was found in Vatican City [Castelli et al., 2012] documenting the event that occurred near Uzès in 1186 (Io VII–VIII MSK). Later, the first widely reported earthquake in the region is the Basel one in 1356 [Lambert et al., 2005, Fäh et al., 2009], being the most important earthquake in the region, together with the 1855 Valais earthquake [Fritsche et al., 2006] and the 1887 Ligurian earthquake [Ferrari, 1991, Larroque et al., 2012], all with an epicentral intensity of IX (i.e. collapse of standard structures).

More generally, the seismicity, as seen from the archives, more or less covers the entire region (Figure 5) with a general trend of decreasing number and intensity of events, while moving away from the Alpine arc and its foreland towards the northwest (Massif Central and Bresse areas). Some specific areas almost lack any historical seismicity, like the Bresse valley between the cities of Lyon and Dijon, the Maures massif north of Toulon, a SW–NE oriented band in the Alps from the Vercors to the Aosta valley in Italy and offshore in the Ligurian Sea. While this low seismicity rate in Bresse,

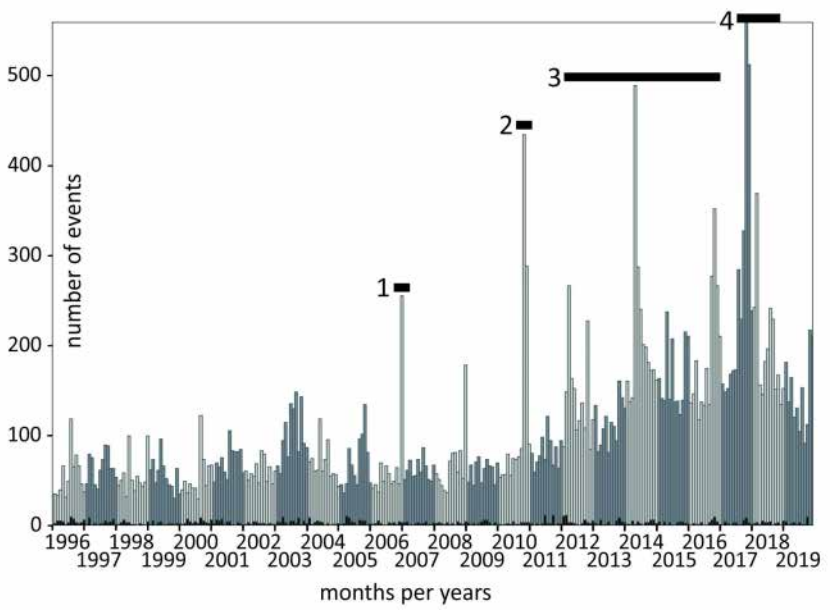

Figure 4. Monthly distribution of earthquakes in SE France from the *CEA*_1996–2019 catalog. Several swarms could be identified: 1. Basel induced swarm [Deichmann and Giardini, 2009]; 2. Sampeyre swarm [Godano et al., 2013]; 3. Ubaye swarms [Thouvenot et al., 2016, Baques et al., 2021]; 4. Maurienne swarm [Guéguen et al., 2021], Var and canton de Vaud (in Switzerland) swarms [Godano et al., 2019, Diehl et al., 2021].

Maures and Vercors areas is consistent with what is observed during the instrumental period, the situation is different for the Ligurian Sea and the internal Alps near the Aosta valley, where the instrumental seismicity rate is high. These observations point to the incompleteness of historical data in both mountainous and maritime areas. For instance, in the Ubaye Valley, the first reported earthquake occurred in 1844 whereas the area has been highly active throughout the 20th century, and especially since the 1959 event and the onset of instrumental networks [Baques et al., 2021].

On the contrary, some areas characterized by poor instrumental seismicity highlight a significant historical seismic activity. This is the case in Provence and the lower Rhône valley where numerous damaging earthquakes [e.g. 1909 Provence earthquake; Baroux et al., 2003] and swarms occurred in previous centuries. To a lesser extent, this is also the case in the Jura mountains (e.g. 1822 Chautagne earthquake), at the shoulders of the Bresse area (e.g. 1783 Bligny earthquake) and in the area that was heavily shaken by the 1755 and 1855 earthquakes (Eastern Valais, Switzerland). Finally, the historical dataset attests to peculiar seismogenic behaviors: the occurrence of swarms (such as in the lower Rhône valley and Tricastin, see later), shallow events (such as in Tricastin and Chasteuil, see later), or repeating events along an individualized fault system (such as along the Middle Durance fault, see later).

4. Seismicity in the different geological domains

Southeast France is made up of a set of juxtaposed and fairly homogeneous geological domains. In order to specify the distribution of seismicity and the potential relationships between earthquakes and mapped faults, we describe the seismicity following those homogeneous geological zones. We discuss the focal mechanisms of the main earthquakes, for more details the reader can refer to the mentioned publications and to the recent synthesis by Mazzotti et al. [2021]. The seismicity maps presented below correspond to extractions from the CEA_1996–2019 catalog according to the geographical limits of each zone which can be found in the supplementary data (Shapefiles_zones).

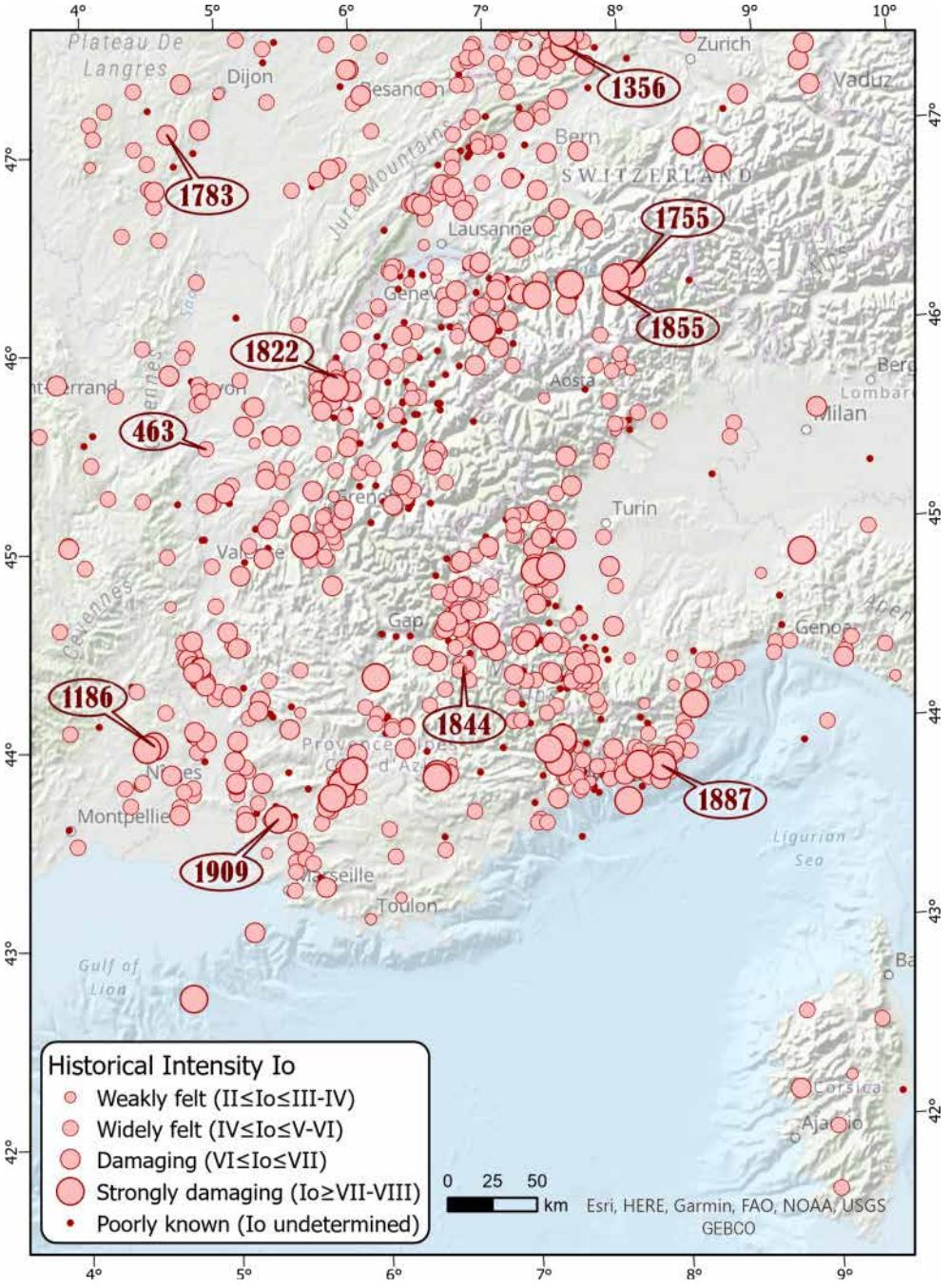

Figure 5. Historical seismicity map in SE France from *SISFRANCE* (Io MSK64).

4.1. *The Jura massif and the Bresse graben*

The Jura mountains are located northward of the western Alpine domain (Figure 7). This arc-shaped massif is a thin-skin fold-and-thrust belt composed of Mesozoic and Cenozoic carbonates and marls which are displaced ~20 km towards the NW since the middle Miocene due to a Triassic evaporite layer of variable thickness [Sommaruga, 1999, Affolter and Gratier, 2004]. The external limit of the arc bor-

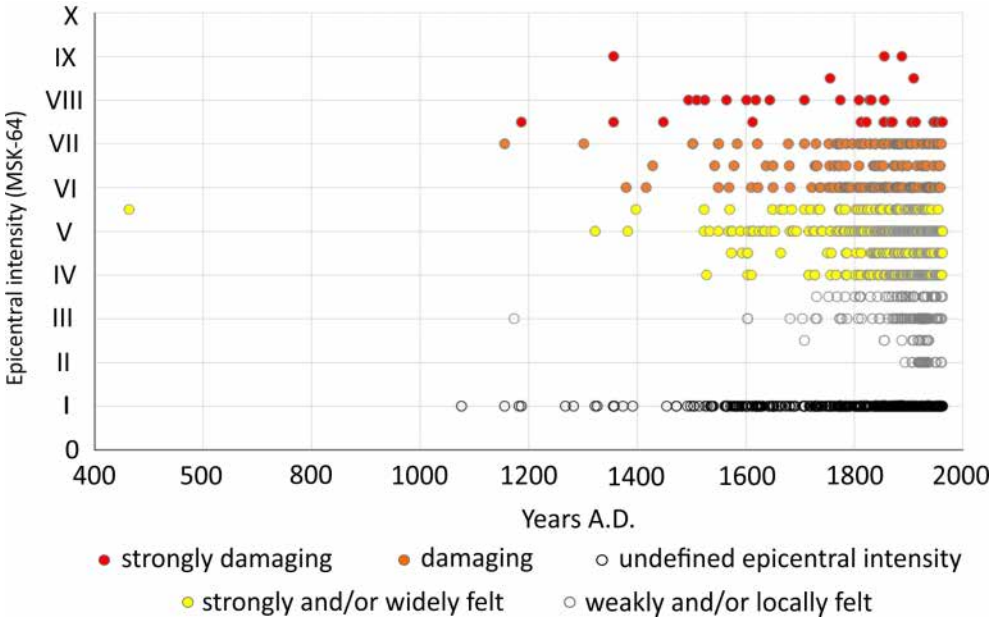

Figure 6. Temporal plot of the historical seismicity recorded in SE France, including the 2055 events of the *SISFRANCE* database, from year 463 to year 1962. Undefined epicentral intensities are arbitrarily plotted along the Io = I axis as presented in Jomard et al. [2021].

ders the Rhine Graben (RG on Figure 7) to the N, the WSW–ENE Rhine–Bresse-Transfer Zone (RBTZ) to the W and the Bresse Graben (BG) to the S and SW. The Molasse Foreland Basin (MFB) marks the internal limit of the Jura arc and its transition with the Alpine belt. The massif is affected by shallow thrust faults oriented parallel to the arc direction and is perpendicularly cross-cut by strike-slip faults possibly developed above pre-existing basement structures, such as the Vuache fault (VB) to the south and the Pontarlier fault (PF) in the middle [Phillippe, 1994, Baize et al., 2011]. N–S normal faults are located, mainly on the external border of the arc and within the Rhine and Bresse grabens and the RBTZ. The Jura massif and the Bresse graben are currently affected by NNW–SSE shortening and strike-slip tectonic regime with the maximum horizontal stress-oriented NW–SE [Rabin et al., 2018]. Actually, several studies have highlighted the complexity and variability of the tectonic style in the area according to the present-day coupling/uncoupling between the basement and its sedimentary cover [e.g. Becker, 2000, Lacombe and Mouthereau, 2002, Madritsch et al., 2008, Rabin et al., 2018].

About 1642 earthquakes have been reported between 1996 and 2019 in the Jura Massif and Bresse graben (Figure 7). The seismicity is spatially unevenly distributed, with fewer events in the Bresse graben, and increasing activity toward NE. In addition, the SW of the area (W of 6° E) exhibits mostly superficial seismic events (<15 km depth, Figure B-S) while deeper earthquakes, down to ~25 km, are recorded in the NE. The epicenter location is well constrained in the area with a primary and secondary gap lower than 180° for 84% and 72% of the locations, respectively [for location criteria quality: e.g. Kissling, 1988, Chatelain et al., 1980, Duverger et al., 2021]. The interpretation of the earthquake depth distribution should however be done cautiously, with a minimum epicentral distance larger than 30 km for more than 50% of the events. The station coverage in the Jura and Bresse graben has been improved recently through the development of *RESIF–EPOS* at the scale of metropolitan France, and through the deployment of local short and long-term seismic networks [e.g. *JURAQUAKE* and AlpArray, Hetényi et al., 2018].

About 95% of the events have magnitude $M_L < 3$. The largest magnitude events ($M_L > 4$) recorded

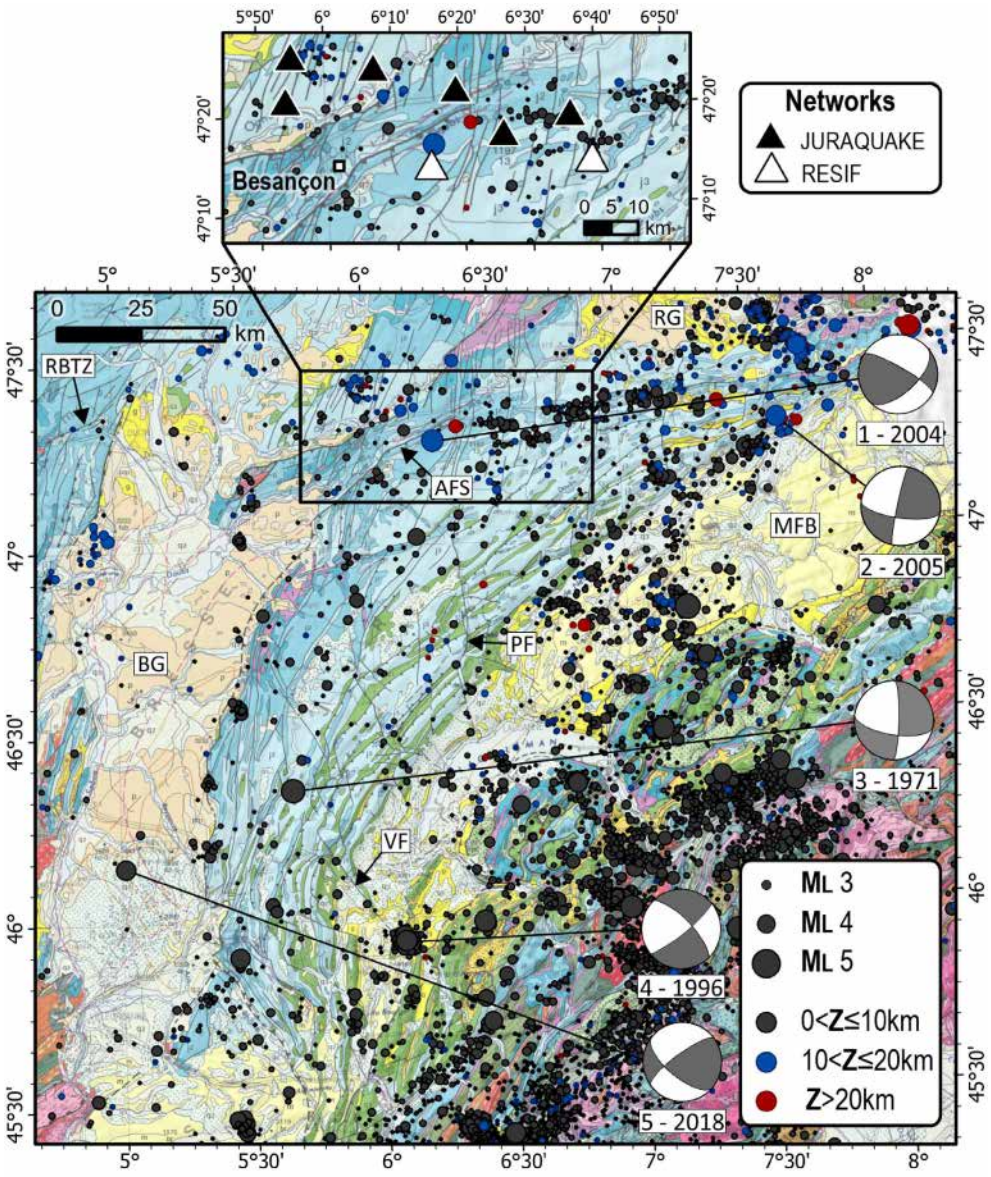

Figure 7. Seismicity overlaid on the geological map of the Bresse–Jura area, from the *CEA*_1996–2019 catalog (all magnitudes) and Chantraine et al. [2003] (pink–red–orange: Paleozoic, blue–green: Mesozoic; yellow–beige–white: Cenozoic; the complete legend of the map is on https://www.geoportail.gouv.fr/donnees/cartes-geologiques). Insert: triangles are seismometers of the *JURAQUAKE* and *RESIF–EPOS* networks around Besançon. Focal mechanisms: 1, Besançon-Roulans earthquake (2004/02/23, M_w 4.5; *Delouis-Géoazur*); 2, Rumisberg [2005/05/12, M_L 4.1; Deichmann et al., 2006]; 3, Jeurre [1971/06/21, M_L 4.4; Sambeth and Pavoni, 1988]; 4, Epagny [1996/07/15, M_L 5.3; Thouvenot et al., 1998]; 5 [2018/11/21, M_w 3.8; *Delouis-Géoazur*].

in the area occurred in the Jura Massif (Figure 7 and Table B-S): the Jeurre earthquake [no. 3 on Figure 7; 1971/06/21, M_L 4.4; Sambeth and Pavoni, 1988], the Epagny earthquake [no. 4; 1996/07/15, M_L 5.3; Thouvenot et al., 1998; see later], the Besançon/Roulans earthquake [no. 1; 2004/02/23, M_L 4.8–M_w 4.5; *Delouis-Géoazur*; Baer et al., 2005] and the Rumisberg earthquake [no. 2; 2005/05/12, M_L 4.1–M_w 3.7; Deichmann et al., 2006]. Only one significant earthquake has occurred so far in the Bresse graben, close to Bourg-en-Bresse (no. 5; 2018/11/21, M_L 4.1–M_w 3.8; *Delouis-Géoazur*).

Focal mechanisms of these events indicate mainly strike-slip to oblique-thrust faulting (Figure 7). In particular, the Besançon/Roulans earthquake is most likely associated with left-lateral thrust movement on a deeply rooted NE–SW structure [Cara et al., 2007, Madritsch et al., 2008]. This event could be attributed to the activity of the Avant-Monts faults system (AFS) where a recurrent seismicity is recorded. A shallower and swarm-like distribution of the seismicity can be observed close to Besançon. The potential role of fluid in triggering microseismicity into this faulted and karstified region is currently investigated based on local seismic recordings with the new *JURAQUAKE* network.

While no significant historical event was recorded in the Bresse area, several damaging earthquakes struck the Jura mountains with Io VII MSK (Figure 8 and *SISFRANCE*): January 18, 1155 in a wide area near Lons-le-Saunier; October 30, 1828 near Besançon; August 11, 1839 near Annecy; April 17, 1936 near Frangy. Two strongly damaging events occurred on October 18, 1356 near Basel (Io IX) and February 19, 1822 in the Bugey area (Io VII–VIII). The Basel earthquake is one of the strongest ever felt in most western Europe, producing heavy damages in the northeastern Jura/South Rhine graben area [Lambert et al., 2005, Fäh et al., 2009] and felt over a wide territory including Paris and Prague. With an estimated M_w 6.5 [Manchuel et al., 2017], its seismogenic source is still being discussed: Meyer et al. [1994] and Ustaszewski and Schmid [2007] favor an oblique-slip reactivation of an ENE-striking basement fault of the RBTZ below the thrusted Jura mountains while Meghraoui et al. [2000] and Ferry et al. [2005] propose a normal faulting along a NNE-striking Rhine graben fault [see also Bellier et al., 2021; Doubre et al., 2021]. The Basel area also suffered recurrent seismic activity over the centuries, especially in 1650 when a sequence of earthquakes occurred with a maximum epicentral intensity of VI–VII (*SISFRANCE*).

4.2. *The South-east basin of France and the Provence*

The South-East Basin of France is made of 2 to more than 10 km thick of Meso-Cenozoic sedimentary rocks covering the Paleozoic basement (Figure 9). A thick layer of Triassic evaporites (salts, gypsum and anhydrite) at the base of the Meso-Cenozoic cover plays an important role in the regional tectonic behavior, allowing fold and thrust décollement tectonics over the basement [e.g. Rangin et al., 2010, Espurt et al., 2019]. On the edges, the SE Basin is over thrusted by the Alpine belt to the East (namely the Vercors (V on Figure 9) and Arc de Castellane frontal thrusts (ACT on Figure 9) to the North and to the South, respectively) and it is bounded by Paleozoic basement to the South (Maures and Esterel massifs, ME) and the West (Massif Central, MC).

From late Paleozoic up to Neogene times, the long-term geological evolution of the SE Basin is characterized by several phases of extensional tectonics, such as the opening of the Tethys ocean during the Jurassic and the opening of the western Mediteranean during the Oligocene, as well as compressional tectonics, such as the Pyrenean orogenesis during the Eocene. Within the basin, those phases successively reactivated large crustal faults such as the Cévennes (CFS), Nîmes (NF), Salon-Cavaillon (SCF) and Middel Durance (MDF) faults [Arthaud and Séguret, 1981, Roure et al., 1992, Séranne, 1999, Espurt et al., 2012, Bestani et al., 2016].

Subsequently, from the Miocene the collision between the Adria and Eurasia plates (Alpine orogeny) causes deformation in the SE basin, which can basically be considered as the foreland basin of both the Pyrenean and Alpine ranges. The Pyrenean north- and south-verging thrusts were then reactivated [Combes, 1984, Villeger and Andrieux, 1987, Champion et al., 2000, Chardon and Bellier, 2003, Rangin et al., 2010, Bestani et al., 2016], whereas the NE-trending crustal-scale strike-slip faults (Cévennes, Nîmes and Middel Durance faults) were activated as transfer fault zones, accommodating a differential N–S shortening [Arthaud and Laurent, 1995, Guyonnet-Benaize et al., 2015]. West of the Durance fault, struc-

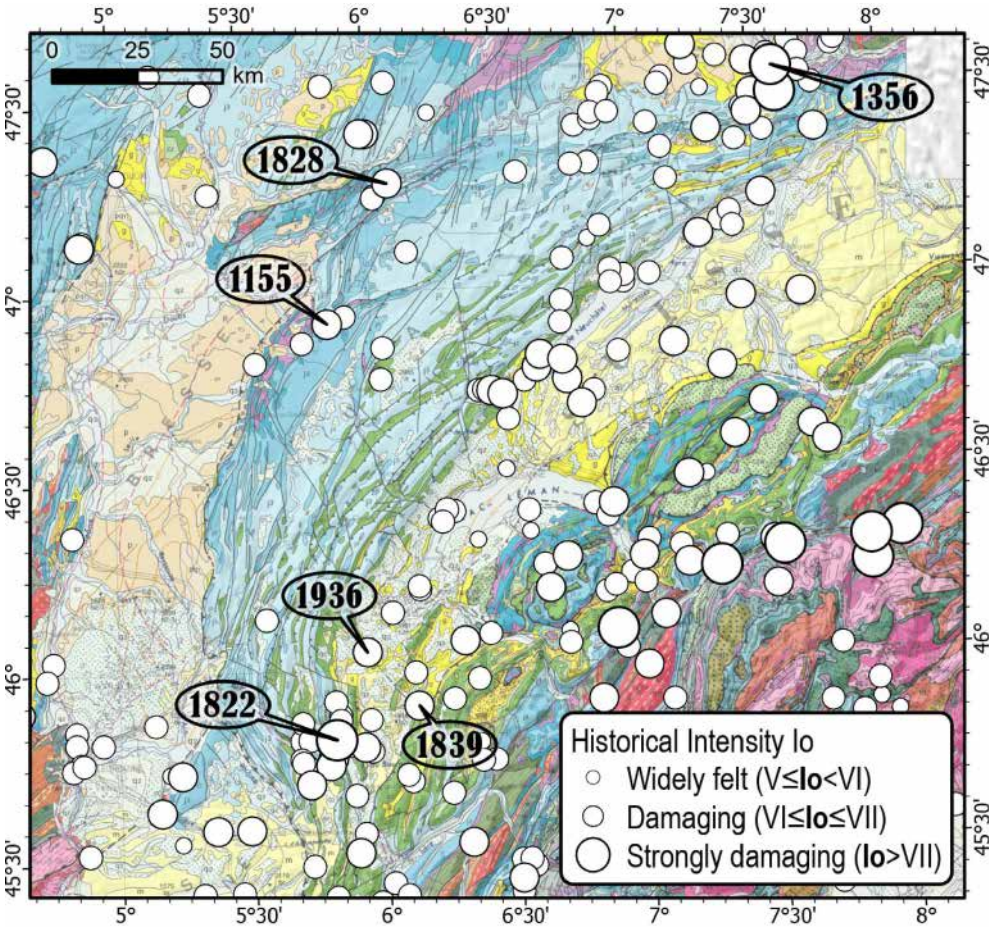

Figure 8. Historical seismicity map of the Jura–Bresse area from *SISFRANCE*.

tural investigations attest that the sedimentary cover is largely decoupled from the basement thanks to the thick evaporitic Triassic layer. [Rangin et al., 2010] propose that this sedimentary cover has been flowing southward because of the uplift of the alpine chain.

The overall rate of seismicity is low in the SE basin (Figure 9), compared to the alpine domain for instance. About 903 events are reported in the *CEA* catalog between 1996 and 2019. The epicenter locations are relatively well constrained with a primary and a secondary azimutal gap less than 180° for 82% and 57% of the events, respectively. Like in Jura, the minimum epicentral distance is larger than 30 km for more than 50% of the events. Although the whole region is entirely and highly prestructured, the distribution of seismicity is heterogeneous and only few earthquakes clearly attest to reactivation of some inherited faults [Cushing et al., 2008, Ritz et al., 2020]. In addition, several areas, such as the Diois–Baronnies (DB), the Ventoux–Lure range (VL), the Cévennes-Ardèche hills and the eastern Provence area are characterized by very few instrumental earthquakes. Earthquake magnitudes are low: only the Largentière (no. 2 on Figure 9; 2011/08/03, M_L 4.3) and the Le Teil (no. 1; 2019/11/11, M_L 5.4) earthquakes exceeded magnitude 4 since 1962 (Table B-S). The focal depths are distributed down to 25 km deep in the crust with a majority of events around 5 km (Figure B-S). A peculiar set of ultra-shallow seismicity, less than 1 km, have been monitored in the Tricastin area (TA) [Thouvenot et al., 2009, see later].

The major seismic structure is the Middle Durance Fault (MDF) along which seismic clusters show a clear alignment with strike-slip focal mechanisms

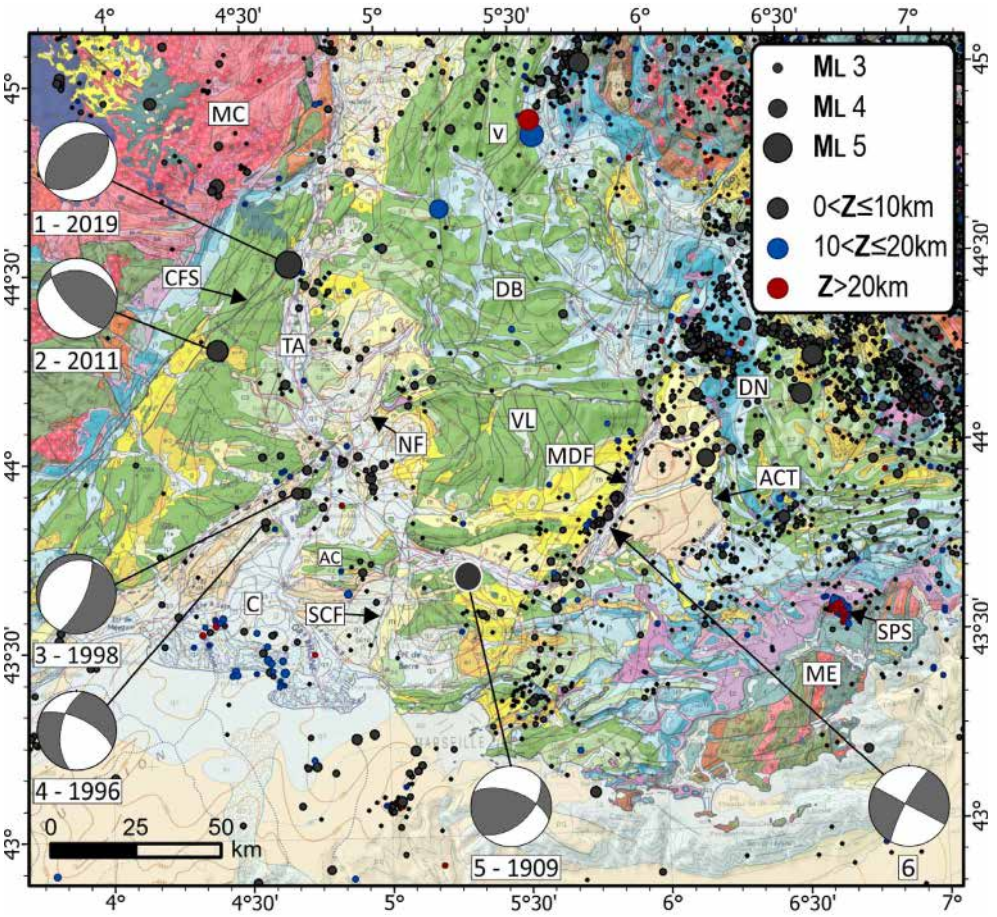

Figure 9. Seismicity overlaid on the geological map of the Southeast basin, from the *CEA*_1996–2019 catalog (all magnitudes, except for the 1909 Provence earthquake from Baroux et al. [2003]) and Chantraine et al. [2003]. Focal mechanisms: 1. Le Teil earthquake [2019/11/11, M_w 4.9; Ritz et al., 2020]; 2. Largentière (2011/08/03, M_L 4.3; *Delouis-Géoazur*); 3. [1998/02/09, M_L 3.1; Baroux et al., 2001]; 4. [1996/03/25, M_L 3.1; Baroux et al., 2001]; 5. Provence earthquake [1909/06/11, M_w 6.0; Baroux et al., 2003]; 6. composite mechanism Durance fault [Cushing et al., 2008].

(no. 6 on Figure 9, see later). The main seismic alignment extends over 70 km along the course of the Durance River and seems to continue for about 40 km to the South toward Marseille. In the Gulf of Lion, another seismic NE–SW alignment, about 20 km long, continues the MDF trace. To the North, the MDF is over-thrusted by the Digne nappe (DN) and the connection with the Lambruissier blind fault remains to be explored. There, a large cluster of microseismicity occurs [Hippolyte and Dumont, 2000, Godard et al., 2020].

Several zones of diffuse seismicity are located along the lower Rhône valley. From North to South, these zones are (Figure 9): (i) the Northeastern tip of the Cévennes faults system (CFS), where the Teil earthquake occurred in 2019, (ii) the Tricastin area (TA) characterized by earthquakes swarms occurrence, (iii) the Nîmes fault area (NF) and (iv) the Camargue coastline (C). The focal depths are less than 10 km except beneath the Camargue delta where depths greater than 20 km are reached (Figure B-S). While the western part of the SE basin is mainly aseismic, the 2 strongest instrumental earthquakes occurred on the northern part of the Cévennes faults system (Largentière and Le Teil, no. 2 and no. 1 on Figure 9), all together with a reverse faulting

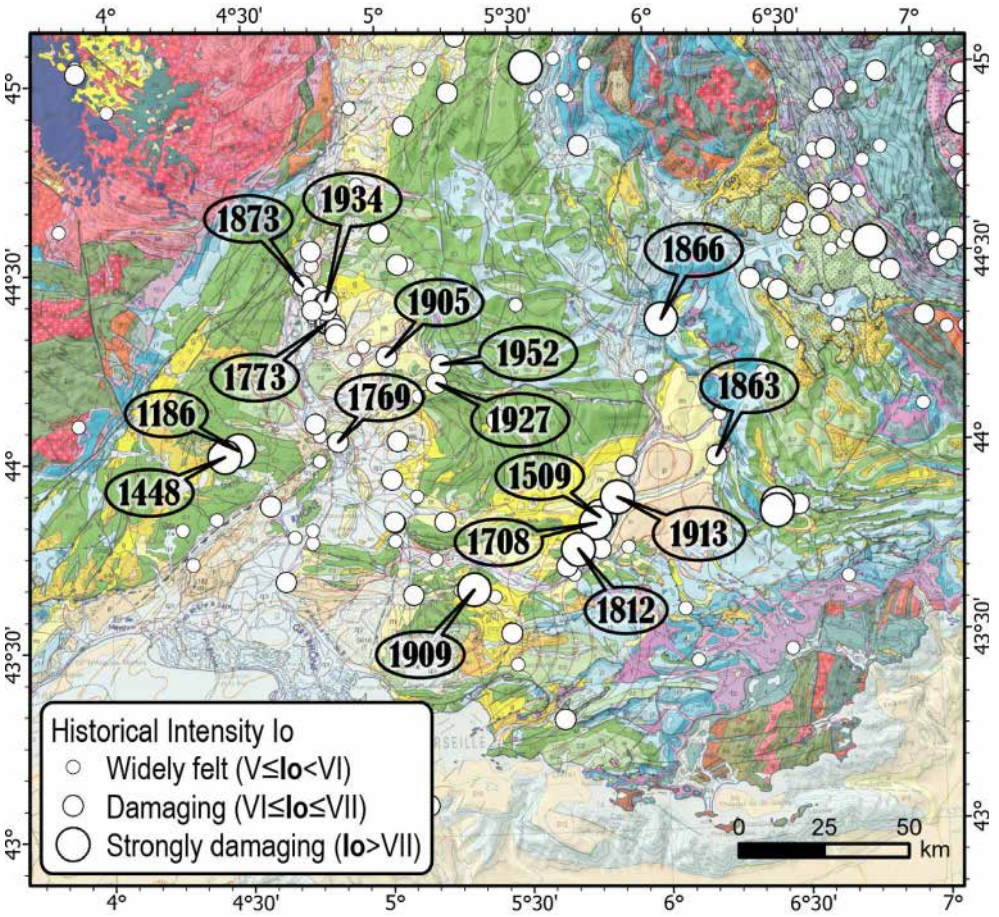

Figure 10. Historical seismicity map of the Southeast basin from *SISFRANCE*.

mechanism and with a focal depth of 4 and 1 km, respectively. Shallow microseismicity is also recorded along the Nîmes fault with normal and strike-slip focal mechanisms [no. 3 and no. 4, Baroux et al., 2001]. A cluster is located at the junction between the Nîmes fault and the Ventoux–Lure thrust fault. South of the Nîmes fault, two clusters are located in the Comtat plain, East of Avignon, and in the Alpilles chain (AC). Finally the Maures and Esterel crystalline massifs of eastern Provence are mostly aseismic but a seismic swarm occurred near St Paul-en-Forêt during February–September 2018 [Godano et al., 2019]: 81 earthquakes with $1 < M_L < 3.5$ and focal depths around 20 km were detected (SPS on Figure 9).

The most damagning historical event is the 1909 Provence earthquake near Lambesc (Io VIII–IX MSK—M_w 6.0). This event is the strongest in France during the 20th century (no. 5 on Figures 9, 10 and *SISFRANCE*). It occurred on the Trévaresse fault [Baroux et al., 2003, Chardon et al., 2005, Bellier et al., 2021]. Many other significant earthquakes (Io > VII) have been reported mainly in the active seismic areas highlighted by the instrumental seismicity and described above (Figure 10): along the Middle Durance Fault (see later), in the lower Rhône valley and close to the Nîmes fault. Although the seismic activity in the Rhône valley is low, several strongly damaging earthquakes have been reported: to the North, several swarms with tens of earthquakes occurred in 1773 (Clansaye, Io VII) and 1934 (Valaurie, Io VII) around the Tricastin area. Likewise, another swam near Châteauneuf-du-Rhone in 1873 (Io VII) may either be related to the aforementioned swarms or to a branch of the Cévennes fault [Jomard et al., 2017].

More to the South, several earthquakes are reported close to the Nîmes fault: in 1186 and 1448 (Uzes, Io VII–VIII) and 1769 (Bedarrides, Io VII). At the northeastern tip of Nîmes fault, at the junction with the Ventoux–Lure thrust fault, three earthquakes were felt in the 20th century: Vaison la Romaine in 1905 (Io VII), Malaucène in 1927 (Io VII) and Pierrelongue in 1952 (Io VII). Finally, two strongly damaging earthquakes occurred in 1863 (Beynes, Io VII) and 1866 (Laragne, Io VII–VIII) along the Southwestern Alps frontal thrust (Digne–Castellane Arc).

4.3. *The western Alpine belt*

The complex structure of the Alpine belt [e.g. Roure et al., 1990, Schmid and Kissling, 2000, Paul et al., 2001, Lardeaux et al., 2006, Thouvenot et al., 2007, Zhao et al., 2016, Solarino et al., 2018; Figure 11], displaying strong changes of crustal nature and thickness with many inherited structures, is the result of the convergence between the Adria and Europe plates which led to the subduction of the Tethys Ocean and, then, to the collision between continental blocks [e.g. Dercourt et al., 1986, Handy et al., 2010]. Crustal shortening started in the internal Western Alps around 50 Ma and continued in the external domain and Jura until 3 Ma. From 35 Ma, due to the WNW-directed movement and counterclockwise rotation of the Adria microplate, the deformation propagated north- and southwestward in a fan-shaped pattern up to the foreland Helvetic and SE basins (MFB and SEB in Figure 12, respectively) [e.g. Tricart, 1984, Ricou and Siddans, 1986, Vialon et al., 1989, Collombet et al., 2002, Bellahsen et al., 2012, Dumont et al., 2011]. During the collision, the shallow mantle body of Ivrea acted as a buttress and the shortening [roughly 100 km along the ECORS-CROP section, e.g. Schmid and Kissling, 2000] was mostly accommodated by wedging, involving the European lower crust.

The present-day orogenic wedge displays outcrops of Meso-Cenozoic sedimentary cover and crystalline basement units belonging to the European margin of the Tethys (external and internal crystalline massifs are remnants of the Variscan basement uplifted during the collision). The sedimentary cover and continental basement are imbricated with crustal oceanic units and the shallow exhumed Ivrea mantle body (~10 km depth). Two main structures underline the curvature of the Alpine arc: the Penninic frontal thrust that separates the external and internal domains of the Alps and the Insubric line that marks the limit between Adriatic and European lithospheres (PFT and IL on Figure 12).

The Alpine domain displays the largest catalog with 24,817 events between 1996 and 2019. The area benefits from a relatively good station coverage inducing well-constrained earthquake locations: about 55% of the events have a minimum epicentral distance less than 20 km, the primary and secondary azimuthal gaps are less than 180° for 81% and 63% of the events, respectively.

The seismicity of the Alpine chain concentrates around two main axes (Figure 11): on the one hand, the Briançonnais arc is parallel to the orogen trend and to the Penninic frontal thrust from the Valais area to the north of the Argentera Massif (V and A on Figure 12) and on the other hand the Piemont arc runs from the Gran Paradiso Massif (GP on Figure 12) to the north of the Argentera without any correspondence with geological structures identified at the surface. Except from these two seismic arcs, in most parts of the belt, epicenters are heterogeneously and diffusely distributed, with some rare alignments on known geological structures [e.g. the Belledonne Border fault (no. 4 on Figure 1, see later), the high Rhône valley between Sion and Martigny in Valais [no. 3 on Figure 1, Diehl et al., 2018], the Saorge–Taggia fault in Liguria [Turino et al., 2009]] and several large swarms (no. 6, 7, 8 on Figure 1). In the subalpine chains, the seismicity rate varies significantly between contiguous domains, such as the poorly seismic Castellane Arc and the highly seismic Nice Arc, for instance [Larroque et al., 2001]. Most of the crystalline massifs are also very poorly seismically active (e.g. Belledonne, Pelvoux, Gran Paradiso and Argentera; B, P, GP and A on Figure 12).

The concentration of seismicity in the Briançonnais arc is located along the zone of the highest relief and thickest crust. The focal mechanisms attest to extensional faulting more or less continuous along the arc (e.g. no. 4, 6, 7 on Figure 11). The direction of extension is roughly perpendicular to the orogen axis and is mainly interpreted as inversion of the Penninic frontal thrust [e.g. Maurer et al., 1997, Sue et al., 1999, Sue and Tricart, 2003, Bilau et al., 2021].

In the north- and southwestern subalpine chains, most of the focal mechanisms confirm that strike-slip

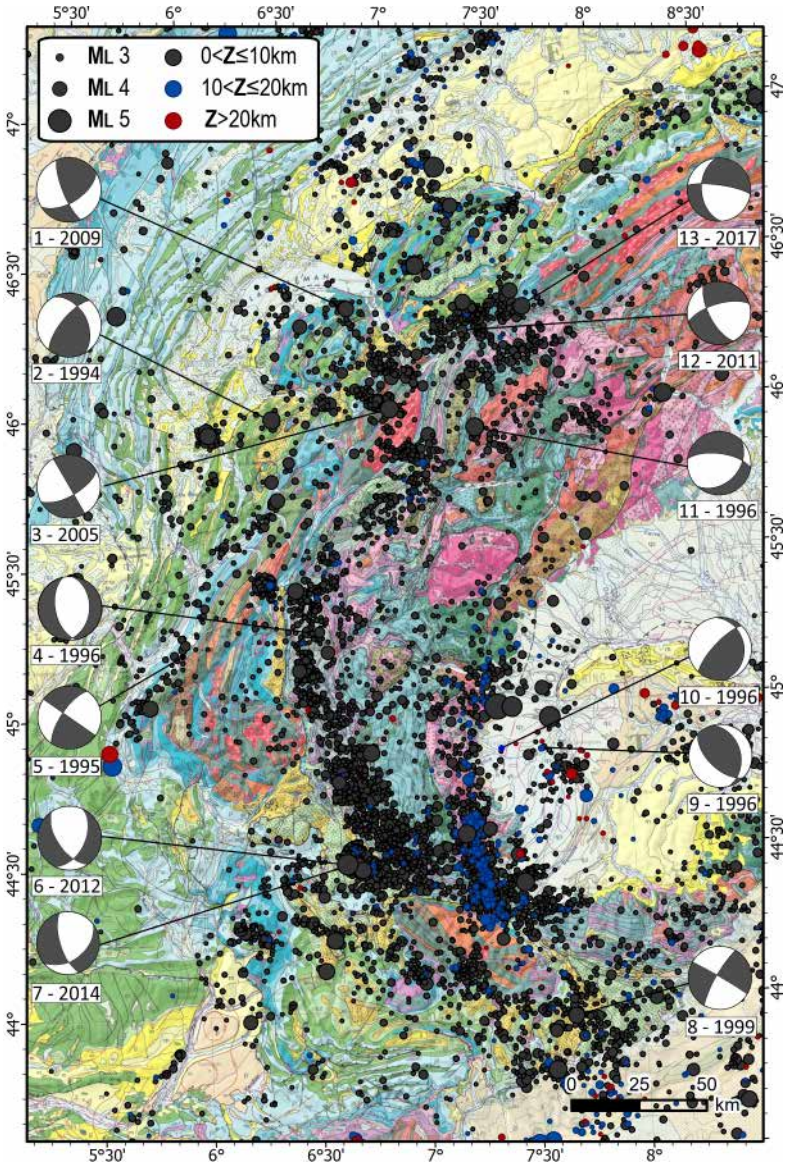

Figure 11. Seismicity overlaid on the geological map of the western Alpine belt, from the *CEA*_1996–2019 catalog ($M_L \geq 2$) and Chantraine et al. [2003]. Focal mechanisms: 1. Morzine earthquake [2009/10/21, M_L 3.5; Deichmann et al., 2012]; 2. Grand Bornand [1994/12/14, M_L 5.1; Fréchet et al., 1996]; 3. Vallorcine [2005/09/08, M_L 4.9; Fréchet et al., 2011]; 4. [1996/11/05, M_L 2.5; Béthoux et al., 2007]; 5. [1995/09/08, M_L 2.5; Thouvenot et al., 2003]; 6. Barcelonnette [2012/02/26, M_L 4.8; Delouis-Géoazur]; 7. Barcelonnette [2014/04/07, M_L 4.8; Delouis-Géoazur]; 8. Blausasc [1999/11/01, M_L 3.4; Courboulex et al., 2007]; 9. [1996/11/22, M_L 2.3, Béthoux et al., 2007]; 10. [1996/11/05, M_L 2.4, Béthoux et al., 2007]; 11. Valpelline [1996/31/03, M_L 4.6; Baer et al., 1999]; 12. [2011/01/08, M_L 3.5; Deichmann et al., 2012]; 13. [2017/06/02, M_L 3.3; Diehl et al., 2021].

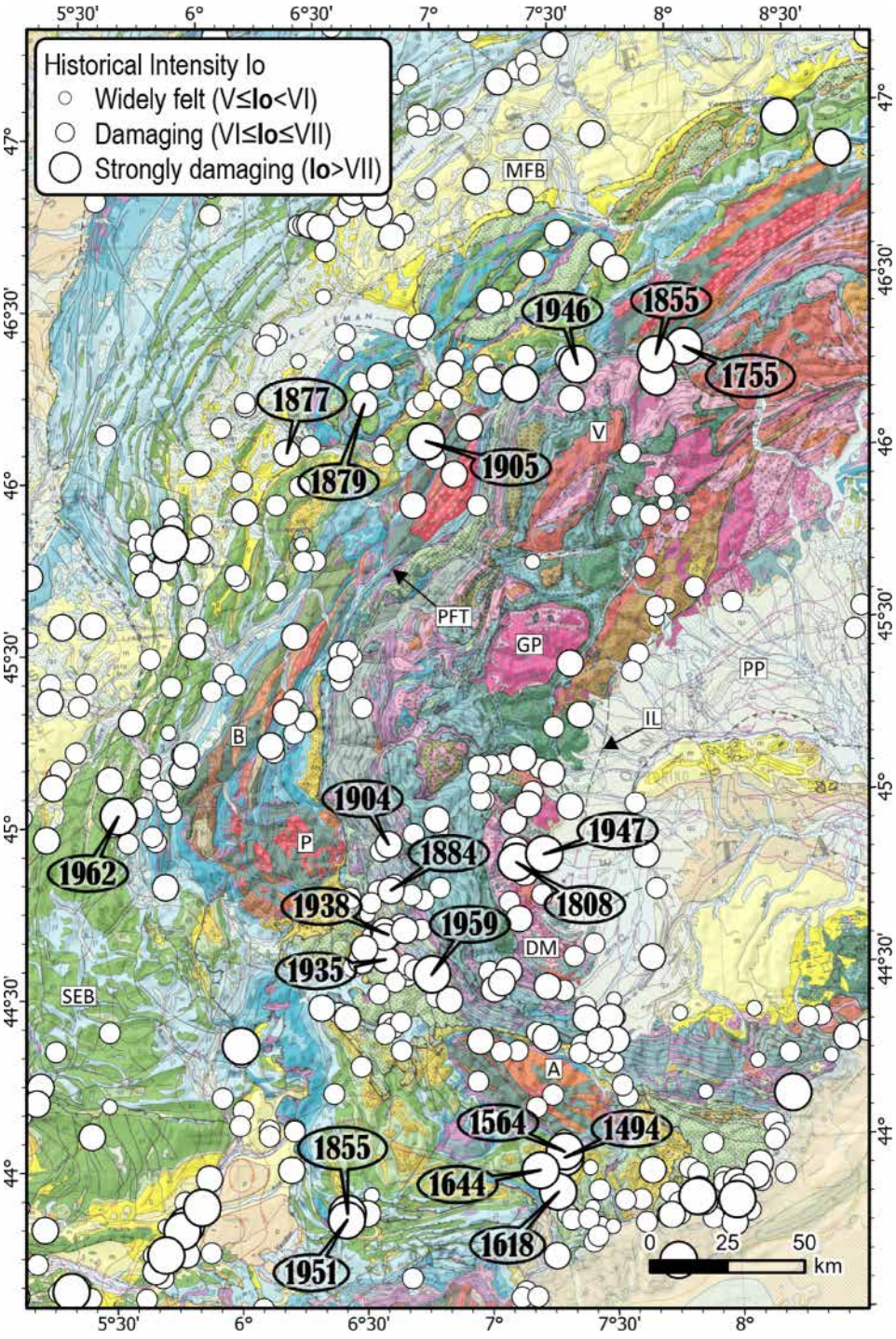

Figure 12. Historical seismicity map of the Western Alps from *SISFRANCE*.

faulting is dominant (e.g. no. 1, 2, 3, 5, 8 on Figure 11). In the southwestern Alps, between 44° N and 45° N, Béthoux et al. [2007] point out that the concentration of hypocenters at 25 km depth east of the Piemont arc is located at the boundary between the mantle wedge of the Ivrea body and the European crust along the southward extend of the Insubric line. Focal mechanisms there are mainly compressive (nos. 9 and 10 on Figure 11) which allow to postulate that this major geological structure is still tectonically active and also underline the sharp change of stress tensor orientation east of the Alpine belt [Eva et al., 1997, Béthoux et al., 2007].

The focal depths observed by the networks is mainly located in the upper crust (Figure B-S) and Deichmann et al. [2000] show that no significant lower crustal seismicity is observed in most of the Western Alps. Nevertheless, the focal depths are in the range of 8–10 km in the Briançonnais arc and 15–20 km in the Piemont arc, clearly indicating a deepening towards the east [Solarino et al., 1997]. This eastward deepening is confirmed by foci deeper than 50 km in the Po Plain [Cattaneo et al., 1999, Eva et al., 2020].

In historical times, several strongly damaging earthquakes have occurred throughout the internal and external part of the Western Alps (Figure 12 and *SISFRANCE*). The Valais earthquakes (near Brig: December 9, 1755, Io VIII–IX MSK; near Visp: July 25, 1855, Io IX; near Sierre: January 15, 1946, Io VIII) are the largest events recognized in the Western Alps in terms of damage. The 1946 event, for instance, triggered numerous landslides, rockfalls and ground cracks [Fritsche and Fäh, 2009], as well as the Rawilhorn rock avalanche that was provoked by the aftershock [Pedrazzini et al., 2016]. These earthquakes occurred nearby an area where current microseismicity shows a clear ENE–WSW alignment, covering ~30 km along the high Rhône valley (Figure 11). No surface faults have been identified yet as potential sources of those Valais events despite some indications of post-glacial activity for the Gemmi Pass Fault, in the epicentral area of the 1946 earthquake [Ustaszewski and Pfiffner, 2008].

Since the 19th century, four earthquakes (November 27, 1884; July 12, 1904; March 19, 1935, July 18, 1938; Figure 12) with Io VII have struck the Queyras-Ubaye area (southern Briançonnais arc). On April 5, 1959 the largest earthquake felt in this area (Io VII–VIII, M_L 5.3) occurred near Saint-Paul-sur-Ubaye [Baques et al., 2021]. This event is located very close to the 2003–2004 Ubaye swarm [Jenatton et al., 2007] and to the 2012/02/26 (M_L 4.8) and 2014/04/07 (M_L 4.8) earthquakes (nos. 6 and 7 on Figure 11, respectively). One can notice that the 1959 event displays a similar focal mechanism [Ménard, 1988] than the 2012 and 2014 earthquakes with dominant normal faulting [Thouvenot et al., 2016]. In the most internal Alps, two large events struck the junction between the Dora Maira massif and the Po plain (DM and PP on Figure 12), on April 2, 1808 (Io VIII) and February 17, 1947 (Io VII–VIII).

In the southern external domain of the Alps, the most significant historical earthquakes correspond to the four events of intensity VIII that occurred in the Vésubie valley (Figure 12): June 23, 1494; July 20, 1564; January 18, 1618 and February 15, 1644. The 1564 "Nissard" earthquake [Vogt, 1992] was the most destructive: two quakes in July 20, 1564 and aftershocks during ~50 days caused the ruin of several villages and at least a hundred deaths. It was felt more than 100 km from the epicentral zone. This sequence of large earthquakes is supposed to be related to the Vésubie fault, a poorly known geological structure [Larroque et al., 2001]. The Castellane arc has been damaged twice, on December 12, 1855 (Io VIII) and on November 30, 1951 (Io VII–VIII) near Chasteuil, while this southern subalpine chain is mainly aseismic during the instrumental period. Bollinger et al. [2010] propose a very shallow source (~1 km) for these two earthquakes.

Finally, in the northern external domain, following the October 8, 1877 (in Faucigny) and December 30, 1879 earthquakes (in Chablais), the Chamonix valley was struck on April 29, 1905 by an Io VII–VIII earthquake, causing strong damage, and was followed by a long series of aftershocks, culminating with the earthquake of August 13, 1905 (Io VII, Figure 12). Based on geological observations, seismological recordings and modeling results, Cara et al. [2017] proposed that the N20° E normal Remuaz fault could be the source of the mainshock (M_w ~ 5.3) at a depth of ~5 km, whereas Manchuel et al. [2017] estimated a deeper hypocentral depth of ~11 km based on macroseismic data. One can notice that in the same area, the shallow M_w 4.5 Vallorcine earthquake (2005/09/08, no. 3 on Figure 11) activated a right-lateral and ENE-striking ~2 km long fault, as shown

by the aftershock sequence [Fréchet et al., 2011]. A sequence of nine earthquakes occurred in the Vercors massif south of Grenoble, between April 12 and July 15, 1962, culminating with the Io VII–VIII event on the April 25 (Figure 12), while this subalpine massif was a low-level seismic area since at least the past five centuries [Grasso et al., 1992].

4.4. *The Ligurian Sea and Corsica*

The Ligurian Sea is at the southern termination of the Alps (Figure 13). It is composed of (1) a northern extensional margin from the Gulf of Lion to Genoa with a continental crust that thins from 29 km to 18 km in a few tens of kilometers seaward; (2) a central part at 2,500 m below sea level with transitional and oceanic crust of atypical reduced thickness (∼4 km) and (3) the southeastern margin of Corsica–Sardinia with a continental crust that thickens up to 30 km below Corsica [Chamoot-Rooke et al., 1999, Rollet et al., 2002]. The Ligurian Sea is considered to be a back-arc basin that opened between 34 and 21 Ma together with the counter-clockwise rotation of the Corsica–Sardinia block [Réhault et al., 1984, Gattacceca et al., 2007, Jolivet et al., 2008]. Several faults are inherited from this rifting episode and mainly evidenced on the northern margin, thus NE–SW normal faults dipping to the south and NW–SE transverse vertical faults bound few tilted blocks [Rollet et al., 2002]. At the foot of the northern margin, a large system of northward dipping reverse faults, the Ligurian faults system (LFS on Figure 13), extends roughly over 80 km between Nice and Savona [Larroque et al., 2011].

The island of Corsica is divided into two geological domains: to the northeast, the "Alpine Corsica" (AC on Figure 13) is made of different nappes of HP-LT metamorphic ophiolites ("schistes lustrés" nappes) thrusted during the Alpine orogeny upon the European margin which corresponds now to the southern domain of Corsica [e.g. Malavieille et al., 1998]. This southern domain, the so-called "Hercynian Corsica" (HC on Figure 13), is made of continental Paleozoic crystalline rocks [Durand-Delga, 1984]. No active fault has been described in Corsica and the main inherited faults are N–S in the Alpine part and NE–SW in the Hercynian part [Chantraine et al., 2003].

The strong crustal heterogeneities and the lack of seismometers in the marine area make difficult the detection and particularly the determination of focal depths of earthquakes [Béthoux et al., 2016]. The area counts 1533 events. Compared with the other areas studied here, the earthquake locations are less constrained. This is most likely due to a sparser station coverage. Only 39% of the events have a primary azimuthal gap less than 180°, and more than 50% of the events have a minimum epicentral distance larger than 50 km. Nevertheless, dense microseismicity and numerous moderate earthquakes are regularly recorded and attest to a continuity of the deformation processes from the continent to the marine area. Some of them were widely felt by the population, such as the offshore Nice event (1989/12/26, M_w 4.2; 1995/04/21, M_w 4.5 and 2001/02/25, M_w 4.6; no. 3, 1 and 2 on Figure 1, respectively and Table B-S), the earthquake close to the center of the basin (1963/07/19, M_w 6.0; no. 4 on Figure 13) and the one offshore of Ajaccio (2011/07/07, M_L 5.3 – M_w 4.9; no. 5 on Figure 13).

The seismicity distribution is heterogeneous in the Ligurian Sea. The focal depths are mainly in the range of 3–15 km with few events down to 20 km (Figure B-S). In the northern domain, most of the epicenters gather at the foot of the margin, aligned N50–60E. Several moderate magnitude reverse faulting earthquakes are related to active faults evidenced by marine geophysical survey [Larroque et al., 2011]. The 1989/12/26 and the 2001/02/25 events activated a western segment of the Ligurian faults system (Figure 13). Two NNW–SSE linear trends subperpendicular to the margin could correspond to faults mapped by Chaumillon et al. [1994] and Augliera et al. [1994]. A cluster develops further offshore in the area of the 1963 earthquake, at the boundary with the oceanic basin, unrelated to known faults.

In the basin, the seismicity is sparse and decrease to the west and to the south. The magnitudes are mainly less than 3 and the focal depths are determined with a large uncertainty. However, several studies pointed out focal depths as deep as 20 km in the center of the basin [Béthoux et al., 2008] and maybe even more deep [Scafidi et al., 2015]. In this area of 4 km thin crust, some events would therefore be located below the Moho interface. In 2011–2013, an unusual seismic activity occurred in the southern part of the basin, 80 km offshore of Ajaccio [Larroque et al., 2016]. The regional networks recorded a sequence of five moderate earthquakes (M_L 3.8–5.3; the major one is no. 5 on Figure 13) with several tens

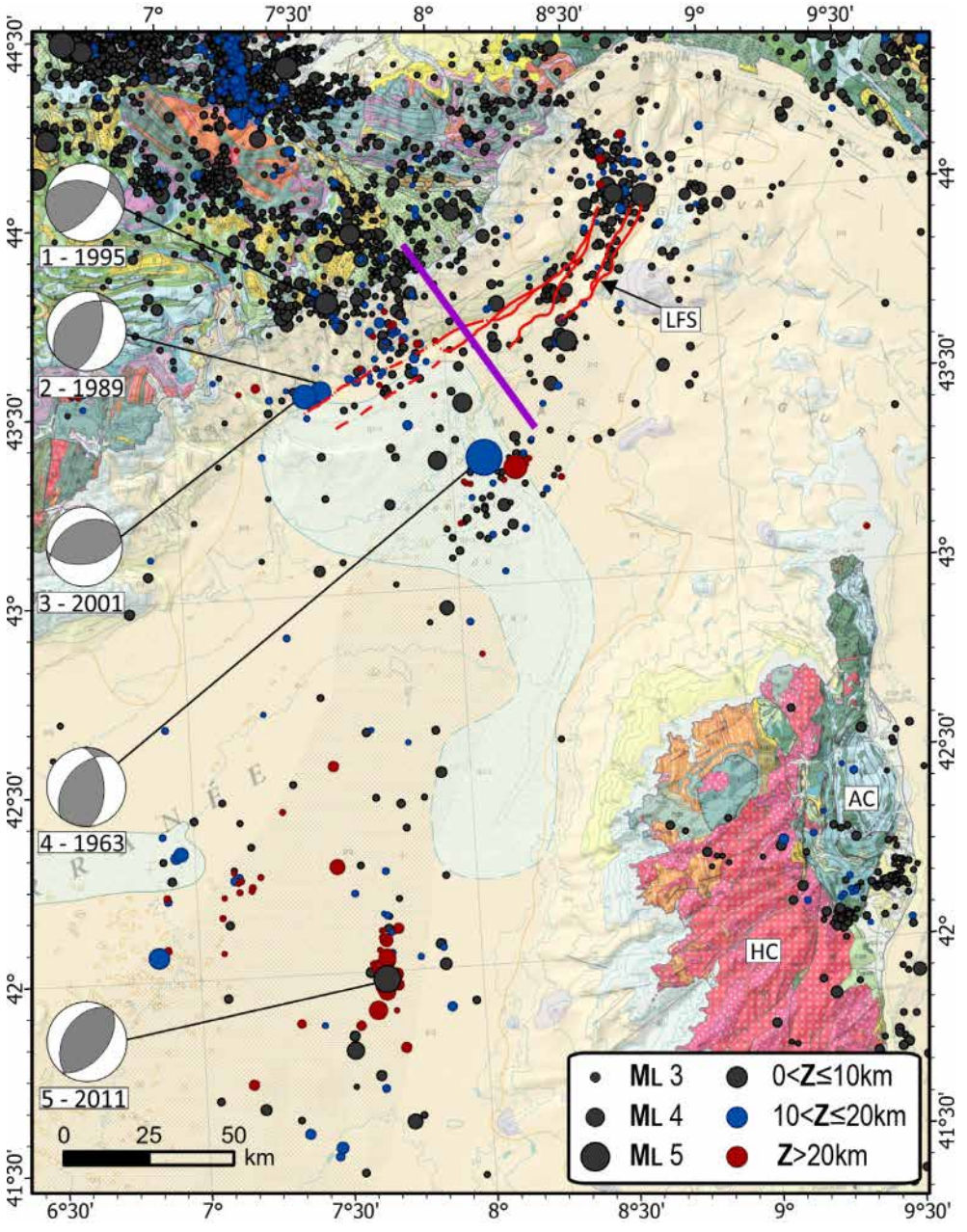

Figure 13. Seismicity overlaid on the geological map of the Ligurian Sea and Corsica, from the CEA_1996–2019 catalog ($M_L \geq 2$) and Chantraine et al. [2003], red lines: the Ligurian faults system from Larroque et al. [2011]. Focal mechanisms: 1. Vintimille earthquake [1995/04/21, M_w 4.5; Courboulex et al., 1998], 2. [1989/12/26, M_w 4.2; Béthoux et al., 1992], 3. [2001/02/25, M_w 4.6; Courboulex et al., 2007], 4. [1963/07/19, M_w 6.0; Bossolasco et al., 1972], 5. [2011/07/07, M_w 4.9; Larroque et al., 2016]. The purple line corresponds to the cross section on Figure 21.

of aftershocks in a low seismicity zone. The estimation of the focal depths is different, according to the methods used and varies from 26 km (Letort et al., 2014 and *CEA* catalog) to a range of 6–13 km [Larroque et al., 2016]. Therefore, the faulting occurred along an unknown fault, in the atypical oceanic crust or in the topmost mantle.

In contrast, the southern Ligurian margin (offshore of western Corsica) is mainly aseismic and the microseismicity is also sparse in Corsica [Ferrandini et al., 1994, Béthoux et al., 2008]. Only two seismic crises occurred in the eastern part of the island, at the limit between the metamorphic units of Alpine Corsica and the eastern coastal plain filled by Cenozoic sedimentary deposits. On the one hand, in 1978–1979 more than 150 earthquakes of low magnitude and low focal depths (~5 km) were recorded [Marillier et al., 1982]. The largest instrumental earthquake known in Corsica, M_L 4.3, occurred during this crisis, on 1978/04/03. On the other hand, in 2012 several tens of earthquakes occurred, more or less aligned with the NE–SW Saint Antoine fault which bounds to the south the eastern coastal plain from the Schistes Lustrés nappe [Caron and Loye-Pilot, 1990].

Most of the focal mechanisms determined in the Ligurian domain are compressive with a P-axis oriented in the NW–SE quadrant (Figure 13). Several of these earthquakes (1989, 2001, for instance) are related to known faults, such as the Ligurian faults system. The active faults during the 1963 M_w 6.0 and the 2011 M_w 4.9 are not evidenced yet. In any case, the deformations in the Ligurian domain are consistent with the ~0.4 mm/yr of shortening between the Corsica–Sardinia continental block and mainland Europe attested by geodetic measurements [Billi et al., 2011, Nocquet, 2012, Masson et al., 2019].

Over the entire Ligurian domain, the seismogenic depth is estimated in the range 5–20 km [Eva et al., 2001, Béthoux et al., 2008] but the *CEA*_1996–2019 catalog and Scafidi et al. [2015] suggest that this depth could be deeper (Figure B-S). In any case, the focal depth distribution below the margins and the basin shows no particular spatial organization.

Discussing the occurrence of historical seismicity in the Ligurian Sea is problematic because macroseismic observation points are rarer as we go back in time. Essentially, the offshore location of the main events may only be established with relatively good confidence starting from the 19th century [Jomard et al., 2021]. Several strongly damaging earthquakes were reported with an epicenter close to the northern Ligurian coast (Figure 14): on May 26, 1831 (Io VIII MSK) and on December 29, 1854 (Io VII–VIII). The strongest event recorded in SE France and neighboring regions over the last 1000 years occurred on February 23, 1887 (Io IX). The so-called "Ligurian earthquake" was felt across a vast area that covered Switzerland and Austria to the north, and reached as far as the eastern Pyrenees to the west and northern Sardinia to the south [Taramelli and Mercalli, 1888, Ferrari, 1991]. At least 600 people died and almost 200 villages suffered great destruction along 100 km of coastline and 20 km inland. In the following year, approximately 200 aftershocks were identified. The macroseismic epicenter is located 30 km off the Ligurian coast and this earthquake produced the only known significant tsunami in the region [Lambert and Terrier, 2011]. The reassessment of the Ligurian earthquake resulted in a magnitude of M_w 6.7–6.9 [Ioualalen et al., 2014, Manchuel et al., 2017]. Larroque et al. [2012] proposed that it corresponds to reverse faulting along the north-dipping Ligurian faults system and thus testifies to the active inversion of the northern margin as the 1989 and 2001 earthquakes (Figure 13, see later).

Four other events have occurred off the northern Ligurian coast: September 5, 1807 (Io VI), February 23, 1818 (Io VII), January 8, 1819 (Io VI), October 16, 1896 (Io VII) and with the events of 1831, 1854 and 1887 this makes seven strong earthquakes in less than 100 years over an area of about 50 km close to the Ligurian faults system. In Corsica, only one strongly damaging event is reported on October 22, 1775 (Io VII), 25 km north of Ajaccio, however poorly characterized.

5. Discussion

The Cenozoic evolution of southeast France and neighboring areas has led to the development of a complex fault networks in the upper crust [e.g. Chantraine et al., 2003]. Several previous works underline the diffuse distribution of seismicity in this region [e.g. Béthoux et al., 1998]. The current very low deformation rate in such an intraplate region makes the relationships between earthquakes and active faults unclear [Camelbeeck et al., 2007, Masson et al., 2019] and often gives rise to discussions among

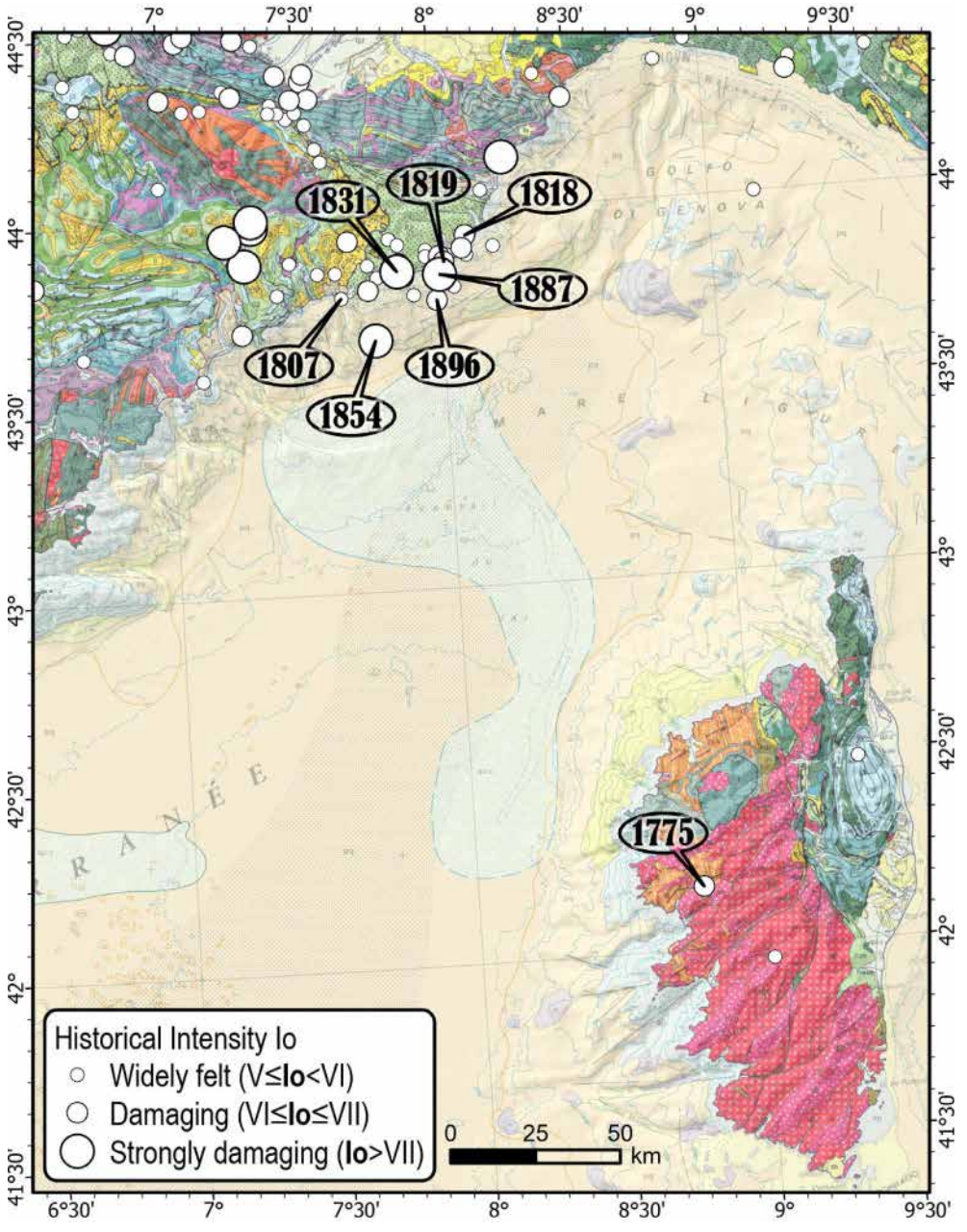

Figure 14. Historical seismicity map of the Liguria Sea and Corsica from *SISFRANCE*.

scientists [e.g. Cévennes faults system: Lacassin et al., 1998, Ambert et al., 1998, Sébrier et al., 1998; Basel-1356 earthquake: Meyer et al., 1994, Meghraoui et al., 2000, Ferry et al., 2005; Nîmes fault: Schlupp et al., 2001, 2002, Mattauer, 2002, Séranne, 2002; Argentera fault system: Larroque et al., 2009, Sanchez et al., 2010]. This leads to the situation that most of the earthquakes occurring in SE France are "from unidentified faults".

The temporal observation window is also an issue. The faults highlighted by instrumental and historical seismicity are undoubtedly active but not all the active faults are necessarily seismic at this time scale. This leads to several paradoxical situations, for

instance: (i) the Nîmes fault and the Salon–Cavaillon fault, in the Southeast basin, are documented to be active from geological and geomorphic data without seismic activity being clearly observed [Carbon et al., 1993, Schlupp et al., 2001, Molliex et al., 2011; NF and NCF on Figure 9], (ii) the Belledonne Border fault is seismically active although no active fault has been mapped at the surface (Thouvenot et al., 2003, Billant et al., 2015; no. 4 on Figure 1, see later), (iii) the La Rouvière fault (LRF on Figure 20) produced the last major earthquake of the area (M_w 4.9, 2019/11/11, no. 1 on Figure 9) while this fault has not been recognized as potentially active from geological and seismological data [Jomard et al., 2017, Ritz et al., 2020], (iv) strong earthquakes (Basel-1356, Liguria-1887, Provence-1909; Figure 5) have occurred along poorly characterized faults [Meyer et al., 1994, Meghraoui et al., 2000, Chardon et al., 2005, Larroque et al., 2012, Bellier et al., 2021], such as those existing throughout SE France and (v) several areas, such as Belledonne, Pelvoux and Argentera crystalline massifs (B, P and A on Figure 12) and the Diois–Barronnies area (DB on Figure 12) are mainly aseismic while they are crossed by as many faults as the neighboring seismic regions (Figure 11).

In the following sections, we discuss: (i) from specific examples, how the improvement of seismological instrumentation and the field geological knowledge have allowed the identification of the relationships between some earthquakes and active faults (Blausasc, Belledonne, Vuache and Middle Durance faults), (ii) the concentration of shallow focal depth in the Rhône–Tricastin area and lastly (iii) the diversity of seismogenic processes in SE France.

5.1. *Active faulting highlighted by microseismicity*

The distribution of microseismicity is often considered as diffuse and therefore difficult to relate to active structures and their seismogenic potential. However, microseismicity can be considered as a consistent proxy to understand the large-scale deformation pattern and mode. It develops in the active zones of the upper crust and a fine analysis of the locations and focal mechanisms help in retrieving a relevant representation of tectonic deformation at the regional scale [e.g. Amelung and King, 1997]. The densification of the permanent networks and the deployment of temporary networks help a lot in clarifying the spatial relationship between microearthquakes and the identified faults, thus several remarkable results have been obtained in recent years. We present some of these in this last section.

5.1.1. *The Belledonne Border fault zone (BBF)*

From 1989, the seismic monitoring by the *SISmalp* network makes it possible to specify the seismicity on the alpine domain and to identify several active geological structures. For instance, from more than 10 years of recording (1989–2000), Thouvenot et al. [2003] precisely located 163 microearthquakes (magnitudes between 0 and 3.5) aligned ~50 km along a N30° E direction on the western flank of the Belledonne crystalline massif (Figure 1). In the external zone of the western Alps, the Belledonne Border seismic alignment (BBF, Figure 15A) is located east of the Grésivaudan valley which separates the uplifted Variscan basement (crystalline massif of Belledonne) from the northwestward thrusted Mesozoic sedimentary cover of the subalpine chains (Bauges, Chartreuse and Vercors massifs). The focal depths are in the range of 5–10 km and 10–15 km along the southern and northern half of the alignment respectively, which attests to earthquakes in the crystalline basement. Along most of its length, the narrowness of the seismic alignment suggests a nearly vertical structure. Most of the focal mechanisms determined are consistent with right-lateral strike-slip faulting along N36° E ± 9° vertical fault planes. Later on, Mathey [2020] provides an update of the *SISmalp* catalog which confirms the seismic alignment and suggests its prolongation northward, beneath the Isère valley.

In the southern part of the seismic alignment, the epicenters gather under the so-called "border hills" (Figure 15B). There, some deformations, such as folds and N50–60° E right-lateral strike-slip faults are related to the Belledonne Middle fault, a 50 km long, at the least, Variscan extension fault zone that trends N50–60° E and dips steeply to the east [BMF, Figure 15B; Barféty and Gidon, 1996]. However, there is no evidence that these deformations are recent and may be related to deep crustal faults. To the north, the seismic alignment loses the spatial relationship with the BMF. In any case, the seismic lineation cannot be explained without postulating a fault zone at depth, buried beneath the sedimentary cover and

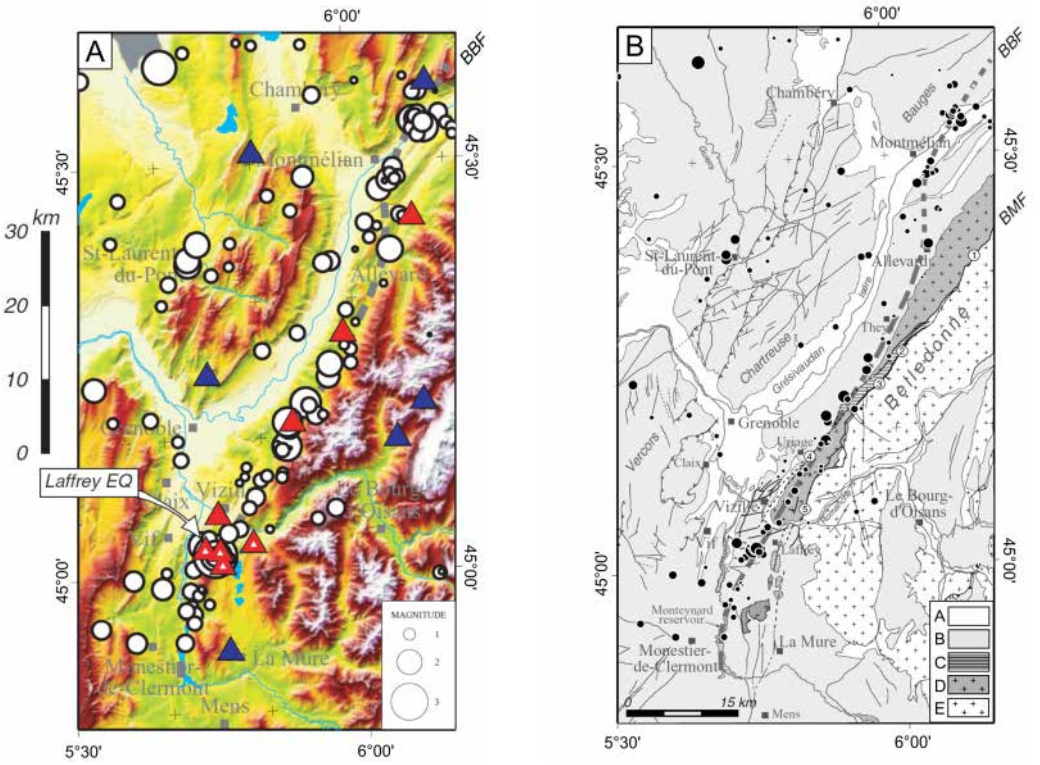

Figure 15. (Modified from Thouvenot et al., 2003): (A) Instrumental seismicity of the Grenoble and western zone of Belledonne for the period 1989–2000 [Thouvenot et al., 2003]. White circles (epicenters); gray dotted lines (approximate trace of the Belledonne border fault, BBF); blue triangles (permanent stations of the Sismalp network); red triangles (stations of the "Belledonne Border Fault" microseismicity campaign, 1998/12–1999/05). The epicenter of the strongest event recorded: the Laffrey earthquake (11/01/1999; M_w = 3.5) is indicated, with the post-seismic recording stations (red dotted triangles). (B) Geological sketch with 1989–2000 epicenters (black dots). A. Quaternary deposits; B. Mesozoic and Cenozoic sedimentary rocks; C. Paleozoic sedimentary rocks; D. and E. Paleozoic crystalline basement. 1 to 5, segments of the Belledonne Middle fault (BMF).

recent sediments, more or less parallel to but different from the BMF. Currently no active fault has yet been identified at the surface in this zone where the topography was largely smoothed by the Isère glacier during the last glacial maximum [Billant et al., 2015].

5.1.2. *The hidden Blausasc fault*

On 1st November 1999 a small earthquake (M_w 3.4) occurred 15 km north of Nice, near the village of Peille (no. 8 on Figure 11). This earthquake was set in the "Arc de Nice" fold-and-thrust belt (southwestern Alps) which corresponds to the deformation of the Mesozoic to Palaeogene sediments above a basal décollement zone in the upper Triassic evaporites [Courboulex et al., 2007]. This earthquake was well recorded by several stations of the permanent networks, located between 6 and 50 km away from the epicenter [Courboulex et al., 2001]. The seismological data allowed to locate the epicenter with an uncertainty of ±1.5 km in latitude and 3 km in longitude. The focal depth was computed at 3 ± 1.5 km and a left-lateral focal mechanism was determined. Courboulex et al. [2001] then proposed that the rupture corresponds to a 600 m long segment belonging to the left-lateral Peille–Laghet fault mapped at the surface.

Following this earthquake, a temporary network of 20 stations were installed in the epicentral area from

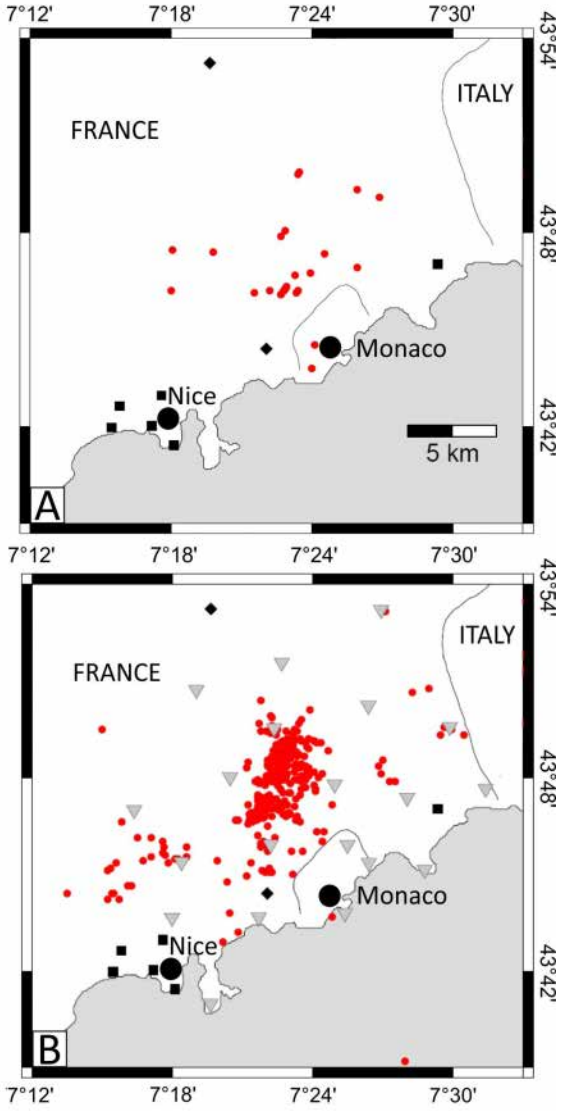

Figure 16. (Modified from Courboulex et al., 2007): The Blausasc swarm. (A) Earthquakes detected during November–December 2000 by the permanent networks (black squares: RAP and black diamonds: ReNaSS). (B) Earthquakes detected during the same period by the permanent and the temporary networks (gray triangles).

October 2000 to April 2001 and a seismic swarm was recorded there during November–December 2000. The results were obtained because the temporary network completely changed the understanding of local active tectonics and seismicity, from what was previously inferred based on the permanent network data alone (Figure 16).

About 350 earthquakes were recorded over a small area of 8 km × 4 km with M_L between 3.2 and 0.1 [Courboulex et al., 2003]. For each of these events, the distance to the closest stations was always smaller than 2.5 km. This allowed to reduce the average uncertainty on the absolute location errors to 1.2 km. A relative relocation based on cross correlation of waveforms enabled also to precisely describe the complexity of the activated structures [Courboulex et al., 2007]. All focal depths were shallower than 3 km and were mainly in the sedimentary cover with also a significant part in the Paleozoic basement.

The major result was the 3D geometry of the swarm: epicenters appeared to be aligned on an 8 km long structure oriented N20° and on a 70° W dip plan (Figure 17). At the surface the alignment of epicenters is superimposed on the Paillon valley. This result highlighted the existence of an active fault plane at depth in the basement, parallel to but 2 km west of the Peille–Laghet fault at the surface. Courboulex et al. [2003, 2007] propose that in the late Miocene times, the Peille–Laghet fault was decoupled from the basement during the SSE thrusting of the sedimentary cover. Therefore, the shallow Peille–Laghet fault being now unrooted from the basement and below the Paillon valley, the seismicity propagates inside the sedimentary cover delineating a new fault (Blausasc fault) which does not reach the surface yet. This example shows a possible mismatch between seismicity and known surface faults in fold-and-thrust belt areas.

5.2. *The Vuache active fault highlighted by the moderate Epagny earthquake*

Although the Epagny earthquake (1996/07/15, no. 4 on Figure 7) did not produce an extensive surface rupture, it is, along with the Le Teil earthquake [Ritz et al., 2020], the only one to have caused noticeable damage and is clearly attributed to an identified fault with surface imprints in metropolitan France [Baize et al., 2011]. Numerous testimonies allowed to define more than 700 intensity data points (*SISFRANCE*).

The mainshock (M_L 5.3) hit the area after a small foreshock (M_L 2, depth ~ 3–4 km) located exactly in the 1996 epicentral zone [Mathey, 2020]. One can

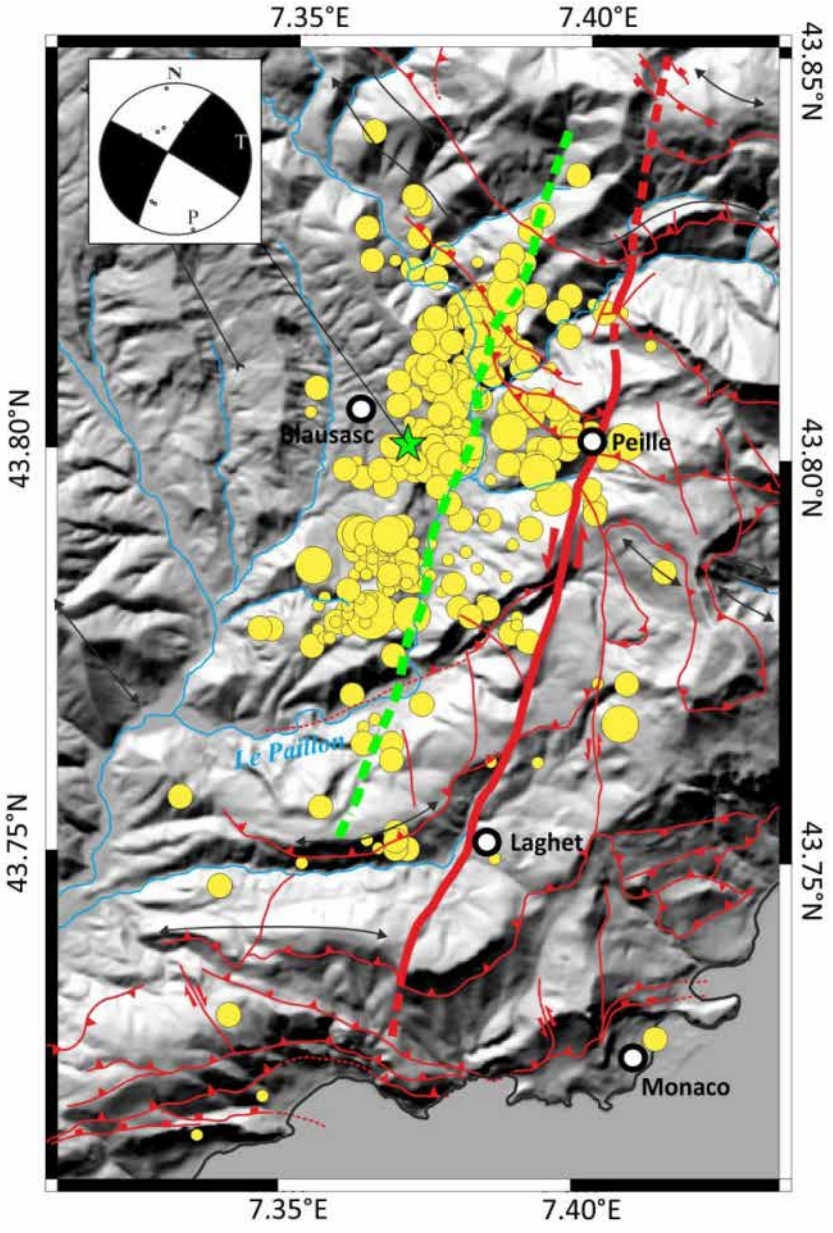

Figure 17. Seismicity and structural map of the Blausasc area. Yellow circles: epicenters of the Blausasc swarm (November–December 2000). Green star: epicenter of the Peille earthquake (1999/11/01) and focal mechanism. The left-lateral Peille–Laghet unrooted fault corresponds to the bold red line and the Blausasc hidden fault to the green dotted line.

notice that a few months before, Le Grand-Bornand earthquake (1994/12/14; M_L 5.1) shook the same area, 25 km away from the 1996 epicenter (Figure 7). The Epagny earthquake was immediately and precisely studied using instrumental [Thouvenot et al., 1998, Courboulex et al., 1999, Dufumier, 2002] and macroseismic data [Scotti et al., 1999]. Seismological data, in particular from the post-seismic network,

allowed defining two 3 km-long subparallel active segments, separated by a ~500 m-wide right stepover (Figure 18). The segment to the north includes the hypocenter of the main shock at its southern end, and the segment to the south includes the foreshock at its northern end. Courboulex et al. [1999] describe the earthquake as a series of at least two subevents, with a rupture propagating towards the SE and potentially mobilizing these two segments. The focal mechanism suggests the left-lateral activation of the nodal plane oriented ~N135° E and dipping 70° toward the NE [Figure 7, Thouvenot et al., 1998].

There were more than 800 aftershocks detected, with the strongest one, M_L 4.2, on July 23 and six with M_L greater than 2 until August 1996 and finally one with M_L 1.7 in 1997. The good accuracy of the focal depths of 400 aftershocks places the main rupture area above 3.5 km, in the brittle sedimentary layers (Jurassic and Cretaceous limestones, Figure 11). The southern segment revealed by the aftershocks and the NW–SE nodal plane of the focal mechanism aligns remarkably with the presumed geological trace of the left-lateral Vuache fault at surface. The Vuache fault is undoubtedly an active fault with long recurrence times for surface rupture event: coseismic cracks were mapped in the airport area after the 1996 earthquake [Thouvenot et al., 1998] but paleoseismological investigations failed to provide evidence for past ruptures in the Holocene sediments from several trenches [Baize et al., 2011, Bellier et al., 2021].

Historically, the area near the Vuache fault had experienced several damaging events (Figure 8): the Frangy earthquake in April 17, 1936 (Io VII MSK) and during the summer of 1839, the town of Annecy underwent a seismic sequence from August 7 to 27, culminating on August 11 (Io VII).

The Vuache fault is a major structure oriented NW–SE, connecting the front of the Western Alps to the Jura massif through the Molasse basin (Figure 7). It is considered as a left-lateral ramp that allowed the transfer of shortening to the Jura Mountains since the Miocene [Donzeau et al., 1998, Baize et al., 2011]. The Vuache fault is nearly 35 km long, with several segments and bends, and gaps or stepovers smaller than 2 km. A major concern remains to determine whether the Vuache fault is a thin-skin structure as proposed by Thouvenot et al. [1998] or whether this fault might have a root deep in the crystalline basement, as proposed based on the analysis of seismic reflection profiles [Baize et al., 2011, De la Taille, 2015].

5.3. *The Middle Durance Fault (MDF) and its seismogenic potential*

The Middle Durance Fault (MDF) forms a system about 70 km long, striking NNE–SSW and consisting of several fault segments marked with geomorphological evidences as well as instrumental and historical seismicity [Figures 9 and 10; Cushing et al., 2008, Le Pichon et al., 2010, Cushing et al., 2014, Guyonnet-Benaize et al., 2015, Bellier et al., 2021]. This major fault (Figure 19) separates, to the west, the "Provençal Panel" (a morphologically rugged zone characterized by a 6–10 km thick folded Meso-Cenozoic sedimentary cover overlying a very thick evaporite Triassic layer) from a less mountainous domain to the east, the Valensole plateau (characterized by a thin sedimentary cover −1 to 2 km—with very thin or absent Triassic evaporites). Together with its prolongation towards the south (the Aix fault), they are considered as a transfer fault with a left lateral-reverse component (western block uplifted; Cushing et al., 2008). This transfer fault connects the Alpine front to the E–W thrusts system of the western Provençal belt [Trévaresse, Aix-Eguille and La Fare thrusts; Terrier et al., 2008].

During the instrumental period, the MDF produced a continuous microseismicity but no earthquake of magnitude greater than 4 (Figure 9). During the historical period however, several strongly damaging events occurred close to the MDF (Figure 10): in 1509 and 1708 (Manosque, Io VIII MSK), 1812 (Beaumont-de-Perthuis, Io VII–VIII MSK) and 1913 (Volx, Io VII–VIII MSK). The Manosque earthquake of August 14, 1708 is well documented and is part of a sequence of earthquakes lasting several months [Quenet et al., 2004]. A significant earthquake may also have occurred in the MDF region in 1601 [Cushing et al., 2014]. Therefore, during historical times the MDF produced strongly damaging earthquakes with a quasi-centennial recurrence.

The current left-lateral slip of the MDF is clearly demonstrated by the analysis of the focal mechanisms determined from the microseismicity recorded by a dense network installed between 1999 and 2006 [Volant et al., 2000 and no. 6 on Figure 9].

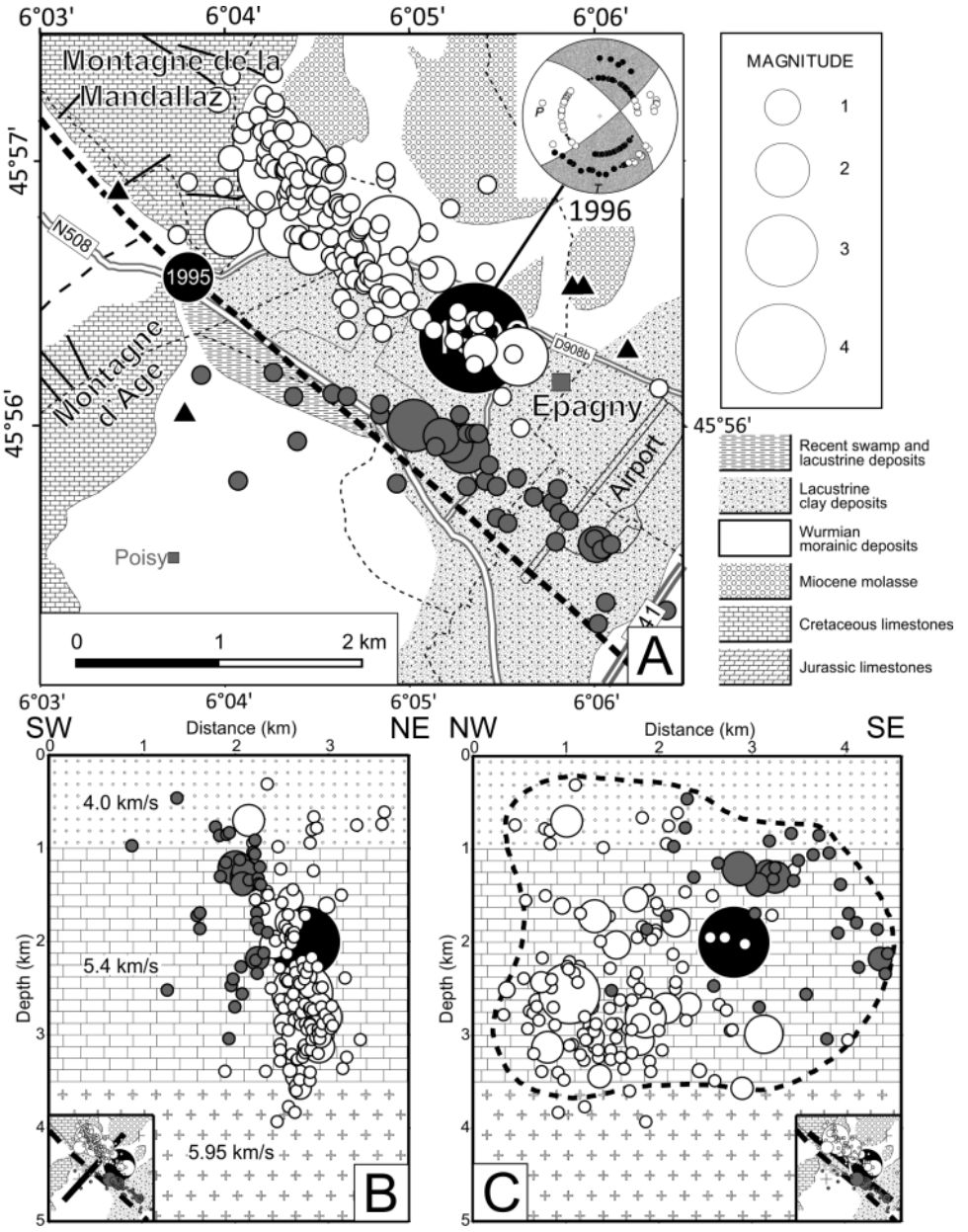

Figure 18. Image of the Vuache active fault plane [modified from Thouvenot et al., 1998]. (A) Aftershock map of the 1996 Epagny earthquake (main shock: big black circle and its focal mechanism), open and shaded circles highlight the northern and southern segments respectively. The dashed line corresponds to the trace of the Vuache fault and the black triangles to the temporary seismologic stations. (B), (C) Two perpendicular cross sections in the aftershocks zone. The dashed line on (C) is the inferred extension of the rupture area (~10 km^2).

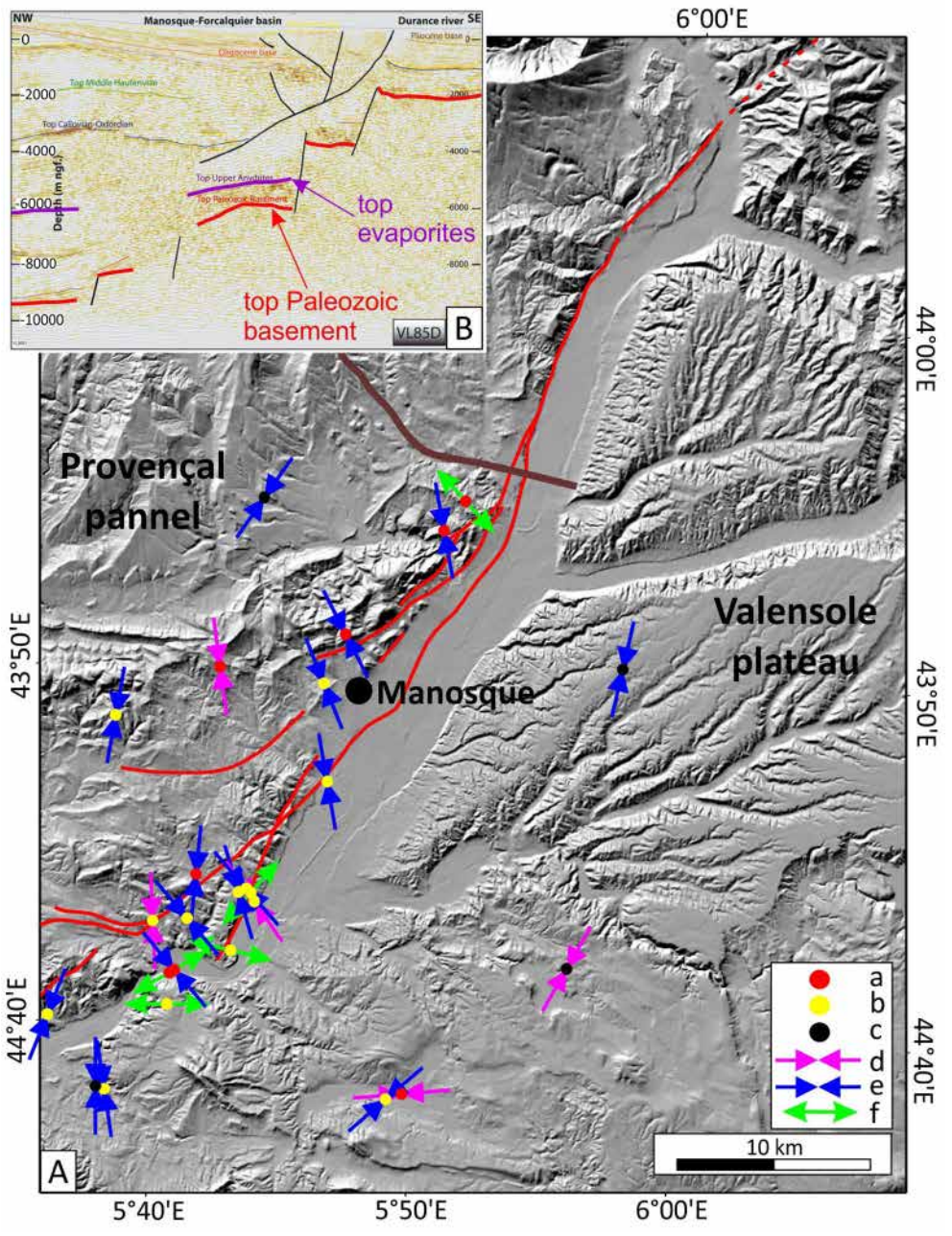

Figure 19. (A) *P*-axes and focal depth along the Durance fault (red line) for the best localized earthquakes [modified from Cushing et al., 2008]. (a) Focal depth >2 km below the basement top (BT), (b) focal depth 2 km below or over BT, (c) focal depth 2 km over BT. Focal solution: (d) reverse, (e) strike-slip, (f) normal. (B) Seismic imagery (profile VL85D, brown line on A, depth is in m) of the Paleozoic basement, Meso-Cenozoic sedimentary cover and geometry of the Middle Durance Fault [from Guyonnet-Benaize et al., 2015].

Following Cushing et al. [2008], the focal depths are in the range of 4–9 km, thus earthquakes are mainly located in the sedimentary cover but also caused by the fault in the crystalline basement. A careful analysis of these focal mechanisms reveals different directions of the *P*-axis of earthquakes: on the one hand a NW–SE compression in the sedimentary cover and on the other hand a NS to NE–SW compression in the basement [Cushing et al., 2008; Figure 19]. Such stress decoupling in the upper crust has also been proposed in the southern subalpine chains [e.g. Madeddu et al., 1996] and is certainly enabled by the thick level of Triassic evaporites.

From a slightly different 3D-crustal model and another relocation code, Le Pichon et al. [2010] proposed that the 1999–2006 seismicity recorded around the MDF is located only in the sedimentary cover. Therefore, the question of the potential involvement of the basement in the deformation, thick-skin versus thin-skin tectonics, remains relevant [Cushing et al., 2008, Le Pichon et al., 2010, Guyonnet-Benaize et al., 2015]. The extension, or not, in the basement of the active part of the fault is a major parameter of the hazard estimation since the activated fault surface largely determines the magnitude of an earthquake. However, considering that the main deformation occurs in the sedimentary cover, the associated potential magnitude of earthquakes is then limited to an upper bound of 6.5 [Cushing et al., 2008]. The potential hazard associated with deep crustal fault located under this thin-skin structure remains unknown till date.

5.4. *Shallow- and ultra-shallow seismicity in the Rhône valley*

On a global scale, seismicity is considered to be shallow when it occurs within a depth of 40 km from the surface of the Earth. In SE France, the majority of earthquakes are in the 3–10 km depth range (Figure B-S), however some areas display a concentration of shallower focal depths.

In the lower Rhône valley, the recent Le Teil earthquake (2019/11/11, M_w 4.9; no. 1 on Figure 9) was a surprise in a place where only 39 small earthquakes (M_L 1.3–2.9) have been recorded for the period 1962–2019, with focal depths in the range of 5–24 km (Figure 20A). The most surprising aspect was the very shallow depth of the 2019 earthquake focus, around 1 km [Delouis et al., 2021] which produced a strong ground motion with a maximum epicentral intensity of VIII (EMS98 macroseismic scale) and a peak ground acceleration exceeding 1 *g* [Causse et al., 2021]. This 2019 M_w 4.9 earthquake together with its shallow focus produced a co-seismic 4.5 km long surface rupture [Ritz et al., 2020]. One must notice that the development of surface rupture for a moderate magnitude earthquake is rare [Moss and Ross, 2011]; it is the first time that such a long co-seismic surface rupture has been described in France. Most often, even for earthquakes of magnitude close to 5, no co-seismic surface rupture is observed and the fault that produced the earthquake has no surface expression and remains unknown [e.g. Perrot et al., 2005, Baques et al., 2021]. Following the Le Teil earthquake, the analysis of the co-seismic rupture allowed us to demonstrate the reactivation of part of the La Rouvière fault (LRF on Figure 20), one segment of the Cévennes faults system [Ritz et al., 2020], Figures 9 and 20A).

Earlier, in December 2002, 20 km south of Le Teil, inhabitants of Clansayes city had heard two strong explosion-like sounds and had felt vibrations. Based on this a network of 15 stations was installed in the Tricastin area [Thouvenot et al., 2009]. Then, from January 10 to April 2003, 51 events were recorded with M_L—0.7–1.4. Thirty eight earthquakes have been precisely relocated, most of them are shallower than 600 m (Figure 20B). A dozen of them hold the record with a maximum depth of 300 m below ground level, and thus have been qualified as ultra-shallow earthquakes by Thouvenot et al. [2009]. This swarm elongates 5 km N–S and no active fault has been identified at the surface [Le Dortz et al., 2021].

Even historical archives attest to periods of several dozen events accompanied by very loud underground noise in the lower Rhône valley between Montélimar and Le Teil to the north and Pierrelatte to the south (Figure 20A, Rothé, 1936). For these earthquake sequences (January–April 1773, July–August 1873 and 1934–1936), Manchuel et al. [2017], taking into account the *SISFRANCE* macroseismic database and intensity prediction equations calibrated in M_w, estimated the equivalent moment magnitude–focal depth for the main shocks as: $3.0 < M_w < 4.1$ and $1 < z < 3$ km.

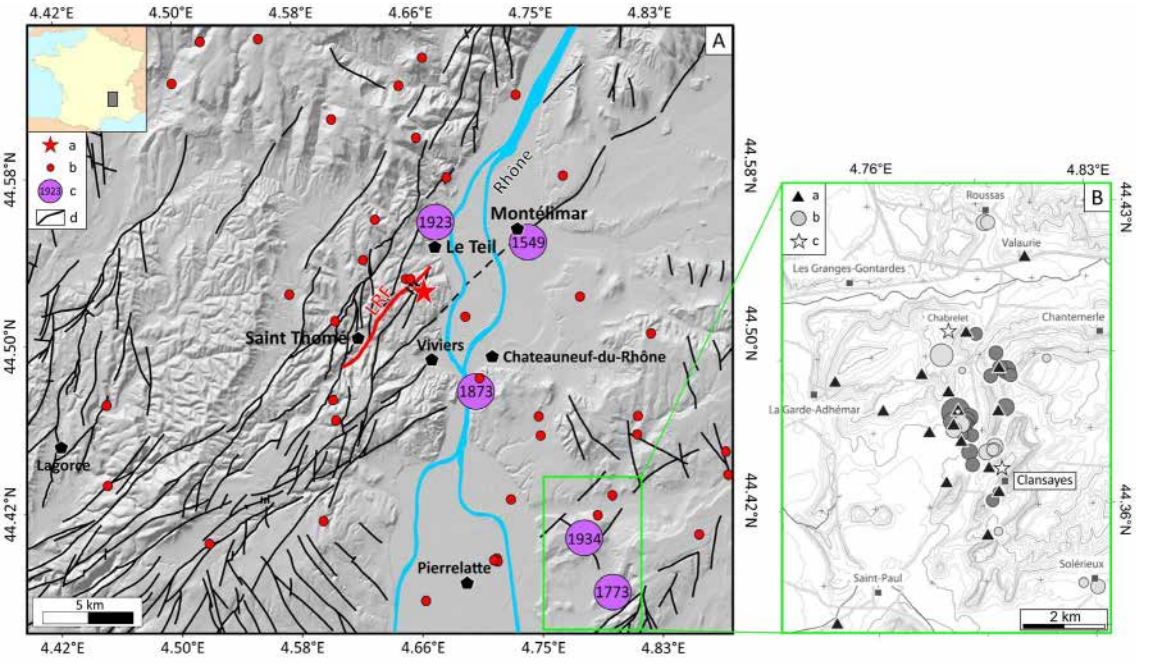

Figure 20. (A) Seismicity and structural map of the lower Rhône valley [modified from Ritz et al. [2020]]: (a) 2019/11/11 Le Teil epicenter; (b) 1962–2018 epicenters (BCSF catalog); (c) historical earthquakes (*SISFRANCE*); (d) fault traces (LRF: La Rouvière fault in red, BRGM geological maps). (B) Focus on the seismic swarm and ultra-shallow earthquakes of the Tricastin area [from Thouvenot et al., 2009]: (a) seismologic stations of the temporary network; (b) the 38 epicenters relocated (events shallower than 300 m below ground level are in lighter shade); (c) approximate position of the 1934–1936 (Chabrelet) and 1773 (Clansayes) swarms.

5.5. *Diversity of seismogenic processes*

Until the 1990s, the driving forces loading the faults in SE France were considered to be the result on the one hand of the convergence between the Africa (Nubia) and Eurasia plates [DeMets et al., 1994] and on the other hand of the counter-clockwise rotation of the Adria microplate [e.g. Vialon et al., 1989]. Twenty years of spatial geodetic measurements in the 1990s and 2000s have clarified the distribution of the movements: the convergence between Nubia and Eurasia is mainly absorbed along the Maghrebides chain in North Africa and only about 10% of this horizontal motion might be accommodated northwards [e.g. Nocquet and Calais, 2004, Serpelloni et al., 2007, Nocquet, 2012], thus restraining the role of the Nubia–Eurasia convergence as the driving forces of deformation over SE France.

Therefore, the variety of current deformation, from the Jura mountains to Corsica, can only be explained by the action/interaction of different processes depending on the location: (i) far-field plate tectonics [Nocquet, 2012, Sánchez et al., 2018, Walpersdorf et al., 2018], including Nubia–Eurasia convergence and counter-clockwise rotation of Adria, (ii) glacial and/or erosion-related isostatic adjustment [e.g. Barletta et al., 2006, Champagnac et al., 2007, Vernant et al., 2013, Chéry et al., 2016], (iii) buoyancy forces related to thickened crust in the internal Alps [e.g. Delacou et al., 2005], (iv) gravity gliding of the sedimentary cover in the Southeast basin of France [Le Pichon et al., 2010, Rangin et al., 2010], (v) crustal fluid circulation often mentioned as the origin of swarms [Leclère et al., 2013, Godano et al., 2013, De Barros et al., 2019].

The resolution of the driving forces of deformation requires taking into account the joint action of all these processes. The reader will find a precise review in Mazzotti et al. [2020]. Finally we address

three particular points concerning: (i) the tectonic and non-tectonic earthquakes in SE France, (ii) the far-field tectonic versus surface and/or deep processes in the Western Alps and (iii) the Ligurian seismicity and the long-term inversion of the northern margin.

5.5.1. *Tectonic and non-tectonic earthquakes in SE France*

The rate of deformation in SE France such as computed by Masson et al. [2019] is extremely low, in the range of 1–2 × 10^{-9} yr^{-1}. Such low values raise the question of the tectonic loading of faults, however the occurrence of the Le Teil earthquake (2019/11/11, M_L 5.4, no. 1 on Figure 9) led Delouis et al. [2019] and Ampuero et al. [2020] to conclude that, although the earthquake was probably triggered by quarry activity since the 19th century (considered as an external forcing), the magnitude reached requires a prior and significant tectonic loading. The tectonic loading of the La Rouvière fault, source of the Le Teil earthquake, at a very weak strain rate is also supported by field evidences of its Holocene–Late Pleistocene tectonic activity [Ritz et al., 2021].

The question of earthquakes induced or triggered by non-tectonic processes, whether anthropogenic or natural, is currently widely debated. The reader may refer to dedicated works for more information [e.g. McGarr et al., 2002, Grigoli et al., 2017]. A triggered earthquake occurs on a tectonically loaded fault and the additional stress related to an external forcing triggers this earthquake which would nevertheless have occurred anyway in the future. As previously mentioned, the large excavation of limestone in a quarry located on the hanging wall of the La Rouvière fault (LRF on Figure 20) is certainly the triggering cause of the Le Teil earthquake [Delouis et al., 2019, Ampuero et al., 2020]. An induced earthquake can occur on a fault that is not tectonically loaded and, in this case, such an earthquake would probably never have occurred in the absence of the external forcing. Most often the focal depths of triggered/induced events are shallow, around 1 km for the 2019 Le Teil earthquake for instance, but the shallow focal depths are not systematic.

Several examples of triggered earthquakes have been highlighted in SE France: (i) Anthropic hydrological forcing such as the filling of reservoirs is assumed to have triggered the Monteynard earthquake (1962/04/25, M_L 5.3, focal depth ~10 km, Figure 12) near Grenoble [Grasso et al., 1992] and the Jeurre earthquake in Jura [1971/06/21, M_L 4.4, focal depth 3 km; Rothé, 1983; no. 3 on Figure 7]. (ii) Natural hydrological forcing caused by a major flood of the Verdon river could have triggered the historical earthquake of Castellane in 1855 (M_L 4.5, focal depth ~1 km; Bollinger et al., 2010; Figure 12) as well as the microseismic crisis following the September 2002 catastrophic storm near Avignon, in the area of the Nîmes fault (Rigo et al., 2008; Figure 9). (iii) At crustal scale, deep-seated fluid circulation is at the origin of the 2003–2004 Ubaye swarm [Daniel et al., 2011, Leclère et al., 2013]; and De Barros et al. [2019] in analyzing the peculiar seismic behavior pointed out the interaction between tectonic process and fluid diffusion in the triggering of the alternating mainshock–aftershocks sequences and swarms during the 2012–2015 seismic crises in Ubaye. (iv) In December 2006, the Basel sequence was particularly well studied: following injection of 11,500 m^3 high-pressure water into a 5 km deep borehole more than 10,500 microearthquakes (maximum M_L 3.4) were detected in the area of injection during the following months [Deichmann and Giardini, 2009]. From analysis of accurate locations and stress drop, Goertz-Allmann et al. [2011] conclude that these earthquakes occurred on pre-existing faults and were triggered by the increase in pore pressure due to the injected water but driven by the ambient tectonic stress. (v) Finally, the origin of the Tricastin ultra-shallow earthquakes (Figure 20B) has not yet been determined. Although the focal depths are less than 500 m under the topographic surface, it has not been established that those events have been triggered by non-tectonic forcing [Thouvenot et al., 2009, Le Dortz et al., 2021].

The strongest earthquake known in SE France and neighboring regions is the 1887/02/23 Ligurian earthquake (M_w 6.7–6.9, Figure 14). Larroque et al. [2012] propose that it occurred onto the Ligurian faults system (LFS on Figure 13), 20 km from the coast line with a focal depth around 15 km and a reverse faulting on a gentle northward dipping fault plane (Figure 21). This earthquake, which occurred 1000 km away from the Africa/Eurasia plate boundary (located in the Maghrebides chain), is a typical large intraplate earthquake. The origin of large intraplate earthquakes was recently discussed by Calais

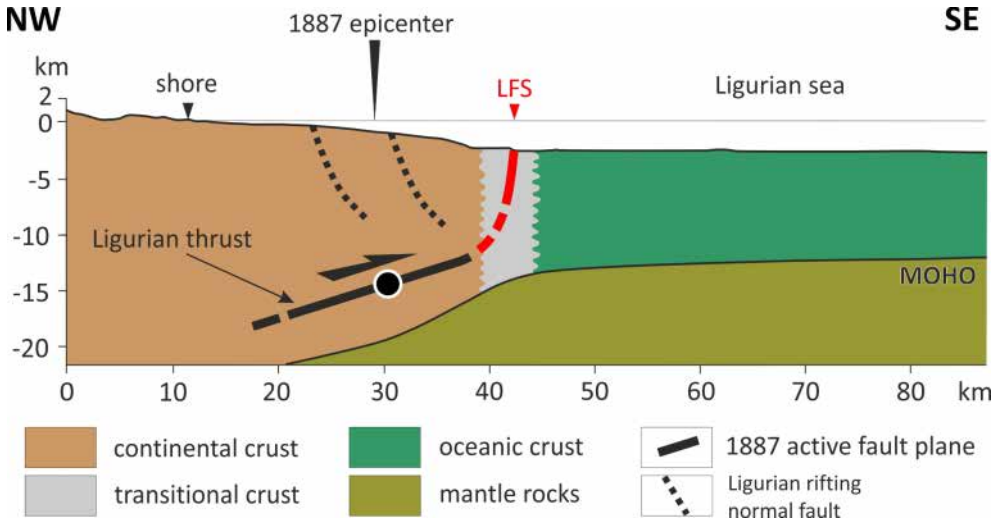

Figure 21. Seismotectonic sketch of the 1887 Ligurian earthquake and main active faults in the northern Ligurian Sea (cross section located on Figure 13). The 1887 earthquake (black dot) occurred along the northward low-dip Ligurian thrust. At shallow depths, the Ligurian Fault System (LFS) is located at the transitional oceanic/continental crust and the dashed black lines are the normal faults inherited from the rifting [modified from Larroque et al., 2012].

et al. [2016] who proposed that such earthquakes occurring in stable continental regions (SCR) are triggered by local and transient external perturbations of stress rather than long-term tectonic loading, as along plate boundaries. Several data suggest that the LFS is a long lived active fault zone working with a very low strain rate, nevertheless producing large cumulated deformation like: (i) the at least 1000 m uplift of the northern margin since 5 Ma [Bigot-Cormier et al., 2004, Larroque et al., 2011], (ii) the high concentration of instrumental and historical seismicity with seven significant earthquakes in the 19th century, including the 1887 event (Figure 14), and (iii) the very low-rate convergence between the Corsica–Sardinia block and the European mainland [Nocquet, 2012, Masson et al., 2019]. Thus, we propose that earthquakes in the northern Ligurian Sea, although far away from a plate boundary, are mainly related to far-field tectonic loading in an active plate interior rather than transient perturbation of stress in a stable continental region.

5.5.2. *Far-field tectonics versus surface and/or deep processes: example from the Western Alps*

In the Western Alps, most of the deformation is located in the internal domain, along and in the vicinity of the two seismic arcs (nos. 1 and 2 in Figures 1 and 11). Several models have been proposed in order to explain the seismicity distribution in the Western Alps, favoring either horizontal indentation [e.g. Tapponnier, 1977] or Adria microplate rotation [e.g. Vialon et al., 1989]. During the 1990–2000 period, it was shown that the main deformation corresponds to orogen-perpendicular extension framed on the periphery by transcurrent zones locally modulated with compressional component [Maurer et al., 1997, Eva and Solarino, 1998, Sue et al., 1999, Kastrup et al., 2004, Delacou et al., 2004, Larroque et al., 2009]. As spatial geodesy does not show any shortening higher than 0.5 mm/yr through the chain [e.g. Nocquet, 2012], this pattern of deformation was interpreted as reactivation of ancient faults mostly resulting from buoyancy forces after cessation of Africa–Europe convergence [e.g. Selverstone, 2005, Delacou et al., 2005]. However, the influence of the counter-clockwise rotation of the Adria microplate was not excluded [Calais et al., 2002].

The most recent seismotectonic study, at the scale of the Western Alps [Mathey, 2020], is based on the *SISmalp* catalog (1987–2014) and a new 3D-crustal velocity model [Potin, 2016]. The quality of hypocenter locations confirms that the seismicity is

distributed along a slab dipping from west to east, at depth between 10–15 km on the western side of the belt (Europe plate) and 25–30 km on the eastern side (Adria microplate) and reaching at least 40 km depth in the Po plain. The reassessment of the deformation pattern, from more than 2000 focal mechanisms (mainly $1 < M_L < 3$) across the chain, confirmed the extension in the internal zones. Moreover this work brings out a new crucial data: the direction of extension appears systematically oblique to the radial direction, deflected by a few tens of degrees in the clockwise sense. This new data therefore suggests a significant influence of the far-field tectonics imposed by the counter-clockwise rotation of the Adria plate with respect to the stable Europe plate leading to a dominant right-lateral strike-slip faulting in the Western Alps [Calais et al., 2002, Serpelloni et al., 2005, D'Agostino et al., 2008, Sánchez et al., 2018, Walpersdorf et al., 2018].

Another recent study [Eva et al., 2020] is based on the reprocessing of 9000 events recorded by the INGV National Central Seismic Network (Italy) from 1986 to 2016 complemented by *RESIF–EPOS* and *SED* (Swiss Seismological Service) data. The first order of the Alpine deformation is common to that in previous works but Eva et al. [2020] particularly point out the role of the opposite-dipping Alpine (toward SE) and Apenninic (toward SW) slabs in the partitioning of deformation. They suggest that the counter-clockwise rotation of Adria has no influence south of 45° N because of the underthrusting of the Adria microplate below the Monferrato thrust front in the western Po plain. This proposition is consistent with the spatial geodetic analysis of Walpersdorf et al. [2018] indicating a decrease of the right-lateral strike-slip component towards the south of the Western Alps and with the dominant extensional deformation along the NNW–SSE high Durance fault pointed out by Mathey et al. [2020]. It is also consistent with the dominant normal faulting along NW–SE faults highlighted during the 2012 and 2014 Ubaye earthquakes [nos. 6 and 7 on Figure 11 and Baques et al., 2021] as well as with the extensional focal mechanisms of earthquakes computed in the Argentera area [Larroque et al., 2009].

Taking into account the recent spatial geodetic results attesting to less than 0.5 mm/yr horizontal motion through the Western Alps versus ~3 mm/yr of present-day uplift in the northern internal zones, several authors [Chéry et al., 2016, Nocquet et al., 2016, Nguyen et al., 2016, Sternai et al., 2019] proposed that the Alpine chain currently deforms mainly under strong influence either from surface processes (such as glacial isostatic adjustment following the last glacial maximum since 15–20 ka) and/or deep processes, related to the European slab detachment and/or lateral variation of rheology in the deep crust and upper mantle. All these processes are themselves at the origin of the isostatic adjustments.

5.5.3. *Ligurian seismicity and long-term inversion of the northern margin*

As previously noticed [e.g. Béthoux et al., 1992, Larroque et al., 2009], earthquakes along the Alps-Ligurian basin junction attest to a compressional tectonic regime (Figure 13) consistent with far-field tectonics and mainly the shortening between the Corsica–Sardinia continental block and the European mainland [Billi et al., 2011, Nocquet, 2012, Masson et al., 2019]. It was recently proposed that the Corsican earthquakes of July 2011 (no. 5 on Figure 13) was related to the southward propagation of this compressional deformation [Larroque et al., 2016].

In the northern Ligurian Sea, Larroque et al. [2011] showed that the current reverse faulting seismicity is mainly related to the north-dipping Ligurian faults system, extended 80 km long from Nice to Savona (LFS on Figure 13 and Figure 21). Morphotectonic data attest to large cumulated deformations since 5 Ma along the LFS that support the uplift of the margin relative to the basin [Bigot-Cormier et al., 2004, Larroque et al., 2011, Sage et al., 2011]. Therefore, the inversion of the margin seems to be controlled by this north-dipping ramp and flat thrust system while the south-dipping normal faults inherited from the Oligo–Miocene rifting remain passive [Sage et al., 2011]. Current earthquakes could then occur along steeply or gently northward dipping fault planes depending on their focal depths.

The current rate of seismicity of the northern margin is significantly higher than that of the surrounding regions (including the southwestern Alps, the northern Apennine and the Corsica–Sardinia block; Béthoux et al., 1998). Béthoux et al. [2008] produced thermomechanical models that account for the strain concentration in the Ligurian Sea

at the transitional oceanic/continental domains as currently observed. Their models point out the strain concentration by a combination of the tectonic forces (related to the shortening between the Corsica–Sardinia block and the European mainland), the geometric effects (related to the strong topography and Moho depth gradients) and the contrast in rheology which leads to a weaker zone at the foot of the northern margin. Thus, the model of Béthoux et al. [2008] could explain the inversion of the margin by the neoformation of a northward dipping thrust inside this weakness zone rather than the reactivation of the inherited normal faults in the shallow continental crust (Figure 21).

6. Conclusion

Southeast France, and surroundings, is an active intraplate zone with heterogeneous low to very low deformation rates (low on the Ligurian margin and very low in Corsica, for instance). Earthquakes there are mainly low to moderate magnitude with 4–5 strong events ($M_w \geq 6$) in 500 years. Except in very rare cases, the instrumental seismicity is heterogeneously distributed across the four major geological domains, the Western Alps and the Ligurian margin being the most active areas. Over a period of 500 years, the distribution of historical seismicity is quite similar to the instrumental seismicity.

While in the 70s the only known relationship between earthquakes and geological structures was limited to the Briançonnais seismic arc and the Penninic Frontal thrust, the regular progress in the detection capacity and in the accuracy of localization now allow generation of a finer image of the active zones and help point out the relationships between earthquakes and several mapped faults (e.g. Belledonne, Durance, Vuache…) and hidden faults (Blausasc). In the same way, microseismic swarms are now rapidly detected owing to instrumentation with temporary networks, and their evolution can be followed precisely. The Ligurian Sea remains the only area where there is no permanent seismological observatory and therefore the seismicity in the basin is very poorly known.

The diversity of seismic behaviors can only be explained because it develops in complex geological domains with large structural inheritance, rheological features, various thermal conditions and with different driving mechanisms that remain largely misunderstood. Thus, the 2019 Le Teil earthquake is surprising both by its location, its focal mechanism and focal depth. The main challenge to refine the image of seismicity concerns the improvement of focal depth determinations. The identification of 3D structures in seismicity requires continued observational efforts as well as the construction of more accurate velocity models, certainly in 3D in such a complex crustal area. Moreover, the accuracy of geodetic measurements, now better than 1 mm/yr, will improve with increasing times series and this should make it possible to link the distribution of seismicity with surface movements and active geological structures. The recent result obtained on the characterization of the Haute Durance fault is an encouragement to continue the joint analysis of seismicity/geodesy, including in areas with low deformation rate.

A better image of the seismicity as well as the budget of the seismic energy released compared to the horizontal and vertical movements measured by space geodesy are needed for understanding the present-day drivers of the deformation throughout SE France. An important bias in this approach remains the temporal scale to be considered because of the long recurrence times of the strongest earthquakes.

A better characterization of seismicity is also a requirement to progress in understanding seismic hazards related to large events and the knowledge of causative geological structures. No catastrophic earthquake has occurred since 1909, however nothing is known about the seismogenic capability of several large active faults (Durance, Belledonne, for instance). Are they able to produce strong earthquakes ($M_w > 6.5$) and at what recurrence intervals? The M_w 4.9 2019 Le Teil earthquake, which occurred on a fault that was not recognized as potentially active, also raises the question of the lack of knowledge of structures capable of being activated by tectonic loading and/or triggered/induced by anthropogenic activities.

Web sites

BCSF, RéNaSS, SI-Hex: http://www.franceseisme.fr/
Delouis-Géoazur:
http://sismoazur.oca.eu/focal_mechanism
GEOFON: https://geofon.gfz-potsdam.de/

JURAQUAKE: https://dataosu.obs-besancon.fr/FR-18008901306731-2019-03-29_JURAQUAKE.html
CEA-LDG: http://www-dase.cea.fr/
OCA: http://sismoazur.oca.eu/
PTB (Physikalisch-Technische Bundesanstalt, DCF77):
https://www.ptb.de/cms/index.php?id=1787&L=1
RSNI: http://www.distav.unige.it/rsni/
RESIF–EPOS: https://www.resif.fr/
SED: http://www.seismo.ethz.ch/en/home/
SISFRANCE: https://sisfrance.net/
SISmalp: https://sismalp.osug.fr/isterre-sismalp

Acknowledgments

We thank all the technical staff from the different labs who for more than 50 years have participated in the installation and maintenance of seismological networks in the southeast. We thank the researchers who have invested heavily in the development of these networks, in particular François Thouvenot for the SISmalp network (1989) and Jean Virieux and Stéphane Gaffet for the TGRS network (1992). We also thank the researchers who participated in the exploitation of these data, in particular Nicole Béthoux and François Thouvenot. Clara Duverger and Gilles Mazet-Roux provided the *CEA* catalog and answered questions, Denis Thiéblemont (BRGM) gave us the vectorized geological map of France. We also thank Jérémy Billant for the discussion about the Belledonne fault and Frédéric Huneau for data on Corsica geology. Lastly, we thank the anonymous reviewer who took the time to carefully read this long manuscript and helped us to clarify the text and figures.

Supplementary data

Supporting information for this article is available on the journal's website under https://doi.org/10.5802/crgeos.69 or from the author.

References

Affolter, T. and Gratier, J. P. (2004). Map view retrodeformation of an arcuate fold-and-thrust belt: The Jura case. *J. Geophys. Res.*, 109(B3), article no. 03404.

Ambert, P., Philip, H., and Ritz, J.-F. (1998). Commentaire à la note de Robin Lacassin, Bertrand Meyer, Lucilla Benedetti, Rolando Armijo et Paul Tapponnier. *C. R. Acad. Sci. Paris*, 327, 857–859. série lia.

Amelung, F. and King, G. C. P. (1997). Large scale tectonic deformation inferred from small earthquakes. *Nature*, 386, 702–705.

Ampuero, J. P., Billant, J., Brenguier, F., Cavalier, O., Courboulex, F., Deschamps, A., Delouis, B., Grandin, R., Jolivet, R., Liang, C., Mordret, A., and Oral, E. (2020). The November 11, 2019 Le Teil, France M5 earthquake: a triggered event in nuclear country. In *EGU General Assembly 2020*. https://doi.org/10.5194/egusphere-egu2020-18295.

Arthaud, F. and Laurent, P. (1995). Contraintes, déformation et déplacement dans l'avant-pays Nord-pyrénéen du Languedoc méditerranéen. *Geodyn. Acta (Paris)*, 8, 142–157.

Arthaud, F. and Séguret, M. (1981). Les structures pyrénéennes du Languedoc et du golfe du Lion (Sud de la France). *Bull. Soc. Géol. Fr.*, XXIII(7), 51–63.

Augliera, P., Béthoux, N., Déverchère, J., and Eva, C. (1994). The Ligurian Sea: newseismotectonic evidence. *Boll. Geofis. Teor. Appl.*, XXXVI, 141–144.

Baer, M., Deichamnn, N., Ballarin Dolffin, D., Bay, F., Delouis, B., Fäh, D., Giardini, D., Kastrup, U., Kind, F., Kradolfer, U., Künzle, W., Röthliberger, S., Schler, T., Sellami, S., Smit, P., and Spühler, E. (1999). Earthquakes in Switzerland and surrounding regions during 1998. *Eclog. Geol. Helv.*, 92/2, 265–273.

Baer, M., Deichamnn, N., Braumiller, J., Husen, S., Fäh, D., Giardini, D., Kästli, P., Kradolfer, U., and Wiemer, S. (2005). Earthquakes in Switzerland and surrounding regions during 2004. *Eclog. Geol. Helv.*, 98/3, 407–418.

Baize, S., Cushing, M., Lemeille, F., Gelis, C., Texier, D., Nicoud, G., and Schwenninger, J. L. (2011). Contribution to the seismic hazard assessment of a slow active fault, the Vuache fault in the southern Molasse basin (France). *Bull. Soc. Géol. Fr.*, 182(4), 347–365.

Baques, M., De Barros, L., Duverger, C., Jomard, H., Godano, M., Courboulex, F., and Larroque, C. (2021). Seismic activity in Ubaye Region (French Alps): A specific behaviour highlighted by mainshocks and swarm sequences. *C. R. Géosci.*, 353(S1), 535–559.

Barféty, J. C. and Gidon, M. (1996). La structure des Collines bordières du Grésivaudan et des secteurs adjacents, à l'est de Grenoble (Isère, France). *Géol. Alp.*, 72, 5–22.

Barletta, V. R., Ferrari, C., Diolaiuti, G., Carnielli, T., Sabadini, R., and Smiraglia, C. (2006). Glacier shrinkage and modeled uplift of the Alps. *Geophys. Res. Lett.*, 33, article no. L14307.

Baroux, E., Béthoux, N., and Bellier, O. (2001). Analyses of the stress field in the southeastern France from earthquake focal mechanisms. *Geophys. J. Int.*, 145, 336–348.

Baroux, E., Pino, N. A., Valensise, G., Scotti, O., and Cushing, M. (2003). Source parameters of the 11 June 1909, Lambesc (Provence, southeastern France) earthquake: A reappraisal based on macroseismic, seismological, and geodetic observations. *J. Geophys. Res.*, 108(B9), article no. 2454.

BCSF (1983). Institut de Physique du Globe de Strasbourg, Observation sismologique: sismicité en France entre 1971 et 1977. http://www.franceseisme.fr/donnees/publi/1971-1977/obs_sismo_1971-77.pdf.

BCSF (2002). Institut de Physique du Globe de Strasbourg, Observation sismologique: sismicité de la France en 1997, 1998 et 1999. In *Sismicité instrumentale*, volume 2. http://www.franceseisme.fr/donnees/publi/1997-1999/OBS_SISMO1997-99Vol2.PDF.

Becker, A. (2000). The Jura Mountains - An active foreland fold-and-thrust belt? *Tectonophysics*, 321(4), 381–406.

Bellahsen, N., Jolivet, L., Lacombe, O., Bellanger, M., Boutoux, A., Garcia, S., Mouthereau, F., Le Pourhiet, L., and Gumiaux, C. (2012). Mechanisms of margin inversion in the external Western Alps: implications for crustal rheology. *Tectonophysics*, 560–561, 62–83.

Bellier, O., Cushing, E. M., and Sébrier, M. (2021). Thirty years of paleoseismic research in metropolitan france. *C. R. Géosci.*, 353(S1), 339–380.

Bestani, L., Espurt, N., Lamarche, J., Bellier, O., and Hollender, F. (2016). Reconstruction of the Provence Chain evolution, southeastern France. *Tectonics*, 35(6), 1506–1525.

Béthoux, N., Fréchet, J., Guyoton, F., Thouvenot, F., Cattaneo, M., Eva, C., Nicolas, M., and Granet, M. (1992). A closing Ligurian sea. *Pure Appl. Geophys.*, 139, 179–194.

Béthoux, N., Ouillon, G., and Nicolas, M. (1998). The instrumental seismicity of the Western Alpes: spatio-temporal patterns analysed with the wavelets transform. *Geophys. J. Int.*, 135, 177–194.

Béthoux, N., Sue, C., Paul, A., Virieux, J., Fréchet, J., Thouvenot, F., and Cattaneo, M. (2007). Local tomography and focal mechanisms in the southwestern Alps: comparison of methodes and tectonic implications. *Tectonophysics*, 432, 1–19.

Béthoux, N., Theunissen, T., Beslier, M. O., Font, Y., Dessa, J. X., Simon, S., Courrioux, G., and Guillen, A. (2016). Earthquake relocation using a 3D a priori geological velocity model from the Western Alps to Corsica: implication to seismic hazard. *Tectonophysics*, 670, 82–100.

Béthoux, N., Tric, E., Chery, J., and Beslier, M. O. (2008). Why is the Ligurian basin (Mediterranean sea) seismogenic? Thermomechanical modeling of a reactivated passive margin. *Tectonics*, 27(5), article no. TC5011.

Bigot-Cormier, F., Sage, F., Sosson, M., Déverchère, J., Ferrandini, M., Guennoc, P., Popoff, M., and Stéphan, J. F. (2004). Déformations pliocènes de la marge nord-Ligure (France): Les conséquences d'un chevauchement crustal sud-alpin. *Bull. Soc. Géol. Fr.*, 175(2), 197–211.

Bilau, A., Rolland, Y., and Schwartz, S. (2021). Extensional reactivation of the penninic frontal thrust 3 Myr ago as evidenced by U-Pb dating on calcite in fault zone cataclasite. *Solid Earth*, 12, 237–251.

Billant, J., Hippolyte, J. C., and Bellier, O. (2015). Tectonic and geomorphic analysis of the Belledonne border fault and its extensions, Western Alps. *Tectonophysics*, 659, 31–52.

Billi, A., Faccenna, C., Bellier, O., Minelli, L., Neri, G., Piromallo, C., Presti, D., Scrocca, D., and Serpelloni, E. (2011). Recent tectonic reorganization of the Nubia-Eurasia convergent boundary heading for the closure of the western Mediterranean. *Bull. Soc. Géol. Fr.*, 182(4), 279–303.

Bollinger, L., Nicolas, M., and Marin, S. (2010). Hydrological triggering of the seismicity around a salt diapir in Castellane, France. *Earth Planet. Sci. Lett.*, 290, 20–29.

Bossolasco, M., Cicconi, G., Eva, C., and Pascale, V. (1972). La rete sismica dell'Istituto Geofisico di Genova e primi risultati sulla sismo-tettonica delle Alpi Marittime ed Occidentali, e del Mar Ligure. *Riv. It. Geofis.*, XXI(5/6), 229–247.

Calais, E., Camelbeeck, T., Stein, S., Liu, M., and Craig, T. J. (2016). A new paradigm for large earthquakes in stable continental plate interiors. *Geophys. Res. Lett.*, 43(20), 10621–10637.

Calais, E., Nocquet, J. M., Jouanne, F., and Tardy, M. (2002). Current strain regime in the Western Alps form continuous Global Positioning System measurements, 1996–2001. *Geology*, 30(7), 651–654.

Camelbeeck, T., Vanneste, K., Alexandre, P., Verbeeck, K., Petermans, T., Rosset, P., Everaerts, M., Warmant, R., and Van Camp, M. (2007). Relevance of active faulting and seismicity studies to assessments of long-term earthquake activity and maximum magnitude in intraplate northwest Europe. In Stein, S. and Mazzotti, S., editors, *Continental Intraplate Earthquakes*, volume 425 of *Geol. Soc. Am. Sp. Pap.*, pages 193–224. Geological Society of America, Boulder, CO.

Cara, M. et al. (2015). Si-Hex: a new catalog of instrumental seismicity for metropolitan France. *Bull. Soc. Géol. Fr.*, 186(1), 3–19.

Cara, M., Schlupp, A., and Sira, C. (2007). *Observations sismologiques: sismicité de la France en 2003, 2004, 2005*. Bureau Central Sismologique Français, Strasbourg. 200 pages. http://www.franceseisme.fr/donnees/publi/2003-2005/OBS_SISMO_2003-05_W.pdf.

Cara, M., Van der Woerd, J., Alasset, P. J., Benjumea, J., and Mériaux, A. S. (2017). The 1905 Chamonix earthquakes: active tectonics in the Mont Blanc and Aiguilles Rouges massifs. *Swiss J. Geosci.*, 110, 631–651.

Carbon, D., Combes, P., Cushing, E. M., and Garnier, T. (1993). Enregistrement d'un paléoseisme dans des sédiments du Pléistocène supérieur dans la vallée du Rhône: quantification de la déformation. *Géol. Alp.*, 69, 33–48.

Caron, J. M. and Loye-Pilot, M. D. (1990). Notice explicative, Carte géol. France (1/50,000), feuille Pietra-di-Verde (1115). BRGM, Orléans, 51 pages.

Castelli, V., Camassi, R., and Molin, D. (2012). The Uzège (Southeastern France) 22 March 1186 earthquake reappraised. *Seismol. Res. Lett.*, 83(3), 604–614.

Cattaneo, M., Augliera, P., Parolai, S., and Spallarossa, D. (1999). Anomalously deep earthquakes in northwestern Italy. *J. Seismol.*, 3, 421–435.

Causse, M., Cornou, C., Maufroy, E., Grasso, J. R., Baillet, L., and El Haber, E. (2021). Exceptional ground motion during the shallow M_w 4.9 2019 Le Teil earthquake, France. *Commun. Earth Env.*, 2(14), article no. 14.

Chamoot-Rooke, N., Gaulier, J. M., and Jestin, F. (1999). Constraints on Moho depth and crustal thickness in the Liguro-Provençal basin from 3D gravity inversion: geodynamic implications. In Durand, B. et al., editors, *Mediterranean Basins*, volume 156, pages 37–62. Geol. Soc. London Special Publication, London.

Champagnac, J. D., Molnar, P., Anderson, R. S., Sue, C., and Delacou, B. (2007). Quaternary erosion-induced isostatic rebound in the western Alps. *Geology*, 35(3), 195–198.

Champion, C., Choukroune, P., and Clauzon, G. (2000). La déformation post-pliocène en Provence occidentale. *Geodyn. Acta*, 13, 67–85.

Chantraine, J., Autran, A., and Cavelier, C. (2003). *Carte géologique de la France (version numérique) à l'échelle du millionième*. BRGM, Orléans, 6ème edition.

Chardon, D. and Bellier, O. (2003). Geological boundary conditions of the 1909 Lambesc (Provence, France) earthquake: structure and evolution of the Trévaresse ridge anticline. *Bull. Soc. Géol. Fr.*, 174(5), 497–510.

Chardon, D., Hermitte, D., Nguyen, F., and Bellier, O. (2005). First paleoseismological constraints on the strongest earthquake in France (Provence) in the twentieth century. *Geology*, 33, 901–904.

Chatelain, J. L., Roecker, S. W., Hatzfeld, D., and Molnar, P. (1980). Microearthquake seismicity and fault plane solutions in the Hindu Kush region and their tectonic implications. *J. Geophys. Res.*, 85, 1365–1387.

Chaumillon, E., Déverchère, J., Réhault, J. P., and Gueguen, E. (1994). Réactivation tectonique et flexure de la marge continentale Ligure (Méditerranée Occidentale). *C. R. Acad. Sci. Paris*, 319, 675–682.

Chéry, J., Genti, M., and Vernant, P. (2016). Ice cap melting and low-viscosity crustal root explain the narrow geodetic uplift of the western Alps. *Geophys. Res. Lett.*, 43, 3193–3200.

Collombet, M., Thomas, J. C., Chauvin, A., Tricart, P., Bouillin, J., and Gratier, J. P. (2002). Counterclockwise rotation of the western Alps since the Oligocene: new insights from paleomagnetic data. *Tectonics*, 21, 11–15.

Combes, P. (1984). *La Tectonique récente de la*

Provence Occidentale: Microtectonique, caractéristiques dynamiques et cinématiques. Méthodologie de zonation tectonique et relations avec la sismicité. PhD thesis, Univ. Louis Pasteur, Strasbourg, France. 192 pp.

Cornou, C. et al. (2021). Rapid response to the M_w 4.9 earthquake of November 11, 2019 in Le Teil, Lower Rhône Valley, France. *C. R. Géosci.*, 353(S1), 441–463.

Courboulex, F., Deichmann, N., and Gariel, J. C. (1999). Rupture complexity of a moderate intraplate earthquake in the Alps: the 1996 M5 Epagny-Annecy earthquake. *Geophys. J. Int.*, 139, 152–160.

Courboulex, F., Deschamps, A., Cattaneo, M., Costi, F., Déverchère, J., Virieux, J., Augliera, P., Lanza, V., and Spallarossa, D. (1998). Source study and tectonic implications of the 1995 Ventimiglia (border of Italy and France) earthquakes (M_L = 4.7). *Tectonophysics*, 290, 245–257.

Courboulex, F., Duval, A. M., Deschamps, A., Lomax, A., and Larroque, C. (2001). Les enseignements du petit séisme de Peille (Alpes-Maritimes, France). *C. R. Acad. Sci. Paris*, 333, 105–112.

Courboulex, F., Larroque, C., Deschamps, A., Gélis, C., Charreau, J., and Stéphan, J. F. (2003). An unknown active fault revealed by microseismicity in the south-east of France. *Geophys. Res. Lett.*, 30(15), 1782–1786.

Courboulex, F., Larroque, C., Deschamps, A., Kohrs-Sansorny, C., Gélis, C., Got, J. L., Charreau, J., Stéphan, J. F., Béthoux, N., Virieux, J., Brunel, D., Maron, C., Duvak, A. M., Perez, J. L., and Mondielli, P. (2007). Seismic hazard on the French Riviera: new data, interpretations and simulations. *Geophys. J. Int.*, 170(1), 387–400.

Cushing, E. M., Baize, S., Nechtchein, S., Bellier, O., Scotti, O., and Baumont, D. (2014). Contexte sismotectonique régional : géologie, sismicité historique et sismotectonique de la région de Manosque. In Poursoulis, G. and Levret, A., editors, *Tremblement de Terre de 1708 à Manosque. Apport d'une Étude Historique et Archéologique à l'évaluation du Risque Sismique en Moyenne Durance*, pages 19–44. Groupe A.P.S., Perpignan.

Cushing, E. M., Bellier, O., Nechtschein, S., Sébrier, M., Lomax, A., Volant, P., Dervin, P., Guignard, P., and Bove, L. (2008). A multidisciplinary study of a slow-slipping fault for seismic hazard assessment: The example of the Middle Durance Fault (SE France). *Geophys. J. Int.*, 172, 1163–1178.

D'Agostino, N., Avallone, A., Cheloni, D., D'Anastasio, E., Mantenuto, S., and Selvaggi, G. (2008). Active tectonics of the Adriatic region from GPS and earthquake slip vectors. *J. Geophys. Res.*, 113, article no. B12413.

Daniel, G., Prono, E., Renard, F., Thouvenot, F., Hainzl, S., Marsan, D., Helmstetter, A., Traversa, P., Got, J. L., Jenatton, L., and Guiguet, R. (2011). Changes in effective stress during the 2003–2004 Ubaye seismic swarm, France. *J. Geophys. Res.*, 116, article no. B01309.

De Barros, L., Baques, M., Godano, M., Helmstetter, A., Deschamps, A., Larroque, C., and Courboulex, F. (2019). Fluid-induced swarms and coseismic stress transfer: a dual process highlighted in the aftershock sequence of the 7 April 2014 earthquake (Ml 4.8, Ubaye, France). *J. Geophys. Res., Solid Earth*, 124, 3918–3932.

De la Taille, C. (2015). *Évaluation de l'activité tectonique quaternaire des failles du Jura Méridional (France)*. PhD thesis, Université Grenoble-Alpes. 246 pp. https://tel.archives-ouvertes.fr/tel-01680848v2/document.

Deichmann, N., Baer, M., Braunmiller, J., Husen, S., Fäh, D., Giardini, D., Kästli, P., Kradolfer, U., and Wiemer, S. (2006). Earthquakes in Switzerland and surrounding regions during 2005. *Eclogae Geol. Helv.*, 99(3), 443–452.

Deichmann, N., Bare, M., Braunmiller, J., Ballardin Dolfin, D., Bay, F., Delouis, B., Fäh, D., Giardini, D., Kastrup, U., Kind, F., Kradolfer, U., Künzle, W., Röthelisberger, S., Schler, T., Salichon, J., Sellami, S., Spühler, E., and Wiemer, S. (2000). Earthquakes in Switzerland and surrounding regions during 1999. *Eclogae Geol. Helv.*, 93, 395–406.

Deichmann, N., Clinton, J., Husen, S., Edwards, B., Haslinger, F., Fäh, D., Giardini, D., Kästli, P., Kradolfer, U., and Wiemer, S. (2012). Earthquakes in Switzerland and surrounding regions during 2011. *Swiss J. Geosci.*, 105, 463–476.

Deichmann, N. and Giardini, D. (2009). Earthquakes induced by the stimulation of an enhanced geothermal system below Basel (Switzerland). *Seismol. Res. Lett.*, 80/5, 784–798.

Delacou, B., Burkhard, M., Champagnac, J. D., and Sue, C. (2004). Present-day geodynamics in the bend of the Western and Central Alps as con-

strained by earthquake analysis. *Geophys. J. Int.*, 158(2), 753–774.

Delacou, B., Sue, C., Champagnac, J. D., and Burkhard, M. (2005). Origin of the current stress field in the western/central Alps: Role of gravitational re-equilibration constrained by numerical modelling. *Geol. Soc. Lond., Sp. Pub.*, 243(1), 295–310.

Delouis, B., Ampuero, J. P., Audin, L., Bernard, P., Brenguier, F., Grandin, R., Jolivet, R., Leloup, H., Ritz, J. F., Vergne, J., Vernant, P., and Voisin, C. (2019). Rapport d'évaluation du groupe de travail (GT) CNRS-INSU sur le séisme du Teil du 11 novembre 2019 et ses causes possibles. http://www.cnrs.fr/sites/default/files/press_info/2019-12/Rapport_GT_Teil_phase1_final_171219_v3.pdf.

Delouis, B., Oral, E., Menager, M., Ampuero, J. P., Guilhem Trilla, A., Régnier, M., and Deschamps, A. (2021). Constraining the point source parameters of the 11 November 2019 M_w 4.9 Le Teil earthquake using multiple relocation approaches, first motion and full waveform inversions. *C. R. Géosci.*, 353(S1), 493–516.

DeMets, C., Gordon, R. G., Argus, D. F., and Stein, S. (1994). Effect of recent revisions to the geomagnetic reversal time scale on estimates of current plate motions. *Geophys. Res. Lett.*, 21(20), 2191–2194.

Dercourt, J., Zonenshain, L. P., Ricou, L. E., Kasmin, V. G., Le Pichon, X., Knipper, A. L., Grandjacquet, C., Sbortshikov, I. M., Geyssant, J., Lepvrier, C., Pechersky, D. H., Boulin, J., Sibuet, J. C., Savostin, L. A., Sorokhtin, O., Westphal, M., Bazhenov, M. L., Lauer, J. P., and Biju-Duval, B. (1986). Geological evolution of the Tethys belt from the Atlantic to the Pamir since the Lias. *Tectonophysics*, 123, 241–315.

Dervin, P., Nechtschein, S., and Cushing, M. (2007). Bilan instrumentation du réseau de la Durance après plus de 10 ans d'exploitation. BERSSIN, Bilan instrumentation du réseau de la Durance après plus de 10 ans d'exploitation, 72 pp. DEI/SARG/2007-028.

Diehl, T., Clinton, J., Cauzzi, C., Kraft, T., Kästli, P., Deichmann, N., Massin, F., Grigoli, F., Molinari, I., Böse, M., Hobiger, M., Haslinger, F., Fäh, D., and Wiemer, S. (2021). Earthquakes in Switzerland and surrounding regions during 2017 and 2018. *Swiss J. Geosci.*, 114, article no. 4.

Diehl, T., Clinton, J., Deichmann, N., Cauzzi, C., Kästli, P., Kraft, T., Molinari, I., Böse, M., Michel, C., Hobiger, M., Haslinger, F., Fäh, D., and Wiemer, S. (2018). Earthquakes in Switzerland and surrounding regions during 2015 and 2016. *Swiss J. Geosci.*, 111, 221–244.

Donzeau, M., Wernli, R., and Charollais, J. (1998). Interprétation nouvelle de la géométrie de l'accident du Vuache dans le Jura meridional: le relais de failles transpressif sénestre Léaz-Champfromier (Ain). *Géol. de la France*, 2, 25–45.

Doubre, C., Meghraoui, M., Masson, F., et al. (2021). Seismotectonics and geodynamic implication in North–Eastern France and neighboring regions. *C. R. Géosci.*, 353(S1), 153–185.

Dufumier, H. (2002). Synthesis of magnitude and focal mechanism computations for the M≥4.5 earthquakes in France for the period 1995–2000. *J. Seismol.*, 6, 163–181.

Dumont, T., Simon-Labric, T., Authemayou, C., and Heymes, T. (2011). Lateral termination of the north-directed Alpine orogeny and onset of westward escape in the Western Alpine Arc: Structural and sedimentary evidence from the external zone. *Tectonics*, 30, article no. TC5006.

Durand-Delga, M. (1984). Principaux traits de la Corse Alpine et corrélations avec les Alpes Ligures. *Mem. Soc. Geol. It.*, 28, 285–329.

Duverger, C., Mazet-Roux, G., Bollinger, L., Guilhem Trilla, A., Vallage, A., Hernandez, B., and Cansi, Y. (2021). A decade of seismicity in metropolitan France (2010–2019): the CEA/LDG methodologies and observations. *BSGF - Earth Sci. Bull.*, 192, article no. 25.

Espurt, N., Hippolyte, J.-C., Saillard, M., and Bellier, O. (2012). Geometry and kinematic evolution of a long-living foreland structure inferred from field data and cross section balancing, the Sainte-Victoire system, Provence, France. *Tectonics*, 31, article no. TC4021.

Espurt, N., Wattellier, F., Philip, J., Hippolyte, J. C., Bellier, O., and Bestani, L. (2019). Mesozoic halokinesis and basement inheritance in the eastern Provence fold-thrust belt, SE France. *Tectonophysics*, 766, 60–80.

Eva, E., Malusà, M. G., and Solarino, S. (2020). Seismotectonics at the transition between opposite-dipping slabs (Western Alpine Region). *Tectonics*, 39(9). https://doi.org/10.1029/2020TC006086.

Eva, E. and Solarino, S. (1998). Variations of stress directions in the western Alpine arc. *Geophys. J. Int.*, 135(2), 438–448.

Eva, E., Solarino, S., Eva, C., and Neri, G. (1997). Stress tensor orientation derived from fault plane solutions in the southwestern Alps. *J. Geophys. Res.*, 102(B4), 8171–8185.

Eva, E., Solarino, S., and Spallarossa, D. (2001). Seismicity and crustal structure beneath the western Ligurian Sea derived from local earthquake tomography. *Tectonophysics*, 339(3–4), 495–510.

Fäh, D., Gisler, M., Jaggi, B., Kästli, P., Lutz, T., Masciadri, V., Matt, C., Mayer-Rosa, D., Rippmann, D., Schwartz-Zanetti, G., Tauber, J., and Wenk, T. (2009). The 1356 Basel earthquake: an interdisciplinary revision. *Geophys. J. Int.*, 178(1), 351–374.

Ferrandini, J., Béthoux, N., Gauthier, A., Fréchet, J., Thouvenot, F., and Fontaine, C. (1994). Première tentative d'étude sismotectonique de la Corse à partir des données d'un réseau sismologique régional de la campagne SISBALIG II. *C. R. Acad. Sci. Paris*, 319, 705–712. série IIa.

Ferrari, G. (1991). The 1887 Ligurian earthquake: a detailed study from contemporary scientific observations. *Tectonophysics*, 193(1–3), 131–139.

Ferry, M., Meghraoui, M., Delouis, B., and Giardini, D. (2005). Evidence for Holocene palaeoseismicity along the Basel–Reinach active normal fault (Switzerland): a seismic source for the 1356 earthquake in the Upper Rhine graben. *Geophys. J. Int.*, 160, 554–572.

Fréchet, J. (2008). Past and future of historical seismicity studies in France. In *Historical Seismology*, pages 131–145. Springer, Dordrecht.

Fréchet, J., Thouvenot, F., Frogneux, M., Deichmann, N., and Cara, M. (2011). The M_w 4.5 Vallorcine (French Alps) earthquake of 8 September 2005 and its complex aftershock sequence. *J. Seismol.*, 15, 43–58.

Fréchet, J., Thouvenot, F., Jenatton, L., Hoang-Trong, P., and Frogneux, M. (1996). Le séisme du Grand-Bornand (Haute Savoie) du 14 décembre 1994: un coulissage dextre dans le socle subalpin. *C. R. Acad. Sci. Paris*, 323, 517–524. IIa.

Fritsche, S. and Fäh, D. (2009). The 1946 Magnitude 6.1 earthquake in the Valais: site-effects as contributor to the damage. *Swiss J. Geosci.*, 102, 423–439.

Fritsche, S., Fäh, D., Gisler, M., and Giardini, D. (2006). Reconstructing the damage field of the 1855 earthquake in Switzerland: historical investigations on a well-documented event. *Geophys. J. Int.*, 166(2), 719–731.

Gattacceca, J., Deino, A., Rizzo, R., Jones, D. S., Henry, B., Beaudoin, B., and Valeboin, F. (2007). Miocene rotation of Sardinia: new paleomagnetic and geochronological constraints and geodynamic implications. *Earth Planet. Sci. Lett.*, 258, 359–377.

Godano, M., Deschamps, A., Delouis, B., Bertrand, E., Chèze, J., Langlaude, P., Martin, X., and Pernoud, M. (2019). The Saint-Paul-en-Forêt seismic swarm: an unusual activity in the seismically quiet Maures Massif (South-Eastern France). In *EGU General Assembly 2019*. https://meetingorganizer.copernicus.org/EGU2019/EGU2019-14600.pdf.

Godano, M., Larroque, C., Bertrand, E., Courboulex, F., Deschamps, A., Salichon, J., Blaud-Guerry, C., Fourteau, L., Charléty, J., and Deshayes, P. (2013). The October–November 2010 earthquake swarm near Sampeyre (Piedmont region, Italy): a complex multicluster sequence. *Tectonophysics*, 608, 97–111.

Godard, V., Hippolyte, J. C., Cushing, E., Espurt, N., Fleury, J., Bellier, O., and Ollivier, V. (2020). Hillslope denudation and morphologic response to a rock uplift gradient. *Earth Surf. Dyn.*, 8, 221–243.

Goertz-Allmann, B. P., Goertz, A., and Wiemer, S. (2011). Stress drop variations of induced earthquakes at the Basel geothermal site. *Geophys. Res. Lett.*, 38(9). https://doi.org/10.1029/2011GL047498.

Grasso, J. R., Guyoton, F., Fréchet, J., and Gammond, J. F. (1992). Triggered earthquakes as stress gauge: implication for the uppercrust behavior in the grenoble area, France. *Pure Appl. Geophys.*, 139(3/4), 579–605.

Grigoli, F., Cesca, S., Priolo, E., Pio Rinaldi, A., Clinton, J. F., Stabile, T. A., Dost, B., Garcia Fernandez, M., Wiemer, S., and Dahm, T. (2017). Current challenges in monitoring, discrimination, and management of induced seismicity related to underground industrial activities: A European perspective. *Rev. Geophys.*, 55, 310–340.

Guéguen, P., Janex, G., Nomade, J., Langlais, M., Helmstetter, A., Coutant, O., Schwartz, S., and Dollet, C. (2021). Unprecedent seismic swarm in the Maurienne valley (2017–2019) observed by the SISmalp Alpine seismic network: operational monitoring and management. *C. R. Géosci.*, 353(S1),

517–534.

Gutenberg, B. and Richter, C. F. (1944). Frequency of earthquakes in California. *Bull. Seismol. Soc. Am.*, 34, 185–188.

Guyonnet-Benaize, C., Lamarche, J., Hollender, F., Viseur, S., Münch, P., and Borgomano, J. (2015). Three-dimensional structural modeling of an active fault zone based on complex outcrop and subsurface data: The Middle Durance Fault Zone inherited from polyphase Meso-Cenozoic tectonics (southeastern France). *Tectonics*, 34, 265–289.

Handy, M. R., Schmid, S. M., Bousquet, R., Kissling, E., and Bernoulli, D. (2010). Reconciling plate-tectonic reconstructions of Alpine Tethys with the geological–geophysical record of spreading and subduction in the Alps. *Earth Sci. Rev.*, 102(3–4), 121–158.

Hetényi, G. et al. (2018). The AlpArray Seismic Network: a large-scale European experiment to image the Alpine orogeny. *Surv. Geophys.*, 39, 1009–1033.

Hippolyte, J.-C. and Dumont, T. (2000). Identification of Quaternary thrusts, folds and faults in a low seismicity area: Examples in the Southern Alps (France). *Terra Nova*, 12, 156–162.

Ioualalen, M., Larroque, C., Scotti, O., and Daubord, C. (2014). The tsunami coastal distribution and hazard along the French–Italian Riviera. *Pure Appl. Geophys.*, 171, 1423–1443.

Jenatton, L., Guiguet, R., Thouvenot, F., and Daix, N. (2007). The 16,000-event 2003–2004 earthquake swarm in Ubaye (French Alps). *J. Geophys. Res.*, 112, article no. B11304.

Jolivet, L., Augier, R., Faccenna, C., Negro, F., Rimmele, G., Agard, P., Robin, C., Rossetti, F., and Crespo-Blanc, A. (2008). Subduction, convergence and the mode of backarc extension in the Mediterranean region. *Bull. Soc. Géol. Fr.*, 179(6), 525–550.

Jomard, H., Cushing, E. M., Palumbo, L., Baize, S., David, C., and Chartier, T. (2017). Transposing an active fault database into a seismic hazard fault model for nuclear facilities – Part 1: Building a database of potentially active faults (BDFA) for metropolitan France. *Nat. Hazards Earth Syst. Sci.*, 17(9), 1573–1784.

Jomard, H., Scotti, O., Auclair, S., Dominique, P., Manchuel, K., and Sicilia, D. (2021). The SISFRANCE database of historical seismicity. State of the art and perspectives. *C. R. Géosci.*, 353(S1), 257–280.

Kastrup, U., Zoback, M. L., Deichmann, N., Evans, K., and Giardini, D. (2004). Stress field variations in the Swiss Alps and the northern Alpine foreland derived from inversion of fault plane solutions. *J. Geophys. Res.*, 109, article no. B01402.

Kissling, E. (1988). Geotomography with local earthquake data. *Rev. Geophys.*, 26, 659–698.

Lacassin, R., Meyer, B., Benedetti, L., Armijo, R., and Tapponnier, P. (1998). Signature morphologique de l'activité de la faille des Cévennes (Languedoc, France). *C. R. Acad. Sci. Paris*, 326, 807–815. série Il.

Lacombe, O. and Mouthereau, F. (2002). Basement-involved shortening and deep detachment tectonics in forelands of orogens: Insights from recent collision belts (Taiwan, Western Alps, Pyrenees). *Tectonics*, 21(4), 12–1–12–22.

Lambert, J. and Terrier, M. (2011). Historical tsunami database for France and its overseas territories. *Nat. Hazards Earth Syst. Sci.*, 11, 1037–1046.

Lambert, J., Winter, T., Dewez, T. J., and Sabourault, P. (2005). New hypotheses on the maximum damage area of the 1356 Basel earthquake (Switzerland). *Quat. Sci. Rev.*, 24(3–4), 381–399.

Lardeaux, J. M., Schwartz, S., Tricart, P., Paul, A., Guillot, S., Béthoux, N., and Masson, F. (2006). A crustal scale cross section of the southwestern Alps combining geophysical and geological imagery. *Terra Nova*, 18(6), 412–422.

Larroque, C., Béthoux, N., Calais, E., Courboulex, F., Deschamps, A., Déverchère, J., Stéphan, J. F., Ritz, J. F., and Gilli, E. (2001). Active and recent deformation at the Southern Alps–Ligurian basin junction. *Neth. J. Geosci. Geol. Mijnbouw.*, 80, 255–272.

Larroque, C., Delouis, B., Godel, B., and Nocquet, J. M. (2009). Active deformation at the southwestern Alps–Ligurian basin junction (France–Italy boundary): evidence for recent change from compression to extension in the Argentera massif. *Tectonophysics*, 467(1–4), 22–34.

Larroque, C., Delouis, B., Sage, F., Régnier, M., Béthoux, N., Courboulex, F., and Deschamps, A. (2016). The sequence of moderate size earthquakes at the junction of the Ligurian basin and the Corsica margin (western Mediterranean): The initiation of an active deformation zone revealed? *Tectonophysics*, 676, 135–147.

Larroque, C., Mercier de Lépinay, B., and Migeon, S. (2011). Morphotectonic and fault–earthquake relationships along the northern Ligurian margin

(western Mediterranean) based on high resolution multibeam bathymetry and multichannel seismicreflection profiles. *Mar. Geophys. Res.*, 32(1–2), 163–179.

Larroque, C., Scotti, O., and Ioualalen, M. (2012). Reappraisal of the 1887 Ligurian earthquake (western Mediterranean) from macroseismicity, active tectonics and tsunami modelling. *Geophys. J. Int.*, 190(1), 87–104.

Le Dortz, K., Bollinger, L., Duverger, C., Vallage, A., Marin, S., and Leroy, Y. (2021). Seismic swarms in Tricastin, lower Rhône Valley (France): review of historical and instrumental seismicity and models. *C. R. Géosci.*, 353(S1), 585–606.

Le Pichon, X., Rangin, C., Hamon, Y., Loget, N., Lin, J., Andreani, L., and Flotte, N. (2010). Geodynamics of the France southeast basin. *Bull. Soc. Géol. Fr.*, 6, 477–501.

Leclère, H., Daniel, G., Fabbri, O., Cappa, F., and Thouvenot, F. (2013). Tracking fluid pressure buildup from 792 focal mechanisms during the 2003–2004 Ubaye seismic swarm, France. *J. Geophys. Res., Solid Earth*, 118, 4461–4476.

Letort, J., Vergoz, J., Gulbert, J., Cotton, F., Sebe, O., and Cano, Y. (2014). Moderate earthquake teleseismic depth estimations: new methods and use of the comprehensive nuclear-test-ban treaty organization network data. *Bull. Seismol. Soc. Am.*, 85(2), 558–560.

Madeddu, B., Béthoux, N., and Stephan, J. F. (1996). Déformations et champs de contraintes récents à actuel dans les Alpes sud-occidentales: approche sismotectonique. *Bull. Soc. Géol. Fr.*, 167, 797–810.

Madritsch, H., Schmid, S. M., and Fabbri, O. (2008). Interactions between thin- and thick-skinned tectonics at the northwestern front of the Jura fold-and-thrust belt (eastern France). *Tectonics*, 27, article no. TC5005.

Malavieille, J., Chemenda, A., and Larroque, C. (1998). Evolutionary model for Alpine Corsica: mechanism for ophiolite emplacement and exhumation of high-pressure rocks. *Terra Nova*, 10, 317–322.

Manchuel, K., Traversa, P., Baumont, D., Cara, M., Nayman, E., and Durouchoux, C. (2017). The French seismic CATalogue (FCAT-17). *Bull. Earthq. Eng.*, 8(16), 2227–2251.

Marillier, F., Gauthier, A., and Vogt, J. (1982). La sismicité en Corse: revue historique et étdude macrosismique de quelques événements récents. *Pure Appl. Geophys.*, 120, 168–185.

Masson, C., Mazzotti, S., and Vernant, P. (2019). Precision of continuous GPS velocities 20 from statistical analysis of synthetic time series. *Solid Earth*, 10, 329–342.

Mathey, M. (2020). *Quantification haute résolution du champ de déformation 3D des Alpes occidentales: interprétations tectoniques et apports à l'aléa sismique*. PhD thesis, Université Grenoble-Alpes. http://www.theses.fr/s189352.

Mathey, M., Walpersdorf, A., Sue, C., Baize, S., and Deprez, A. (2020). Seismogenic potential of the High Durance Fault constrained by 20 yr of GNSS measurements in the Western European Alps. *Geophys. J. Int.*, 222, 2136–2146.

Mattauer, M. (2002). Commentaire sur l'article: "Mouvement post-messinien sur la faille de Nîmes…". *Bull. Soc. Géol. Fr.*, 173, 595.

Maurer, H., Burkhard, M., Deichmann, N., and Green, G. (1997). Active tectonism in the central Alps: contrasting stress regimes north and south of the Rhone Valley. *Terra Nova*, 9(2), 91–94.

Mazzotti, S., Abagnac, C., Bollinger, L., Oscanoa, K. C., Delouis, B., Do Paco, D., Doubre, C., Godano, M., Jomard, H., Larroque, C., and Laurendeau, A. (2021). FMHex20: A database of earthquake focal mechanisms in metropolitan France and conterminous Western Europe. *BSGF - Earth Sci. Bull.*, 192, article no. 10.

Mazzotti, S., Jomard, H., and Masson, F. (2020). Processes and deformation rates generating seismicity in metropolitan France and conterminous Western Europe. *BSGF - Earth Sci. Bull.*, 191, article no. 19.

McGarr, A., Simpson, D., and Seeber, L. (2002). Case histories of induced and triggered seismicity. In *International Handbook Earthquake Eng. Seismol.*, volume 81A, pages 647–661. Academic Press (Int'l Assoc. Seismol. & Phys. Earth's Interior, Committee on Education, Ed).

Medvedev, S. V., Sponheuer, W., and Karnik, V. (1967). Seismic intensity scale version 1964. Publication No. 48 of the Institut fur Geodynamik, 69 Jena (D D R).

Meghraoui, M., Delouis, B., Ferry, M., Giardini, D., Huggenberger, P., Spottke, I., and Granet, M. (2000). Active normal faulting in the upper Rhine graben and paleoseismic identification of the 1356. *Basel Earthq. Sci.*, 293, 2070–2073.

Ménard, G. (1988). *Structure et cinématique d'une chaîne de collision. Les Alpes occidentales et centrales*. PhD thesis, Univ. J. Fourier, Grenoble. 268 pp. http://www.theses.fr/1988GRE10018.

Meyer, B., Lacassin, R., Brulhet, J., and Mouroux, B. (1994). The Basel earthquake: which fault produced it? *Terra Nova*, 1, 54–63.

Molliex, S., Bellier, O., Terrier, M., Lamarche, J., Martelet, G., and Espurt, N. (2011). Tectonic and sedimentary inheritance on the structural framework of Provence (SE France): Importance of the Salon-Cavaillon fault. *Tectonophysics*, 501(1–4), 1–16.

Moss, R. and Ross, Z. E. (2011). Probabilistic fault displacement hazard analysis for reverse faults. *Bull. Seismol. Soc. Am.*, 101, 1542–1553.

Nguyen, H. N., Vernant, P., Mazzotti, S., Khazaradze, G., and Asensio, E. (2016). 3D GPS velocity field and its implications on the present-day postorogenic deformation of the western Alps and Pyrenees. *Solid Earth Discuss.*, 7(5), 1349–1363.

Nicolas, M., Bethoux, N., and Madeddu, B. (1998). Instrumental seismicity of the Western Alps: a revised catalogue. *Pure Appl. Geophys.*, 152, 707–731.

Nocquet, J. M. (2012). Present-day kinematics of the Mediterranean: a comprehensive overview of GPS results. *Tectonophysics*, 579, 220–242.

Nocquet, J. M. and Calais, E. (2004). Geodetic measurements of crustal deformation in the Western Mediterranean and Europe. *Pure Appl. Geophys.*, 161, 661–681.

Nocquet, J. M., Sue, C., Walpersdorf, A., Tran, T., Lenôtre, N., Vernant, P., Cushing, M., Jouanne, F., Masson, F., Baize, S., Chéry, J., and van der Beeck, P. A. (2016). Present-day uplift of the western Alps. *Sci. Rep.*, 6(1), article no. 28404.

Paul, A., Cattaneo, M., Thouvenot, F., Spallarossa, D., Béthoux, N., and Fréchet, J. (2001). A three dimensional crustal velocity model of the southwestern Alps from local earthquake tomography. *J. Geophys. Res.*, 106(B9), 19367–19389.

Pedrazzini, A., Humair, F., Jaboyedoff, M., and Tonini, M. (2016). Characterisation and spatial distribution of gravitational slope deformation in the Upper Rhone catchment (Western Swiss Alps). *Landslides*, 13(2), 259–277.

Perrot, J., Arroucau, P., Guilbert, J., Déverchère, J., Mazabraud, Y., Rolet, J., Mocquet, A., Mousseau, M., and Matias, J. (2005). Analysis of the Mw 4.3 Lorient earthquake sequence: a multidisciplinary approach to the geodynamics of the Armorican Massif, westernmost France. *Geophys. J. Int.*, 162, 935–950.

Phillippe, Y. (1994). Transfer Zone in the southern Jura Thrust Belt (eastern France): geometry, development and comparison with analogue modelling experiments. In Mascle, A., editor, *Hydrocarbon and Petroleum Geology of France*, volume 4 of *Europ. Assoc. Petrol. Geol. Spec. Publ.*, pages 327–346. Springer.

Potin, B. (2016). *Les Alpes occidentales: tomographie, localisation de séismes et topographie du Moho*. PhD thesis, University Grenoble-Alpes. 245 pp. https://tel.archives-ouvertes.fr/tel-01539221/document.

Quenet, G., Baumont, D., Scotti, O., and Levret, A. (2004). The 14 August 1708 Manosque, France earthquake: New constraints on the damage area from in-depth historical studies. *Ann. Geophys.*, 47, 583–595.

Rabin, M., Sue, C., Walpersdorf, A., Sakic, P., Albaric, J., and Fores, B. (2018). Present-day deformations of the Jura arc inferred by GPS surveying and earthquake focal mechanisms. *Tectonics*, 37, 3782–3804.

Rangin, C., Le Pichon, X., Loget, N., Hamon, Y., and Crespy, A. (2010). Gravity tectonics in the SE basin (Provence, France) imaged with seismic data. *Bull. Soc. Géol. Fr.*, 6, 503–530.

Réhault, J. P., Boillot, G., and Mauffret, A. (1984). The western Mediterranean basin geological evolution. *Mar. Geol.*, 55, 447–477.

Ricou, L. E. and Siddans, A. (1986). Collision tectonics in the western Alps. In Coward, M. and Ries, A. C., editors, *Collision Tectonics*, volume 19, pages 229–244. Geol. Soc. London Sp. Pub., London.

Rigo, A., Béthoux, N., Masson, F., and Ritz, J.-F. (2008). Seismicity rate and wave–velocity variations as consequences of rainfall: the case of the catastrophic storm of September 2002 in the Nîmes Fault region (Gard, France). *Geophys. J. Int.*, 173, 473–482.

Ritz, J. F., Baize, S., Audin, L., Authemayou, C., Kaub, C., Lacan, P., Leclerc, F., Manchuel, K., Mugnier, J. L., Ortuño, M., Rizza, M., and Vassallo, R. (2021). Perspectives in studying active faults in metropolitan France. *C. R. Géosci.*, 353(S1), 381–412.

Ritz, J. F., Baize, S., Ferry, M., Larroque, C., Audin, L., Delouis, B., and Mathot, E. (2020). Surface rupture

and shallow fault reactivation during the 2019 M_w 4.9 Le Teil earthquake, France. *Comm. Earth Env.*, 1, article no. 10.

Rollet, N., Déverchère, J., Beslier, M. O., Guennoc, P., Réhault, J. P., Sosson, M., and Truffert, C. (2002). Back arc extension, tectonic inheritance and volcanism in the Ligurian Sea, Western Mediterranean. *Tectonics*, 21, 6–1–6–23.

Rothé, J. P. (1936). Les tremblements de terre en France en 1934. *Ann. Inst. Phys. Globe*, 2, 88–110.

Rothé, J. P. (1942). La sismicité des Alpes occidentales. *Bull. Soc. Géol. Fr.*, 5ième série(II), 295–320.

Rothé, J. P. (1983). La sismicité de la France entre 1971 et 1977. *Annales de l'Institut de Physique du Globe de Strasbourg*, page 209. http://www.franceseisme.fr/donnees/publi/1971-1977/obs_sismo_1971-77.pdf.

Roure, F., Brun, J. P., Colletta, B., and Van den Driessche, J. (1992). Geometry and kinematics of extensional structures in the Alpine Foreland Basin of southeastern France. *J. Struct. Geol.*, 14, 503–519.

Roure, F., Heitzmann, P., and Polino, R. (1990). Deep structures of the Alps. *Mem. Soc. Geol. Fr.*, 156, 367.

Sage, F., Beslier, M. O., Thinon, I., Larroque, C., Dessa, J. X., Migeon, S., Angelier, J., Guennoc, P., Schreiber, D., Michaud, F., Stéphan, J. F., and Sonnette, L. (2011). Structure and evolution of a passive margin in a compressive environment: example of the south-western Alps-Ligurian basin junction during the Cenozoic. *Mar. Pet. Geol.*, 28, 1263–1282.

Sambeth, U. and Pavoni, N. (1988). A seismotectonic investigation in the Geneva Basin, southern Jura Mountains. *Eclogea Geol. Helv.*, 8(2), 433–440.

Sanchez, G., Rolland, Y., Schreiber, D., Giannerini, G., Corsini, M., and Lardeaux, J. M. (2010). The active fault system of SW Alps. *J. Geodyn.*, 49(5), 296–302.

Sánchez, L., Völksen, C., Sokolov, A., Arenz, H., and Seitz, F. (2018). Present-day surface deformation of the Alpine region inferred from geodetic techniques. *Earth Syst. Sci. Data*, 10(3), 1503–1526.

Scafidi, D., Barani, S., De Farrari, R., Feretti, G., Pasta, M., Pavan, M., Spallarossa, D., and Turiono, C. (2015). Seismicity of North Western Italy during the last 30 years. *J. Seismol.*, 19, 201–218.

Schlupp, A., Clauzon, G., and Avouac, J.-P. (2001). Mouvement post messinien sur la faille de Nîmes: implications pour la sismotectonique de la Provence. *Bull. Soc. Géol. Fr.*, 172, 697–711.

Schlupp, A., Clauzon, G., and Avouac, J. P. (2002). Réponse au commentaire de M. Séranne sur l'article "Mouvement post-messinien sur la faille de Nîmes: implications pour la sismotectonique de Provence". *Bull. Soc. Géol. Fr.*, 173, 592–594.

Schmid, S. M. and Kissling, E. (2000). The arc of the western Alps in the light of geophysical data on deep crustal structure. *Tectonics*, 19(1), 62–85.

Scotti, O., Baumont, D., Quenet, G., and Levret, A. (2004). The French macroseismic database SISFRANCE: objectives, results and perspectives. *Ann. Geophys.*, 47(2/3), 571–581.

Scotti, O., Levret, A., and Hernandez, B. (1999). Détermination des caractéristiques des séismes pour les études d'aléa sismique: comparaison des évaluations macrosismiques et instrumentales. 5ème colloque National de l'AFPS, ENS Cachan (France) 42–47.

Sébrier, M., Bellier, O., Peulvast, J.-P., and Vergély, P. (1998). Commentaire à la note de Robin Lacassin, Bertrand Meyer, Lucilla Benedetti, Rolando Armijo et Paul Tapponnier. *C. R. Acad. Sci. Paris*, 327, 855–856. série IIa.

Selverstone, J. (2005). Are the Alps collapsing? *Ann. Rev. Earth Planet. Sci.*, 33, 113–132.

Séranne, M. (1999). The Gulf of Lions continental margin (NW Mediterranean) revisited by IBS: an overview. In Durand, B., Jolivet, L., Horvath, F., and Séranne, M., editors, *The Mediterranean Basins*, volume 156, pages 15–36. Geol. Soc. London Sp. Pub., London.

Séranne, M. (2002). Commentaire sur l'article "Mouvement post-messinien sur la faille de Nîmes: implications pour la sismotectonique de la Provence". *Bull. Soc. Géol. Fr.*, 6, 589–591.

Serpelloni, E., Anzidei, M., Baldi, P., Casula, G., and Galvani, A. (2005). Crustal velocity and strain-rate fields in Italy and surrounding regions: New results from the analysis of permanent and non-permanent GPS networks. *Geophys. J. Int.*, 161(3), 861–880.

Serpelloni, E., Faccena, C., Spada, G., Dong, D., and Williams, D. P. (2013). Vertical GPS ground motion rates in the Euro-Mediterranean region: new evidence of velocity gradients at different spatial scales along the Nubia–Eurasia plate boundary. *J. Geophys. Res.*, 118, 6003–6024.

Serpelloni, E., Vannucci, G., Pondrelli, S., Argnani, A., Casula, G., Anzidei, M., Baldi, P., and Gasperini, P. (2007). Kinematics of the Western Africa-Eurasia

plate boundary from focal mechanisms and GPS data. *Geophys. J. Int.*, 169(3), 1180–1200.

Solarino, S., Kissling, E., Sellami, S., Smriglio, G., Thouvenot, F., Granet, M., Bonjer, K. P., and Slejko, D. (1997). Compilation of a recent seismicity data base of the greater Alpine region from several seismological networks and preliminary 3D tomographic results. *Ann. Geophys.*, 40(1), 161–174.

Solarino, S., Malusà, M. G., Eva, E., Guillot, S., Paul, A., Schwartz, S., Zhao, L., Aubert, C., Dumont, T., Pondrelli, S., Salimbeni, S., Wang, Q., Xu, X., Zheng, T., and Zhu, R. (2018). Mantle wedge exhumation beneath the Dora-Maira (U)HP dome unravelled by local earthquake tomography (Western Alps). *Lithos*, 296–299, 623–636.

Sommaruga, A. (1999). Décollement tectonics in the Jura foreland fold-and-thrust belt. *Mar. Pet. Geol.*, 16(2), 111–134.

Sternai, P., Sue, C., Husson, L., Serpelloni, E., Becker, T. W., Wilett, S. D., Faccenna, C., Di Giulio, A., Spada, G., Jolivet, L., Valla, P., Petit, C., Nocquet, J. M., Walpersdorf, A., and Castelltort, S. (2019). Present-day uplift of the European Alps: Evaluating mechanisms and models of their relative contributions. *Earth Sci. Rev.*, 190, 589–604.

Sue, C., Thouvenot, F., Fréchet, J., and Tricart, P. (1999). Widespread extension in the core of the Western Alps revealed by earthquake analysis. *J. Geophys. Res.*, 104, 25611–25622.

Sue, C. and Tricart, P. (2003). Neogene to ongoing normal faulting in the inner western Alps: A major evolution of the late alpine tectonics. *Tectonics*, 22(5), article no. 1050.

Tapponnier, P. (1977). Evolution tectonique du système alpin en Méditarranée: Poinçonnement et écrasement rigide-plastique. *Bull. Soc. Géol. Fr.*, 19, 437–460.

Taramelli, T. and Mercalli, G. (1888). Il terremoto ligure del 23 febbraio 1887. *Ann. dell'Ufficio Centrale Meteorol. Geodinamico Italiano, II*, 8(4), 331–626.

Terrier, M., Serrano, O., and Hanot, F. (2008). Reassessment of the structural framework of western Provence (France): Consequence on the regional seismotectonic model. *Geodyn. Acta*, 21, 231–238.

Thouvenot, F., Fréchet, J., Jenatton, L., and Gamond, J. F. (2003). The Belledonne border fault: identification of an active seismic strike-slip fault in the western Alps. *Geophys. J. Int.*, 155, 174–192.

Thouvenot, F., Fréchet, J., Tapponnier, P., Thomas, J. C., Le Brun, B., Ménard, G., Lacassin, R., Jenatton, L., Grasso, J. R., Coutant, O., Paul, A., and Hatzfeld, D. (1998). The M_L 5.3 Epagny (French Alps) earthquake of 1996 July 15: a long awaited event on the Vuache fault. *Geophys. J. Int.*, 135, 876–892.

Thouvenot, F., Jenatton, L., and Gratier, J. P. (2009). 200 m-deep earthquake swarm in Tricastin (lower Rhône Valley, France) accounts for noisy seismicity over past centuries. *Terra Nova*, 21, 203–201.

Thouvenot, F., Jenatton, L., Scafidi, D., Turino, C., Potin, B., and Ferretti, G. (2016). Encore Ubaye: Earthquake Swarms, Foreshocks, and Aftershocks in the Southern French Alps. *Bull. Seismol. Soc. Am.*, 106, 2244–2257.

Thouvenot, F., Paul, A., Fréchet, J., Béthoux, N., Jenatton, L., and Guiguet, R. (2007). Are there really superposed Mohos in the south-western Alps? New seismic data from fan-profiling reflections. *Geophys. J. Int.*, 170, 1180–1194.

Tricart, P. (1984). From passive margin to continental collision: a tectonic scenario for the western Alps. *Am. J. Sci.*, 284, 97–120.

Turino, C., Scafidi, D., Eva, E., and Solarino, S. (2009). Inference on active faults at the Southern Alps-Ligurian basin junction from accurate analysis of low energy seismicity. *Tectonophysics*, 475, 470–479.

Ustaszewski, K. and Schmid, S. (2007). Neotectonic activity in the Upper Rhine Graben-Jura Mountains junction (North-Western Switzerland and adjacent France). *Bull. Angew. Geol.*, 12(1), 3–19.

Ustaszewski, M. and Pfiffner, A. (2008). Neotectonic Faulting, Uplift and Seismicity in the Central and Western Swiss Alps. In Siegesmund, S., Fugenschuh, B., and Froitzheim, N., editors, *Tectonic Aspects of the Alpine-Dinaride-Carpathian System*, volume 298, pages 231–249. Geol. Soc. London Sp. Pub., London.

Vernant, P., Hivert, F., Chéry, J., Steer, P., Cattin, R., and Rigo, A. (2013). Erosion induced isostatic rebound triggers extension in low convergent mountain ranges. *Geology*, 41, 467–470.

Vialon, P., Rochette, P., and Ménard, G. (1989). Indentations and rotations in the western Alpine arc. In Coward, M. P., Dietrich, D., and Park, R. G., editors, *Alpine Tec-tonics*, volume 45, pages 329–339. Geol. Soc. London, Spec. Publ., London.

Villeger, M. and Andrieux, J. (1987). Phases tectoniques post-Eocènes et structuration polyphasée

du panneau de couverture nord provençal (Alpes externes méridionales). *Bull. Soc. Géol. Fr.*, 8, 147–156.

Vogt, J. (1992). Le "complexe" de la crise sismique nissarde de 1564. *Quaternaire*, 3(3–4), 125–127.

Volant, P., Berge-Thierry, C., Dervin, P., Cushing, M., Mohammadioun, G., and Mathieu, F. (2000). The south eastern Durance fault permanent network: Preliminary results. *J. Seismol.*, 4, 175–189.

Walpersdorf, A., Pinget, L., Vernant, P., Sue, C., Deprez, A., and Renag, t. (2018). Does long-term GPS in the Western Alps finally confirm earthquake mechanisms? *Tectonics*, 37(10), 3721–3737.

Zhao, L., Paul, A., Malusà, M. G., Xu, X., Zheng, T., Solarino, S., Guillot, S., Schwartz, S., Dumont, T., Salimbeni, S., Aubert, C., Pondrelli, S., Wang, Q., and Zhu, R. (2016). Continuity of the Alpine slab unraveled by high-resolution P wave tomography. *J. Geophys. Res.*, 121, 8720–8737.